Aus dem Laser-Forschungslabor und Labor für
Tumorimmunologie, LIFE-Zentrum Großhadern,
Institut der Universität München
Vorstand: Prof. Dr. Ronald Sroka

Verbesserung der Sensitivität von Glioblastomzelllinien gegenüber der Photodynamischen Therapie durch Blockung des ABCG2-Transporterproteins

Dissertation

zum Erwerb des Doktorgrades der Medizin
an der Medizinischen Fakultät der
Ludwig-Maximilians-Universität München

vorgelegt von
Patricia Müller
aus Leinefelde

2022

Mit Genehmigung der Medizinischen Fakultät

der Ludwigs-Maximilians-Universität München

Berichterstatter:	Prof. Dr. Wolfgang Zimmermann
Mitberichterstatter:	Prof. Dr. Rainer Glaß
	Prof. Dr. Andreas Leunig
Mitbetreuung durch den promovierten Mitarbeiter:	Dr. Herbert Stepp
Dekan:	Prof. Dr. med. Thomas Gudermann

Tag der mündlichen Prüfung: 14.07.2022

Affidavit

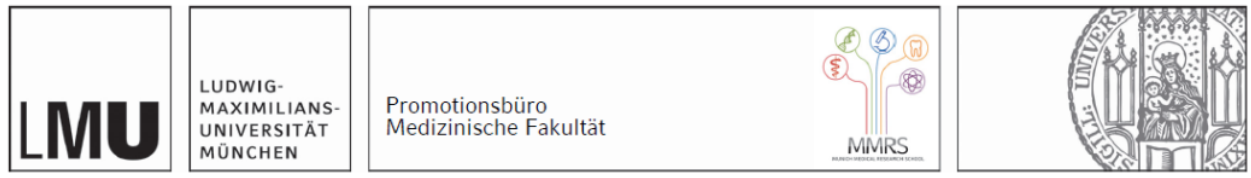

Affidavit

I hereby declare, that the submitted thesis entitled:

„Improving the sensitivity of *glioblastoma multiforme* derived cell lines to photodynamic therapy by inhibiting the ABCG2 transporter protein“

is my own work. I have only used the sources indicated and have not made unauthorized use of services of a third party. Where the work of others has been quoted or reproduced, the source is always given.

I further declare that the submitted thesis or parts thereof have not been presented as part of an examination degree to any other university.

Munich, 10.08.2022 Patricia Müller

…… ……..

place, date Signature doctoral candidate

Table of content

List of abbreviations

A

ABCB1	ATP-binding cassette subfamily B member 1
ABCB6	ATP-binding cassette subfamily B member 6
ABCG2	ATP-binding cassette subfamily G member 2
AKT	Serine/threonine kinase 1
ALAD	Delta-aminolevulinic acid dehydratase
ALAS	Delta-aminolevulinic synthase

B

BBB	Blood-brain barrier
BCRP	Breast cancer resistance protein

C

Ce6	Chlorin e6
CNS	Central nervous system
CSC	Cancer stem cell

E

EGFR	Epidermal growth factor receptor

F

FBS	Fetal bovine serum
FDA	Food and Drug Administration
FECH	Ferrochelatase
FGR	Fluorescence-guided resection

G

GBM	*Glioblastoma multiforme*
GSC	Glioma stem cells

H

HCP-1	Heme carrier protein-1
HGF	Hepatocyte growth factor
HIF	Hypoxia-inducible transcription factor

I

IDH	Isocitrate dehydrogenase
IGF	Insulin-like growth factor
iPDT	interstitial photodynamic therapy

M

MEK	Mitogen-activated protein kinase
MGMT	O^6-Methylguanine-DNA methyltransferase
MRI	Magnetic resonance imaging
mRNA	Messenger ribonucleic acid
mTOR	Mechanistic target of rapamycin
MTT	3-(4,5-Dimethylthiazol-2-yl)-2,5-diphenyl-2H-tetrazolium bromide

N

NADPH	Nicotinamide adenine dinucleotide phosphate
NFκB	Nuclear factor kappa-B

O

OS	Overall survival

P

PANC	Pancreatic cancer cell line
PBGD	Porphobilinogen synthase
PDD	Photodynamic diagnosis
PDGF	Platelet-derived growth factor

PDT	Photodynamic therapy
PEPT1/2	Peptide transporter 1/2
PFS	Progression free survival
PI3K	Phosphoinositide 3-kinase
PpIX	Protoporphyrin IX
PS	Photosensitizer
PTEN	Phosphatase and tensin homolog
P16	Cyclin dependent kinase inhibitor 2A

R

Ras	Rat sarcoma
Rb	Retinoblastoma
ROS	Reactive oxygen species

S

SP	Side population

T

TGF	Transforming growth factor
TMZ	Temozolomide
TP53	Tumor protein P53
TTFields	Tumor Treating Fields

V

VEGF	Vascular endothelial growth factor

W

WHO	World Health Organization

5-ALA	5-Aminolevulinic acid

List of publications

2018

Sara A. Abdel Gaber, Patricia Müller, Wolfgang Zimmermann, Dirk Hüttenberger, Rainer Wittig, Mahmoud H. Abdel Kader, Herbert Stepp. ABCG2-mediated suppression of chlorin e6 accumulation and photodynamic therapy efficiency in glioblastoma cell lines can be reversed by KO143. Journal of Photochemistry & Photobiology, B: Biology 2018;178:182-191.

2020

Patricia Müller, Sara A. Abdel Gaber, Wolfgang Zimmermann, Rainer Wittig, Herbert Stepp. ABCG2 influence on the efficiency of photodynamic therapy in glioblastoma cells. Journal of Photochemistry & Photobiology, B: Biology 2020;210:111963.

1. My contribution to the publications

1.1. Contribution to Paper I

I supported my colleague Dr. Sara Abdel Gabel during the implementation of the experiments published in “Sara A. Abdel Gaber, Patricia Müller, Wolfgang Zimmermann, Dirk Hüttenberger, Rainer Wittig, Mahmoud H. Abdel Kader, Herbert Stepp. ABCG2-mediated suppression of chlorin e6 accumulation and photodynamic therapy efficiency in glioblastoma cell lines can be reversed by KO143. Journal of Photochemistry & Photobiology, B: Biology 2018;178:182-191”. Particularly the investigations of the serum-dependent chlorin e6 efflux caused by the ABCG2 transporter were supported by me. Furthermore, we planned and worked together on the experiments comparing the ABCG2-mediated suppression of Ce6 and PpIX PDT efficacy.

1.2. Contribution to Paper II

I performed all the experiments together with statistical analysis shown in the graphs published in the paper “Patricia Müller, Sara A. Abdel Gaber, Wolfgang Zimmermann, Rainer Wittig, Herbert Stepp. ABCG2 influence on the efficiency of photodynamic therapy in glioblastoma cells. Journal of Photochemistry & Photobiology, B: Biology 2020;210:111963” with conceptual support from my supervisors. Furthermore, I wrote the Introduction, the Material and Methods and Results parts and was supported by my colleague Dr. Gaber with the Discussion section.

2. Introduction

2.1. Objective

Treatment of *glioblastoma multiforme* (GBM) with photodynamic therapy (PDT) is a new and encouraging therapy, but there are some obstacles that need to be resolved. The ATP-binding cassette superfamily G member 2 (ABCG2) is a transmembrane protein (Khot et al., 2020) which exports photosensitizers like protoporphyrin IX (PpIX) and chlorin e6 (Ce6) out of the cell, potentially reducing PDT efficiency. Therefore, the goals of this work were:

1. Analyze if high levels of ABCG2 in glioma cell lines turn off the ability of the cells to accumulate effectively phototoxic concentrations of PpIX or chlorin e6.
2. Examine if the inhibition of the ABCG2 protein function results in an increased accumulation of the photosensitizers PpIX and chlorin e6.
3. Investigate if blocking of ABCG2 increases the sensitivity of tumor cells to photodynamic therapy.
4. Figure out if cancer stem cells feature a higher resistance to PDT because of their elevated ABCG2 expression.

The main focus of my research was to increase photosensitizer accumulation by blocking the ABCG2 multidrug transporter and, therefore, improving PDT efficiency.

2.2. *Glioblastoma multiforme*: a fatal brain tumor

Diffuse gliomas are the most prevalent brain tumors in adults (14.5% of all CNS tumors) (Ostrom et al., 2020). They derive from glial cells, which consist of astrocytes, oligodendrocytes and microglia, and are usually responsible for providing protection as well as support for neurons in the brain. The World Health Organization (WHO) includes in their updated classification from 2016 the grade II and III astrocytomas, grade II and III oligodendrogliomas and high grade IV astrocytomas called *glioblastoma multiforme* (GBM) in this category (Onizuka et al., 2020) with GBM being the most common (57.7% of all gliomas) and aggressive primary malignant brain tumor in adults (Ostrom et al., 2020). Fifty percent of the patients with primary GBM show a clinical history of less than 3 months from first symptoms to diagnosis. They occur especially in elderly

patients and typically show some genetic alterations like EGFR overexpression, *PTEN* mutation or cyclin dependent kinase inhibitor 2A/p16 gene deletions. Secondary GBM arise from prior low-grade astrocytomas during a longer period in younger patients (Alifieris and Trafalis, 2015). They often contain *TP53* mutations. Although primary and secondary glioblastomas display some molecular differences, the current standard treatment is very similar (Kleihues and Ohgaki, 1999).

Symptoms of patients with GBM are connected to the function of the affected area and may include persistent headaches, vomiting, new onset of seizures, focal neurologic deficits, changes in personality, confusion or memory loss due to the tumor pressure on the brain or spinal cord (Davis, 2016). The incidence has raised marginally over the last 20 years mainly due to modernized diagnostic imaging equipment and longevity of people in developed countries. It occurs in 3.23 per 100.000 people in the United States. The median age at diagnosis is 65 years and it is 1.58 times more prevalent with men than with women. The five-year relative survival rate is 7.2% and the median survival regardless of the treatment is eight months (Ostrom et al., 2020). Apart from rare cases of genetic predisposition and exposure to irradiation, no risk factors could be verified (Le Rhun et al., 2019). Also, early detection of the tumor with diagnostic devices is difficult. Standard magnetic resonance imaging (MRI) is the most sensitive method for detecting GBM initially; but, as soon as the tumor can be identified via imaging, it is at an advanced state (Alexander and Cloughesy, 2017).

2.3. Therapeutic advances in the treatment of *glioblastoma multiforme*

Current standard of care comprises maximal safe resection of the tumor and subsequently treatment with adjuvant radiotherapy and chemotherapy with the alkylating agent temozolomide (TMZ) (Cramer and Chen, 2019). TMZ has an excellent permeability into the central nervous system (CNS) and 96-100% bioavailability (Alifieris and Trafalis, 2015). Radiotherapy in combination with concomitant and adjuvant TMZ results in a median overall survival (OS) of 14.6 months and a two-year survival rate of 26.5% (Stupp et al., 2005). Successful surgical debulking of the tumor is restricted by its invasive growth pattern and the impossibility to excise with a sufficient safety margin. Because of the early development of resistance and occurrence of side effects, chemo- and radiotherapy have also limited potency resulting in a high rate of relapses (Stepp and Stummer, 2018, Claes et al., 2007). 80% of recurrences are found in the region adjoining the resection cavity (Cramer and Chen, 2019). Once a relapse occurs, therapeutic options are limited. The causes of failure are still largely unknown, although many possible

obstacles for an effective treatment have been proposed. Consequently, new therapy approaches are urgently needed (Petrecca et al., 2013, Thon et al., 2019).

The molecular processes leading to GBM formation are still not fully understood, but there has been extensive research towards the molecular analysis of this tumor. Despite these efforts only a few molecular attributes, O^6-methylguanine-DNA methyltransferase (MGMT) promoter methylation and IDH1/2 mutation, are regarded clinically significant (Cloughesy et al., 2014, Weller et al., 2012). GBMs featuring IDH1 mutations have a more favorable prognosis and are more frequently found in secondary GBM (73%) but rarely in primary GBM (3.7%). Therefore, in clinical trials they are increasingly considered separately (Nobusawa et al., 2009). Methylation of the gene promotor encoding the DNA repair enzyme MGMT and concomitant silencing of the gene is important for a successful treatment with temozolomide. MGMT is a repair enzyme which removes alkyl groups from the O^6 position of guanine and, subsequently, antagonizing the genotoxic effects of alkylating drugs like TMZ. (Esteller et al., 2000). MGMT promoter methylation occurs in 45% of patients diagnosed with GBM and has become an important predictor for a favorable outcome in patients treated with alkylating agents. The overall survival (OS) of patients with a MGMT promoter methylation combined with chemotherapy with TMZ and radiotherapy was 21.7 months versus 12.7 months in patients with an unmethylated MGMT promoter (Hegi et al., 2005).

Several different therapeutic approaches have been investigated. Promising initial results have been reported 2015 in a study conducted by Stupp *et al*. There it was shown that by adding TTFields to the maintenance TMZ therapy the median progression-free survival could be prolonged from 4.0 to 7.1 months and overall survival could be extended from 15.6 months to 20.5 months in a medium follow-up of 38 months (Stupp et al., 2015). TTFields are a locoregionally delivered antimitotic therapy that intervenes with the division of cells and the assembly of cell compartments. During this treatment transducer arrays deliver low-intensity, intermediate-frequency (200 Hz), alternating electric fields. They are applied to the shaved scalp for not less than 18 hours a day and lead to a disruption of cell division (Kirson et al., 2007, Fonkem and Wong, 2012). Many clinical trials focus on glioblastoma-intrinsic targets to interfere with the oncogenic signaling pathways. The most relevant signaling pathways involved in GBM include, among others, tyrosine kinase receptor-triggered pathways (like EGF, PDGF, VEGF, HGF, TGF receptors) and their downstream signaling pathways RAS, mTOR, PI3K/PTEN/AKT, RB and TP53 (Crespo et al., 2015, Ohgaki et al., 2004). Unfortunately, until now, monotherapies interfering with these pathways show disappointing results (Sathornsumetee et al., 2007). There is a growing

interest in targeting the microenvironment of tumor cells comprising the monocyte/microglia/macrophage compartment, blood vessels or T cells (Le Rhun et al., 2019). A multitude of anti-angiogenic targeted therapies e.g. with bevacizumab have been evaluated in clinical trials as monotherapy or in combination with various additional agents, all with no significant overall survival benefit for patients with glioblastoma (Yang et al., 2017). Immune checkpoint inhibitors have been investigated clinically, but they seem to be less successful in the treatment of GBM compared to malignant melanomas or non-small-cell lung cancer (Lakin et al., 2017, Maxwell et al., 2017).

2.4. Photodynamic Therapy: An encouraging approach for treating *glioblastoma multiforme*

An encouraging strategy for the detection and treatment of GBM is the use of photodynamic diagnosis (PDD), fluorescence-guided resection (FGR) and photodynamic therapy (PDT). They are based on a two-step process consisting of administration of a photosensitizer and its activation by light at a particular wavelength which leads to emission of fluorescence at the tumor site. With an adequate intensity of light the following photochemical reaction is believed to generate reactive oxygen species (ROS) which elicit cell death. This process is named PDT (McNicholas et al., 2019).

During surgical debulking, FGR is used for a better visibility of the tumor margin. A phase III clinical trial conducted by Stummer *et al.* comparing 5-ALA PDD versus conventional microsurgery with white light for malignant gliomas showed that it considerably increased progression-free survival (difference between groups after a medium follow-up of 35.4 months for the 6 month progression free survival (PFS) was 19.9%) (Stummer et al., 2006), implying that 5-ALA PDD is an efficient method for the intra-operative diagnosis of GBM leading to enhanced safe resection. However, most patients recruited for that study still presented a progression of the disease, partly due to tumor cells that have infiltrated normal brain tissue or reside somewhere else as tumor-initiating cells in stem cell niches (Kawai et al., 2019, Stepp and Stummer, 2018).

The main principle of PDT is the highly selective photosensitizer accumulation in malignant cancer tissue (Kawai et al., 2019). It requires light, a photosensitizer and molecular oxygen. The photosensitizer is activated by exposure to light of a specific wavelength into an electronically excited state from which it either relaxes back to the ground state by generating heat or emitting

fluorescence, or it can switch to a metastable triplet state from which the energy can be transferred to molecular oxygen generating reactive oxygen species (ROS) like free radicals or singlet oxygen ($^1O_2$). In all cases, the photosensitizer has returned back to its ground state, ready to absorb more light and generate further ROS (Figure 1). PDT particularly damages tumor cells nearby the intracellular location of the photosensitizer while sparing neighboring normal tissue due to the short distance of migration for singlet oxygen (i.e. 0.02-1 μm) and its brief lifespan (i.e. 0.04-4 μs) (Mahmoudi et al., 2019). Cytotoxic ROS provoke tumor cell death via different mechanisms comprising damage of intracellular organelle membranes such as mitochondria, the endoplasmic reticulum and lysosomes (Khot et al., 2020, Cramer and Chen, 2019). PDT can kill tumor cells via three main types of cell death: apoptotic, necrotic and autophagy-associated cell death. The subcellular localization of the photosensitizer plays an important part in the dominating type of cell death as well as the light and drug dose used (Abrahamse and Hamblin, 2016). Cell necrosis is usually affiliated with damage occurring at higher PDT light doses leading to cell membrane disintegration, while apoptotic cell death is associated with lower doses of sensitizing drugs or light. Apoptosis may be associated with nuclear factor kappa-B (NFκB) damage in the cytoplasm as well as mitochondrial Bcl-2 photodamage and release of cytochrome c. Autophagy features a role in either enhancing or inhibiting cell death following PDT (Mroz et al., 2011). Additionally to its direct cytotoxic effects, PDT may also damage the microvasculature of the tumor by occlusion of blood vessels with the potential to induce local ischemia (Hirschberg et al., 2008). Furthermore, it can lead to immunogenic cell death inducing a host immune response against cancer via cytotoxic T cells (Castano et al., 2006).

The first approval of PDT which used the photosensitizer Photofrin was obtained in Canada 1993 for treating bladder cancer. The U.S. Food and Drug Administration (FDA) gave their first approval for advanced obstructive esophageal cancer in 1995 and for the treatment of early-stage non-small-cell lung cancer in 1998 (Gunaydin et al., 2021, Sheng et al., 2020). In Japan, the chlorin derived photosensitizer talaporfin sodium obtained approval for intra-operative PDT for malignant brain tumors in 2013 (Akimoto, 2016). More recently, the FDA approved 5-ALA for use as an intraoperative optical imaging agent for FGR in patients with gliomas in 2017 (FDA, 2018). In oncology, PDT is being proved clinically for treating cancers of the head and neck, skin, brain, lung, breast, intraperitoneal cavity, pancreas and prostate (Dolmans et al., 2003, Iyer et al., 2007).

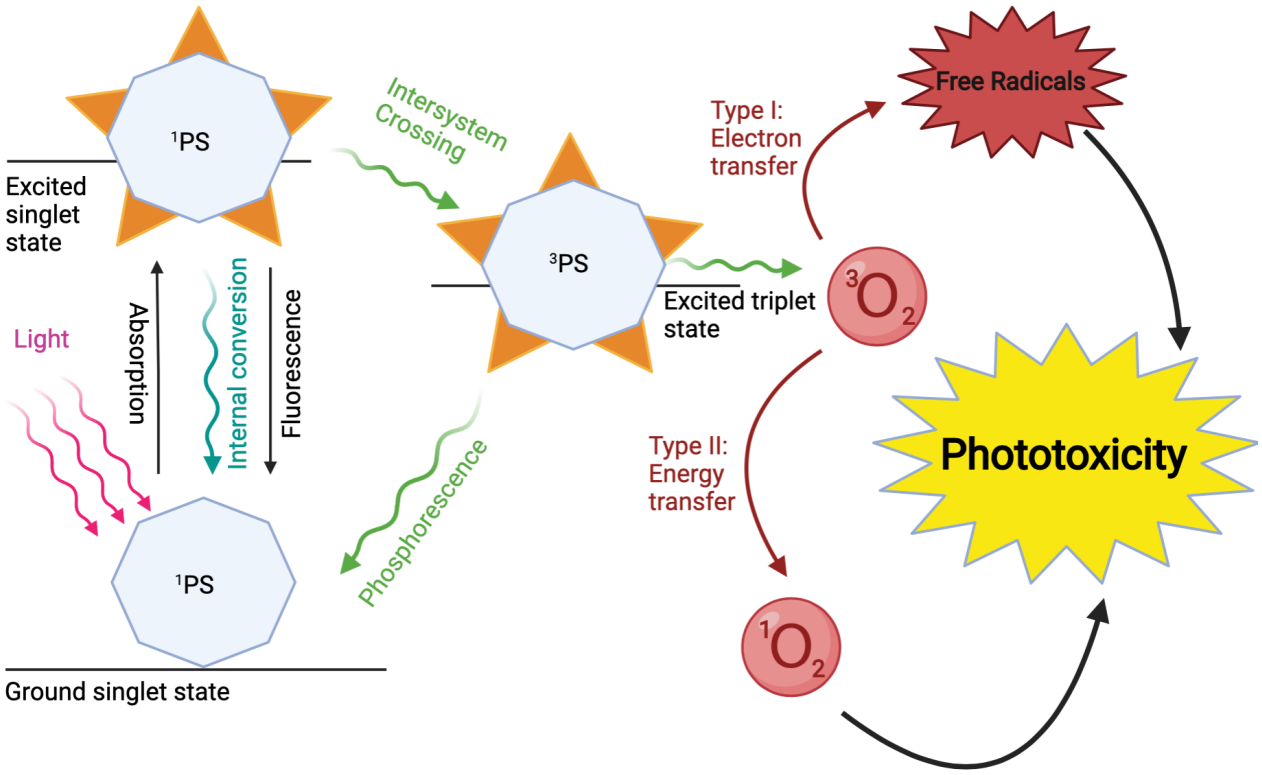

Figure 1: Principle of photodynamic therapy: When a photosensitizer (PS) molecule absorbs photon energy one of its outer electrons is excited from the ground singlet state to an excited singlet state. From there, it either relaxes to the ground state by excitation of vibration (thermal relaxation) or emission of a fluorescence photon, or it undergoes intersystem crossing to an excited triplet state which can generate reactive oxygen species (ROS) via a type I reaction (formation of free radicals) or a type II reaction (formation of singlet oxygen). These reactions ultimately lead to phototoxicity. ((Sai et al., 2021), modified)

In GBM, immediately after having completed FGR, the application of PDT to the resection cavity can minimize the risk of a local relapse (Vermandel et al., 2021). It can even completely replace surgery by using a stereotactic approach. Interstitial PDT (iPDT) is based on the oral administration of a photosensitizer or a photosensitizer precursor followed by a stereotactic insertion of fiber optic diffusers into the tumor to deliver visible light irradiation to the tumor mass (Stepp and Stummer, 2018, Cramer and Chen, 2019). One safety issue is the possible induction of edema which, when reaching functional brain tissue, can lead to neurological deficits. However, in most cases the edema resolves within a few days by application of steroids (Mathews et al., 2011).

2.5. Photosensitizers for photodynamic therapy

The optimal photosensitizer for utilization in malignant tissue must have a highly favorable safety profile and should preferentially accumulate in high concentrations in tumor cells. First generation photosensitizer Photofrin® was the first PDT agent that was approved by the FDA for obstructive esophageal cancer in 1995 (FDA, 2011). Despite Photofrin® was widely utilized in the treatment of different cancers, its clinical use was limited by its side effect profile, especially the prolonged skin photosensitization and low tissue penetration. Therefore, investigations of other photosensitizers were needed. Second generation photosensitizers have a better specified chemical composition compared to first generation photosensitizers and comprise a broad spectrum of drugs like porphyrins (e.g. 5-ALA-derived), chlorins (e.g. chlorin e6) or pheophorbides (Zhang et al., 2018).

Chlorin e6 (Ce6) is a well-studied preformed photosensitizer which is administrated exogenously. It is associated with being highly efficient in the generation and activation of singlet oxygen by light with wavelengths in the far-red spectral range which is suitable for deep penetration into tissue. Ce6 absorbs at a wavelength of 664 nm offering an enhanced light penetration into brain tumor tissue in comparison to photosensitizers such as Photofrin (630 nm) or 5-ALA-based PpIX (633-635 nm) (Abdel Gaber et al., 2018). In a clinical study implemented by Sheleg *et al.* PDT with Ce6 showed an effective response in the treatment of patients with melanoma skin metastases and was also well tolerated (Sheleg et al., 2004). For glioma cells, Ce6 has only been used so far in a rat C6 glioma model where it induced coagulation necrosis and apoptosis (Namatame et al., 2008).

Among the commercially available photosensitizers**,** 5-ALA acts as a photosensitizer precursor and is metabolized endogenously to the fluorescent and phototoxic protoporphyrin IX (PpIX) (Stepp and Stummer, 2018). In mammals, it is the first compound during porphyrin biosynthesis and the immediate precursor of heme in the heme synthesis pathway. Physiologically, 5-ALA is produced by the enzyme ALA synthase (ALAS) from succinyl-coenzyme A and glycine inside the mitochondria and gets exported to the cytoplasm thereafter. Externally applied 5-ALA is transported inside the cytoplasm via passive diffusion through the cell membrane or by active transport by different transporters including the amino acid transporters PEPT1 and PEPT2 (Figure 2). There, synthesis of the intermediate coproporphyrinogen III takes place and subsequently its transport from the cytoplasm into the mitochondria by the ATP-binding cassette transporter ABCB6 (Kawai et al., 2019). In the mitochondria, coproporphyrinogen III is converted

to the photosensitizer PpIX which is finally converted to heme by the enzyme ferrochelatase via insertion of Fe^{2+} into the porphyrin ring (Kobuchi et al., 2012, Layer et al., 2010). Under normal conditions 5-ALA synthesis is inhibited by high levels of free heme but when applied systemically, the negative feedback mechanism that heme exerts on the enzyme ALA synthase is bypassed, thereby catalyzing the natural production of 5-ALA which temporarily boosts PpIX generation (Collaud et al., 2004).

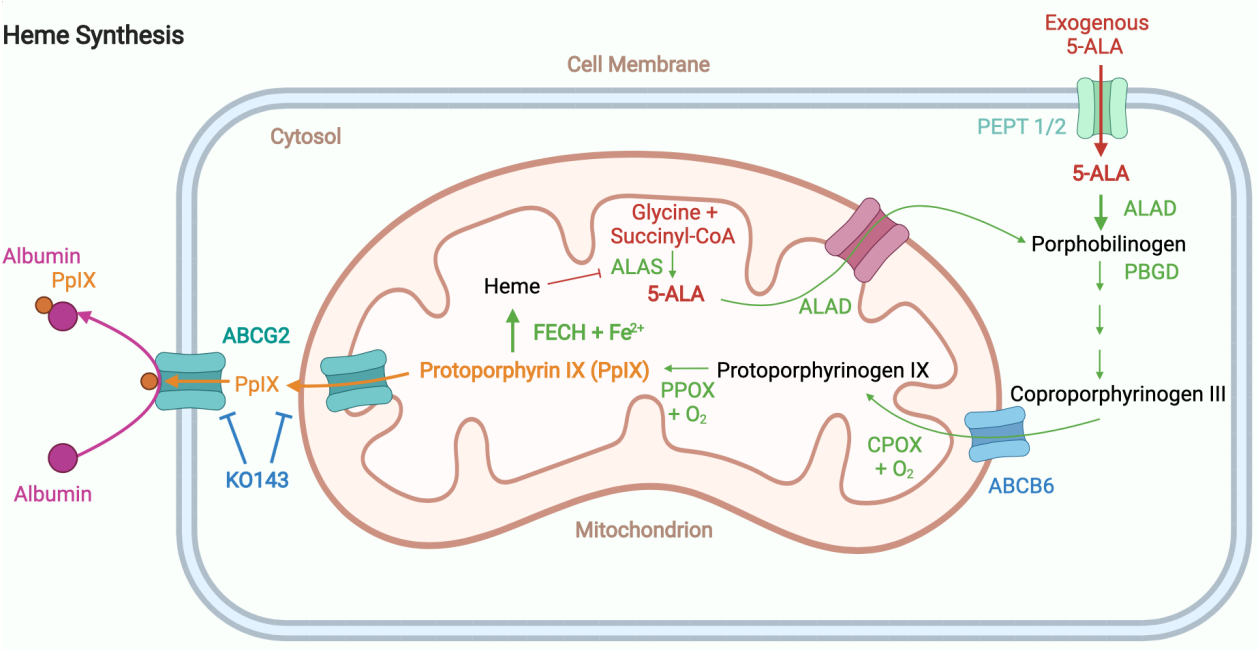

Figure 2. Role of mitochondrial ABCG2 in the regulation of ALA-mediated PpIX accumulation in cancer cells. The arrows in green represent product conversions, orange arrows preferred transport directions across cell or mitochondrial membranes of heme biosynthetic building blocks and red arrows inhibiting pathways. 5-ALA: 5-aminolevulinic acid, PEPT 1/2: oligopeptide transporter 1/2; ABCG2: ABC transporter G2, ABCB6: ABC transporter B6, FECH: ferrochelatase, PpIX: protoporphyrin IX, CPOX: coproporphyrinogen oxidase, ALAD: ALA-dehydrogenase, PBGD: porphobilinogen deaminase, PPOX: protoporphyrinogen oxidase, ALAS: ALA synthase. ((Kobuchi et al., 2012), modified)

When PpIX is excited with red light at a wavelength of 635 nm it transfers the energy from light to oxygen, thereby generating reactive singlet oxygen which is cytotoxic and can damage or kill tumor cells (Stepp and Stummer, 2018) (Figure 1). Clinically, for FGR or PDT of GBM, 5-ALA (Gliolan®, ALAGLIO®, medac GmbH, Wedel, Germany) is dissolved in 50 ml of drinking water with a concentration of 20 mg/kg body weight and applied orally three to four hours before anesthesia begins (EMA, 2007). By using a non-fluorescent precursor, a higher fluorescence contrast can be obtained, because it avoids unspecific fluorescence background from the circulation or interstitial space (Stepp and Stummer, 2018). Investigations of the therapeutic safety

and efficiency of 5-ALA-induced PpIX showed an acceptable risk profile at a promising outcome in clinical trials on PDT of GBM (Johansson et al., 2013, Lietke et al., 2021).

2.6. Selective PpIX accumulation in tumor cells

The selective PpIX accumulation in brain tumor tissue depends on several factors. Normally, 5-ALA cannot pass the blood-brain-barrier (BBB), but gliomas induce the growth of neo-blood vessels leading to a deficit of the BBB morphology and function, therefore, molecules might be able to leak through these vessels (Ennis et al., 2003). Furthermore, the PpIX accumulation rates in tumor tissue can be increased by an upregulated expression of PEPT1 and PEPT2 transporters which are essential for 5-ALA uptake (Hagiya et al., 2013, Zimmermann and Stan, 2010). Increased levels of PEPT1 mRNA could be observed in renal cell carcinoma cells (da Rocha Filho et al., 2015), non-small cell lung cancer cell lines (Omoto et al., 2019) and bladder cancer tissue (Hagiya et al., 2013). Moreover, enhanced transport of coproporphyrinogen III due to increased expression of its transport protein ABCB6 has been observed to correlate positively with accumulation of PpIX in murine erythroleukemia cells (Krishnamurthy et al., 2006) and in human glioma cells (U251, T98, U87) (Zhao et al., 2013). Another significant step is the conversion from PpIX to heme by the enzyme ferrochelatase (FECH) by inserting ferrous iron (Fe^{2+}) into the PpIX molecule and thereby disabling both, fluorescence and phototoxicity (Stepp and Stummer, 2018, Ohgari et al., 2005). In glioblastoma cells (Teng et al., 2011), colon cancer tissue (Kemmner et al., 2008), bladder cancer tissue (Hagiya et al., 2013) and renal cell carcinoma cells (da Rocha Filho et al., 2015) the expression of the FECH mRNA is decreased resulting in preferred PpIX accumulation in these cancerous cells with respect to surrounding normal tissue. The tumor specific down-regulation of FECH could partially be caused by the indirect influence of tumor suppressor proteins on the FECH activity (Sawamoto et al., 2013, Stepp and Stummer, 2018). Moreover, the expression of the enzymes ALA-dehydrogenase (ALAD) and porphobilinogen deaminase (PBGD), which also play a part in the heme synthesis pathway, are elevated in breast cancer tissue (Navone et al., 1990) resulting in increased biosynthesis of PpIX (Yang et al., 2015).

Various studies have been conducted aiming to increase PpIX accumulation. Co-incubating human urothelial carcinoma cells (Inoue et al., 2009), rat glioma stem cells (C6) (Wang et al., 2017) and squamous carcinoma cells (Anayo et al., 2018) with 5-ALA and iron chelators resulted in a low availability of iron, which is necessary for converting PpIX to heme, and therefore increased the PpIX concentration. Another study conducted by Fisher *et al.* showed that

hypothermia during 5-ALA incubation leads to a tumor cell selective enhancement in the median mitochondrial accumulation of PpIX in different glioma cell lines like U251 and U87 cells. Neuroprotective effects of the normal brain against PDT could be observed when applied *in vivo*. Possible underlying reasons for this observation have been reported to comprise reduction of metabolic activities and stabilization of high-energy phosphate molecules. The increased mitochondrial PpIX content observed under these conditions indicates a double benefit of hypothermia: protection of neurons and improved PDT (Fisher et al., 2013, Fisher et al., 2017, Yenari and Han, 2012). It has also been observed that low levels of the cofactor NADPH, which is needed to break down heme into bilirubin by the enzyme heme oxygenase, correlates with PpIX accumulation in glioma cells. Compared to their wildtype counterparts, IDH1-mutant human glioma cells (U87) exhibiting lower levels of NADPH indeed showed a stronger fluorescence following incubation with 5-ALA (Kim et al., 2015, McNicholas et al., 2019).

Another observation is that hypoxia is a frequent characteristic of the tumor microenvironment leading to higher concentrations of hypoxia-inducible transcription factors (HIF) which alter some 5-ALA-based PDT-relevant pathways including heme synthesis. They induce the expression of FECH (Liu et al., 2004) and heme oxygenase (Lee et al., 1997) leading to an increased conversion of PpIX to heme in gastric cancer cells (Otsuka et al., 2015). Approaches which target HIF and improve tumor oxygenation are potentially enhancing 5-ALA-induced fluorescence and PDT efficiency. Additionally, pretreatment of cells with calcitriol (Chen et al., 2014), methotrexate (Sinha et al., 2006, Anand et al., 2009) or 5-fluorouracil (Maytin et al., 2018) leads to an upregulation of coproporphyrinogen oxidase (CPOX) resulting in increased PpIX concentrations.

The selective PpIX accumulation is a major advantage of 5-ALA compared to other photosensitizers. A protein that correlated with decreased PpIX accumulation is the ABCG2 transporter (Kawai et al., 2019, Kobuchi et al., 2012). Inhibiting the activity of ABCG2 elevated PpIX accumulation in triple negative breast cancer cells (Palasuberniam et al., 2015), in lung adenocarcinoma cells (Kobuchi et al., 2012) and glioblastoma cells (U251) (Abdel Gaber et al., 2018, Muller et al., 2020), thus, it represents another important target to enhance PpIX accumulation in brain tumors.

2.7. Overcoming ABCG2-mediated resistance to PDT

The ABCG2 transporter, also called breast cancer resistance protein (BCRP), is primarily found in the cell membrane and inner mitochondrial membrane (see Figure 2). It transports various endogenous and exogenous drugs like doxorubicin, methotrexate or mitoxantrone (Natarajan et al., 2012) out of the cell. This transporter is physiologically expressed in the placenta, where it protects the fetus from xenobiotics in the maternal blood (Mao, 2008). It also occurs in the BBB (Nicolazzo and Katneni, 2009), the apical membrane of intestinal, liver and kidney cells as well as in the blood-testis barrier (Vlaming et al., 2009). Moreover, ABCG2 is overexpressed in cancer stem cells, where it can efflux xenobiotics or photosensitizers out of the cell which reduces chemotherapy sensitivity and PDT toxicity, therefore limiting the efficacy of this treatments (Muller et al., Ding et al., 2010). Thus, the ABCG2 transporter is mediating multidrug resistance and treatment failure in cancers. Numerous investigations have been performed in an attempt to reverse this drug resistance caused by cancer stem cells and improve chemosensitivity (Zhou et al., 2021).

ABCG2 can be effectively blocked by various agents like the fungal toxin fumitremorgin C and its nontoxic analog KO143, specific antibodies or receptor tyrosine kinase inhibitors (Sun et al., 2013, Robey et al., 2011, Abdel Gaber et al., 2018). Some of these inhibitors can also block ABCG2 located on the inner mitochondrial membrane, where 5-ALA-based PDT is thought to be most effective in destructing tumor cells (Kobuchi et al., 2012). Clinically approved ABCG2 inhibitors are receptor tyrosine kinase inhibitors such as gefitinib, sorafenib and imatinib (Sun et al., 2013). In a clinical setting, administrating an ABCG2 blocker prior to PDT treatment may be an effective way to enhance the therapeutic result. Most studies were done *in vitro* investigations, therefore, more *in vivo* studies need to be conducted.

A lot of different studies have been performed trying to enhance PDT efficiency by downregulating or blocking the ABCG2 protein. Some studies revealed that ABCG2 mediates the reduction of ROS toxicity by hindering the NFκB pathway which aids PDT by stimulating an immune response and mediating oxidative stress. Inhibition of ABCG2 activity usually increases generation of ROS in the context of PDT, although identification of the exact molecular pathways requires further exploration (Nie et al., 2018, Khot et al., 2020).

A study conducted by Kurokawa *et al.* showed that hyperthermia (1 hour at 42ºC) can enhance PDT by downregulating ABCG2 and upregulating heme carrier protein-1 (HCP-1) (Kurokawa et

al., 2019). Some studies investigated the impact of cell culturing medium containing fetal bovine serum (FBS) on ABCG2 activity. Ogino *et al.* showed that T24 urothelial carcinoma cells incubated with 5-ALA with or without FBS showed significantly higher PpIX levels in the FBS-free medium. A 5-ALA dose- and time-dependent PpIX accumulation could be detected as well as higher extracellular levels of PpIX when FBS was present in the medium indicating that PpIX export by ABCG2 in T24 cells is dependent on serum concentration (Ogino et al., 2011) (see Figure 2).

In vitro studies where breast cancer cells were cultured under chronic glucose deprivation by adding glycolysis inhibitors after 5-ALA incubation showed a potentiated PpIX accumulation and 5-ALA-based PDT cytotoxicity (Wyld et al., 2002, Golding et al., 2013). Inhibition of glycolysis led to nutrient stress in the cancer cells by depleting ATP levels which also led to an inactivation of ABC transporters (Nakano et al., 2011). These studies propose that targeting glucose metabolism can potentially improve 5-ALA-mediated PDT.

Moreover, Yoshioka *et al.* demonstrated that PpIX fluorescence in cancer cells incubated with 5-ALA can be boosted by inhibiting one of the Ras downstream signaling elements, the Ras/mitogen-activated protein kinase (MEK). Inhibition of MEK decreased PpIX efflux from malignant cells by reducing the expression level of ATP-binding cassette subfamily B member 1 (ABCB1) transporter. Additionally, MEK inhibition reduced the FECH activity, the enzyme which is responsible for the conversion of PpIX to heme (Yoshioka et al., 2018, Chelakkot et al., 2019, Muller et al., 2020).

2.8. Are glioma stem cells causing failure of PDT?

A small subpopulation of cancer cells called side population (SP) cells have a lot of features separating them from mature, differentiated cells. They express organ-specific surface markers like CD44 or CD133 (Brown et al., 2017) and show an upregulation of ABC transporters (Begicevic and Falasca, 2017). SP cells can be isolated from cancer cells via flow cytometry by staining with Hoechst 33342 or rhodamine 123 dye (Bertoncello and Williams, 2004), which are substrates of the ABCG2 transporter, therefore, these cells show a lower fluorescence compared to non-SP tumor cells, because the dye is effluxed by this transporter. SP cells could be identified in glioblastoma cell lines (U87) and various other cancer cell lines (Hirschmann-Jax et al., 2004) and are expected to comprise the cancer stem cells (CSC) of the tissue. It could be shown that rat glioma C6 SP cells can produce both SP and non-SP cells in culture as well as neurons and glial

cells. Therefore, they are mainly accountable for the *in vivo* malignancy of this cell line (Kondo et al., 2004).

CSC are associated with high tumorigenicity, capacity of self-renewal, ability to differentiate, high stem cell marker expression (Clarke et al., 2006) as well as chemo- and radiotherapy resistance. They show several known molecular mechanisms contributing to the improved survival like expression of anti-apoptosis proteins, a dormant state, an active DNA repair capacity or high expression of ABC transporters (Hirohashi et al., 2016, Dean et al., 2005) for creating an optimal microenvironment for survival. Glioma stem cells (GSC) can stimulate angiogenesis via production of VEGF and differentiation into pericytes (Cheng et al., 2013). They can be a helpful target for immunotherapy or inhibition of significant pathways. Focusing on stem cell signaling pathways is an emerging research area that already presents some auspicious results.

Furthermore, expression of ABCG2 is affiliated with stem cell-like characteristics of glioblastoma tumor cells and is assumed to be responsible for chemotherapy resistance. Moreover, ABCG2 expression leads to lower PpIX levels, therefore, such cells require higher PpIX levels or light doses to be killed (Abdel Gaber et al., 2018). In vitro studies showed that main population-derived cells accumulated significantly more 5-ALA-derived PpIX than SP-defined C6 glioma CSCs (Wang et al., 2017). It has also been observed that ABCG2 expression correlated inversely with the PpIX fluorescence in pancreatic cancer cell lines (PANC-1). The cells with the highest ABCG2 expression level and lowest PpIX fluorescence rate showed a high ability for sphere forming and tumor formation suggesting that cell lines with a high ABCG2 expression are enriched with CSCs and exhibit a low PpIX content, but PpIX fluorescence could be increased by ABCG2 inhibition (Kawai et al., 2019).

More obstacles supporting potential PDT failure is variability in the light and drug dose-dependent tumor cell sensitivity. Inside viable GBM tumor tissue PpIX and Ce6 rates can differ widely due to the heterogeneity of the tumor. Moreover, its infiltrative growth pattern causes an insufficient distribution of the photosensitizer or light leading to an inadequate tumor cell destruction (Johansson et al., 2010, Eleouet et al., 2000, Stepp and Stummer, 2018). For the commonly used wavelength of 635 nm, light penetration depths in various types of tissue have been described to be limited to a distance between 1-5 mm (Quirk et al., 2015). Additionally, it has been described that an unspecific PpIX accumulation also occurs in endothelial cells leading to the formation of edema caused by phototoxicity if PDT is applied (Ito et al., 2005).

With the ambition to improve outcomes of PDT with patients suffering from GBM the main focus of this work lies in the relationship between ABCG2 expression and Chlorin e6-/5-ALA-based PDT efficiency in U251 und U87 glioblastoma derived cell lines. We largely excluded the influence of parameters beside ABCG2 by using a glioblastoma cell model with a switchable ABCG2 expression vector to answer the main question: Can PDT efficiency be improved by blocking the ABCG2 transporter and, therefore, increase photosensitizer accumulation?

3. Summary

Photodynamic therapy (PDT) with 5-aminolevulinic acid (5-ALA) or chlorin e6 (Ce6) is an encouraging new therapeutic procedure for the treatment of malignant brain tumors. 5-ALA is a natural precursor of protoporphyrin IX (PpIX), a potent mitochondrially assembled photosensitizer, which accumulates tumor-selectively following systemic delivery of 5-ALA, while Ce6 can be administered directly. The ATP-binding cassette transporter ABCG2 acts as a physiologically substantial player in porphyrin and chlorin efflux from cells. ABCG2 is also linked with stemness attributes. In this work, we examine the impact of ABCG2 on the sensitivity of glioblastoma cells to 5-ALA- and Ce6-based PDT.

We have used the U251MG glioblastoma cell line with controllable ABCG2 expression (sU251MG-V with doxycycline-inducible ABCG2 overexpression; control cells U251MG-EV containing the empty expression vector). Cells containing the vector expressed slightly more surface ABCG2 than the empty vector cells ("leakiness" of the vector). For both photosensitizers we observed an increasing cellular accumulation based on fluorescence measurements at higher concentrations as well as a light fluence- and Ce6-/PpIX-concentration-dependent PDT phototoxicity. Although induction of ABCG2 led to a strong increase of ABCG2 expression on the cell surface and, therefore, reduced the fluorescence and phototoxicity significantly in cells with high ABCG2 expression, intracellular PpIX levels dropped only modestly compared to empty vector cells, even though a more pronounced decrease might have been assumed. In cells incubated with Ce6 two major peaks identifying the accumulating photosensitizer could be detected in ABCG2-expressing cells indicating two cell populations with low and high expression of the transgene whereas only one major peak was observed in the empty vector cells. By blocking the cells with the ABCG2 inhibitor KO143 a further enhanced PpIX fluorescence could be detected in both cell types, indicating an expression of some endogenous ABCG2 in the empty vector cells. The leakiness of the vector already led to a substantial decrease of the PpIX content and phototoxicity, despite only a small rise of ABCG2 expression on the plasma membrane could be observed. ABCG2 inhibition by tyrosine kinase inhibitor sorafenib and a blocking anti-ABCG2 antibody led to an increase of the Ce6-mediated fluorescence, whereas no significant effect on the PpIX fluorescence was exerted. This difference could be due to the ability of KO143 to block not only the cell surface ABCG2, but also the mitochondrial ABCG2.

Incubation with fetal calf serum (FCS) protein decreased the intracellular Ce6 and PpIX accumulation. This demonstrates that ABCG2-mediated efflux is facilitated by FCS. Indeed, when the cells were treated with the ABCG2 inhibitor KO143 throughout the efflux period, the efflux was almost always lowered to the same level as observed in the absence of FCS. The reliance of efflux kinetics on FCS was more pronounced during incubation with 5-ALA than with Ce6. Another discrepancy is the ongoing increase of PpIX concentration in serum-free medium which can be explained by the continuous synthesis of PpIX from 5-ALA at minimal PpIX efflux.

In U87 glioblastoma cells derived from spheres, expression of ABCG2 was enhanced and Ce6 accumulation and phototoxicity reduced compared to adherent monolayer U87 cells. This indicates that expression of ABCG2 is correlated with stem-like features in the GBM-derived cell line U87 and is assumed to be accountable for PDT resistance due to decreased accumulation of the photosensitizer.

In conclusion, the experiments showed that stemness-associated expression of ABCG2 causes a decreased Ce6 and PpIX accumulation and an accordingly reduced photosensitivity of this glioblastoma cell line. For 5-ALA-PDT, the degree of phototoxicity corresponded well with the PpIX level, but to a smaller extent with the measured ABCG2 expression. The induction of the vector resulted in a pronounced ABCG2 signal increase, whereas the enhancement of survival after PDT was rather modest. Inhibiting ABCG2 with KO143 more than restored the photosensitivity for 5-ALA-PDT. When Ce6 was used as a photosensitizer, KO143-induced decrease of survival was much less distinctive. An obvious explanation for this interesting finding is the suspected location of ABCG2 in the mitochondrial membrane in addition to the cell membrane, where it affects the PpIX accumulation but has no influence on the chlorin e6 content.

Combining Ce6- or 5-ALA-based PDT with an ABCG2-inhibitor might be an encouraging approach to destruct glioblastoma stem cells in the future.

4. Zusammenfassung

Photodynamische Therapie (PDT) mit 5-Aminolävulinsäure (5-ALA) oder Chlorin e6 (Ce6) ist ein vielversprechender neuer Therapieansatz bei der Behandlung maligner Hirntumore. 5-ALA ist ein natürlicher Vorläufer von Protoporphyrin IX (PpIX), einem potenten im Mitochondrium produziertem Photosensibilisator, welcher nach systemischer Applikation von 5-ALA tumorselektiv akkumuliert, während Ce6 direkt verabreicht werden kann. Das ATP-bindende Transporterprotein ABCG2 spielt eine physiologisch bedeutsame Rolle beim Porphyrin- und Chlorin-Efflux aus Zellen. Weiterhin werden Stammzelleigenschaften mit ABCG2 assoziiert. In dieser Forschungsarbeit untersuchen wir die Rolle von ABCG2 auf die Empfindlichkeit von Glioblastomzellen gegenüber 5-ALA- und Ce6-basierter PDT.

Wir verwendeten die Glioblastomzelllinie U251MG mit kontrollierbarer ABCG2-Expression (sU251MG-V mit Doxycyclin-induzierbarer ABCG2-Überexpression; Kontrollzellen U251MG-EV mit leerem Expressionsvektor). Zellen, die den Vektor enthielten, exprimierten etwas mehr ABCG2 auf der Oberfläche als die Leervektorzellen („Undichtigkeit“ des Vektors). Für beide Photosensibilisatoren beobachteten wir eine zunehmende zelluläre Akkumulation gemessen anhand ihrer Fluoreszenz bei steigenden Dosierungen sowie eine licht- als auch Ce6-/PpIX-konzentrationsabhängige Phototoxizität gegenüber der PDT. Obwohl die ABCG2-Induktion das ABCG2 auf der Zellmembran drastisch erhöhte und demnach die Fluoreszenz und Phototoxizität in den ABCG2-überexprimierenden Zellen signifikant reduzierte, war die Reduktion von intrazellulärem PpIX im Vergleich zu den Leervektorzellen eher moderat, obwohl man eine viel stärkere Reduktion erwartet hätte. In mit Ce6 inkubierten Zellen konnten zwei Fluoreszenzpeaks während der Akkumulation des Photosensibilisators in ABCG2-exprimierenden Zellen nachgewiesen werden, was auf zwei Zellpopulationen mit niedriger und hoher Expression des Transgens hinweist, während nur ein Hauptpeak in den Leervektorzellen beobachtet wurde. Durch Blockung der Zellen mit dem ABCG2-Inhibitor KO143 konnte für beide Zelltypen eine, über das Ausgangsniveau hinaus, gesteigerte PpIX-Fluoreszenz detektiert werden, woraus sich eine endogene ABCG2-Expression der Leervektorzellen ableiten lässt. Die bereits durch den nicht-induzierten ABCG2-Vektor leicht erhöhte Expression von ABCG2 auf der Zellmembran führte bereits zu einer erheblichen Reduzierung der PpIX-Spiegel und zu verminderter Phototoxizität. ABCG2-Hemmung mit dem Tyrosinkinaseinhibitor Sorafenib und einem blockierenden ABCG2-Antikörper führte zu einer gesteigerten Ce6-vermittelten Fluoreszenz, während keine signifikante PpIX-Erhöhung in mit 5-ALA inkubierten Zellen detektiert werden konnte. Dieser Unterschied

könnte darauf beruhen, dass KO143 nicht nur das ABCG2 auf der Zelloberfläche blockiert, sondern auch das mitochondriale ABCG2.

Inkubation mit fetalem Kälberserum (FCS) verminderte die intrazelluläre Akkumulation von Ce6 und PpIX. Dies weist auf einen FCS-unterstützten ABCG2-vermittelten Efflux hin. Bei Koinkubation mit KO143 während der Effluxperiode reduzierte sich der Efflux auf das Niveau, welches auch ohne FCS erreicht wurde. Die Abhängigkeit der Effluxkinetik von FCS war ausgeprägter, wenn Zellen mit 5-ALA inkubiert wurden als mit Ce6. Ein weiterer Unterschied ist der progrediente PpIX-Anstieg in serumfreiem Medium, offenbar aufgrund der anhaltenden PpIX-Synthese aus 5-ALA bei minimalem PpIX-Efflux.

In U87-Glioblastomzellen, welche aus Tumorzellspheres stammten, war die ABCG2-Expression erhöht und die Ce6-Akkumulation sowie die Phototoxizität im Vergleich zu der adhärenten U87-Monolayer-Zellkultur reduziert. Dies deutet darauf hin, dass die ABCG2-Expression mit stammzellähnlichen Eigenschaften in der Glioblastomzelllinie U87 assoziiert ist und vermutlich für die Resistenz gegenüber der PDT aufgrund einer verringerten Akkumulation des Photosensibilisators verantwortlich ist.

Zusammenfassend zeigten die Experimente deutlich, dass die stammzellassoziierte ABCG2-Expression zu einer verminderten Akkumulation der Photosensibilisatoren Ce6 und PpIX und einer entsprechend verringerten Photosensitivität in dieser Glioblastomzellpopulation führt. Die observierte Phototoxizität korrespondierte mit dem PpIX-Gehalt für 5-ALA-PDT, verhielt sich jedoch in geringerem Maße kongruent zu dem beobachteten Niveau der ABCG2-Expression. Die Induktion des Vektors führte zu einem sehr ausgeprägten ABCG2-Signal, während die Steigerung der Überlebensrate nach PDT eher moderat war. Eine Hemmung von ABCG2 durch KO143 stellte die Lichtempfindlichkeit für 5-ALA-PDT wieder her. Bei Verwendung von Ce6 als Photosensibilisator war die Abnahme der Überlebensrate, die auch durch KO143 induziert werden konnte, weitaus geringer. Dies könnte daran liegen, dass ABCG2 vermutlich neben der Zellmembran auch in der Mitochondrienmembran lokalisiert ist, wo es die PpIX-Akkumulation, jedoch nicht den Ce6-Gehalt beeinflusst.

Eine Kombination von Ce6- oder PpIX-basierter PDT mit einem ABCG2-Inhibitor könnte in Zukunft eine vielversprechende Methode sein, Glioblastomstammzellen zu zerstören.

Journal of Photochemistry & Photobiology, B: Biology 178 (2018) 182–191

Contents lists available at ScienceDirect

Journal of Photochemistry & Photobiology, B: Biology

journal homepage: www.elsevier.com/locate/jphotobiol

ABCG2-mediated suppression of chlorin e6 accumulation and photodynamic therapy efficiency in glioblastoma cell lines can be reversed by KO143

Sara A. Abdel Gaber[a,b,*], Patricia Müller[a,f], Wolfgang Zimmermann[c,f], Dirk Hüttenberger[d], Rainer Wittig[e], Mahmoud H. Abdel Kader[b], Herbert Stepp[a,f]

[a] Laser-Forschungslabor, LIFE-Zentrum, Klinikum der Universität München, Feodor-Lynen-Str. 19, 81377 München, Germany
[b] Pharmaceutical Biology Department, Photochemistry and Photodynamic Therapy Research Group, German University in Cairo, 5th settlement, 11835, New Cairo, Egypt
[c] Labor für Tumorimmunologie, LIFE-Zentrum, Klinikum der Universität München, Feodor-Lynen-Str. 19, 81377 München, Germany
[d] Apocare Pharma GmbH, Hauptstrasse 198, 33647 Bielefeld,Germany
[e] Institut für Lasertechnologien in der Medizin und Messtechnik an der Universität Ulm, Helmholtzstr. 12, 89081 Ulm, Germany
[f] Urologische Klinik, Klinikum der Universität München, Marchioninistr. 15, 81377 München, Germany

ARTICLE INFO

Keywords:
Photodynamic therapy
Chlorin e6
ABCG2
Glioblastoma
Cancer stem cells

ABSTRACT

Background: Photodynamic therapy (PDT) of malignant brain tumors is a promising adjunct to standard treatment, especially if tumor stem cells thought to be responsible for tumor progression and therapy resistance were also susceptible to this kind of treatment. However, some photosensitizers have been reported to be substrates of ABCG2, one of the membrane transporters mediating resistance to chemotherapy. Here we investigate, whether inhibition of ABCG2 can restore sensitivity to photosensitizer chlorin e6-mediated PDT.

Methods: Accumulation of chlorin e6 in wild type U87 and doxycycline-inducible U251 glioblastoma cells with or without induction of ABCG2 expression or ABCG2 inhibition by KO143 was analyzed using flow cytometry. In U251 cells, ABCG2 was inducible by doxycycline after stable transfection with a tet-on expression plasmid. Tumor sphere cultivation under low attachment conditions was used to enrich for cells with stem cell-like properties. PDT was done on monolayer cell cultures by irradiation with laser light at 665 nm.

Results: Elevated levels of ABCG2 in U87 cells grown as tumor spheres or in U251 cells after ABCG2 induction led to a 6-fold lower accumulation of chlorin e6 and the light dose needed to reduce cell viability by 50% (LD50) was 2.5 to 4-fold higher. Both accumulation and PDT response can be restored by KO143, an efficient non-toxic inhibitor of ABCG2.

Conclusion: Glioblastoma stem cells might escape phototoxic destruction by ABCG2-mediated reduction of photosensitizer accumulation. Inhibition of ABCG2 during photosensitizer accumulation and irradiation promises to restore full susceptibility of this crucial tumor cell population to photodynamic treatment.

1. Introduction

Despite multimodal and aggressive treatment, glioblastoma multiforme (GBM) remains connected with a dismal prognosis. Median survival of < 15 months and two year survival of 26.5% result from state of the art surgery and radiochemotherapy [1]. Among the plethora of experimental treatment options tried in case of recurrence, PDT with different photosensitizers has a long standing history. Initially, mostly Photofrin was used as a photosensitizer [2] and long-term survivors were occasionally reported [3]. The side-effect profile with this photosensitizer, however, significantly increased with increasing light dose [4]. Therefore, the investigation of other photosensitizers for PDT of GBM, such as 5-ALA induced PpIX [5] or Chlorin e6 [6] is highly warranted.

One of the open questions is, whether drug resistance mediated by drug efflux transporters, especially expressed in cancer stem cells [7], is also a critical issue with photosensitizers. In GBM, a cell population, over-expressing membrane transporter ABCG2 and other stem cell markers is made responsible for escaping chemotherapy and to cause recurrence [8,9]. Some photosensitizers are known substrates of ABCG2 and, therefore, stem cells the critical cell population of glioblastoma might therefore be resistant to PDT [10].

Chlorin e6 (Ce6) has so far been reported in clinical applications only for some derivatives, called Talaporfin (Laserphyrin, NPe6, LS11,

* Corresponding author at: Pharmaceutical Biology Department, Photochemistry and Photodynamic Therapy Research Group, German University in Cairo, 5th settlement, 11835 New Cairo, Egypt.
E-mail address: sara.abdel-gaber@guc.edu.eg (S.A. Abdel Gaber).

https://doi.org/10.1016/j.jphotobiol.2017.10.035
Received 8 July 2017; Received in revised form 26 October 2017; Accepted 28 October 2017
Available online 28 October 2017
1011-1344/

MACE (mono-(L)-aspartyl chlorin e6), ME2906, Aptocine, Litx) [6,11], SnCe6, Photolon [12], Radachlorin [13] or Photoditazin. But the pure trisodium salt of chlorin e6 is as well highly active [14,15] and is currently used in clinical trials [16]. In Japan, Talaporfin is approved for PDT of glioblastoma [6,17,18]. The absorption wavelength of Ce6 of 664 nm offers an improved light penetration into brain tumor tissue compared to photosensitizers such as Photofrin (630 nm) or 5-ALA-based PpIX (633–635 nm).

Little is known about the interaction of Ce6 with the membrane transporter ABCG2. Robey et al. [10] reported on Ce6 being a substrate of ABCG2 and correspondingly, PDT sensitivity was decreased in ABCG2-overexpressing cells. However, possible measures to inhibit ABCG2 were only investigated with regard to cellular fluorescence, but not with regard to consequences for PDT efficiency. Similarly, Gonzalez-Lobato et al. [19] used Ce6 as a reporter of ABCG2 activity and found that fumitremorgin C (FTC) blocks Ce6 transport by ABCG2. However, the consequences for PDT efficiency were not investigated.

Here, we report on the differential accumulation of Ce6 in U87 and U251 glioblastoma cell lines, where the U251 cell line was transfected with either an empty vector (U251-EV) or an inducible vector coding for human ABCG2 (U251-V). U87 cells were also grown as tumor spheres with the aim to increase the fraction of stem-like cells and to explore, whether Ce6 accumulation is different under these conditions. We also investigated the PDT efficiency and the effect of blocking ABCG2 by KO143 and sorafenib.

2. Materials and Methods

2.1. Cell Lines and Cell Culture

The human glioblastoma cell line U87MG was obtained from the Institut für angewandte Zellkultur, Dr. Toni Lindl GmbH (Munich, Germany). U251MG-L106 is a genetically engineered subclone of U251MG cells containing a single Flp recombinase target (FRT) site [20] which was kindly provided by the Genome & Proteome Core Facility of the German Cancer Research Centre (Heidelberg, Germany). U251MG-L106 was utilized for site-specific integration of a vector for doxycycline (Dox)-inducible expression of ABCG2 (resulting in U251-V) and the corresponding empty control vector (resulting in the isogenic control clone U251-EV), respectively. Cells were cultured in complete DMEM medium supplied with 10% fetal calf serum (FCS, Biochrom AG, Berlin, Germany), 100 U/ml penicillin, 100 µg/ml streptomycin, 100 µM non-essential amino acids and 1 mM sodium pyruvate (GIBCO/Invitrogen, Karlsruhe, Germany) at 37 °C with 5% CO_2 in a humidified atmosphere. U251MG-L106 transfectants were routinely maintained in the presence of 150 µg/ml hygromycin (Sigma-Aldrich Chemie, Munich, Germany).

2.2. Sphere Formation

Cells were grown as spheres in 75 cm^2 ultra-low attachment flasks (Corning Costar, Amsterdam, Netherlands) at a density of 120 cells/10 ml and cultured for 5 days. Medium consisted of serum free DMEM F-12 supplemented with 2% (*v*/v) B27 (Invitrogen, Life Technologies GmbH, Darmstadt, Germany), 0.08% (w/v) basic fibroblast growth factor and 0.08% (w/v) epidermal growth factor (Sigma-Aldrich Chemie, Munich, Germany). Spheres consisting of > 10 cells were counted using an inverted microscope (Leica DMIL, Wetzlar, Germany). For experiments, cells were dissociated from the spheres using Biotase (GIBCO/Invitrogen, Karlsruhe, Germany) and cells were cultured in tissue culture plates.

2.3. Flow Cytometry

Cells were washed with pre-warmed phosphate-buffered saline (PBS) and incubated for 15 min in the incubator with 1 × trypsin (Lonza Rockland Inc., USA) in PBS to allow cell detachment or sphere dissociation. Trypsinization was stopped by the addition of complete medium and cells were collected by centrifugation for 5 min at 251 × *g*/1500 rpm. Non-specific binding was blocked by incubating the cells for 20 min at 37 °C in blocking buffer (0.5% human serum albumin in PBS). For quantitation of ABCG2 expression, cells were incubated for 1 h at room temperature with 2–4 µg/ml of mouse monoclonal anti-ABCG2 antibody 5D3 (Santa Cruz Biotechnology, USA) diluted with binding buffer (2% human serum albumin in PBS). Cells were washed with PBS three times to remove excess antibody. As a negative control an isotype matched control antibody (normal mouse $IgG2_b$, Santa Cruz Biotechnology, Heidelberg, Germany) was used. Cells were then incubated for 30 min with 10 µg/ml goat anti-mouse polyclonal antibodies conjugated with fluorescein isothiocyanate (FITC; Dianova, Hamburg, Germany) and diluted with binding buffer at room temperature in the dark. Finally cells were washed once with PBS, placed on ice and fluorescence was measured using a FACSCalibur flow cytometer (BD Biosciences, Heidelberg, Germany) with an excitation wavelength of 488 nm and fluorescence detection with filter 2. A minimum of 3 × 10^4 viable cell events were recorded per sample. BD CellQuest™ software (version 4.0.2) was used for data acquisition and data were processed using FlowJo software (version 8.8.6; Tree Star, Ashland, Oregon, USA). For discrimination of live/dead cells, 7-aminoactinomycin D (7-AAD) or propidium iodide (BD Biosciences, Heidelberg, Germany) was used.

2.4. Photosensitizer Generation and Loading

Tumor cells (6 × 10^4 per well) were plated in 24-well plates (Nunc GmbH, Wiesbaden, Germany) and grown over night in DMEM with 10% FCS or for 72 h in the same medium supplemented with 1 ng/ml doxycycline to induce ABCG2 expression. Cells were washed with FCS- and phenol red-free DMEM. The cells were incubated in FCS- and phenol red-free medium with 5–160 µM Ce6 (Apocare Pharma, Bielefeld, Germany) for 4–12 h. To assess the effect of FCS on uptake, DMEM was either serum-free or supplied with 2% or 10% FCS. The influence of FCS on Ce6 loss from cells was tested by incubation of the cells after washing with serum-free medium in medium with 0%, 2% or 10% FCS for 1–16 h. To evaluate the influence of ABCG2 on Ce6 accumulation, U251-V cells with or without induction of ABCG2 expression by doxycycline were incubated with Ce6 in the presence or absence of the ABCG2 inhibitors KO143 (1.5 µM; Sigma-Aldrich Chemie, Munich, Germany), sorafenib (3.2 µM; LC Laboratories, Woburn, USA) or the anti-ABCG2 antibody 5D3 (2 µg/ml). U251-EV cells were treated the same way as a control. To compare the results obtained with an exogenously added photosensitizer with the endogenously generated photosensitizer protoporphyrin IX (PpIX) in some experiments Ce6 was replaced by the precursor 5-aminolevulinic acid (5-ALA; 200 µg/ml; Medac GmbH, Hamburg, Germany) for 12 h. 5-ALA stock solutions (1 mg/ml) were freshly prepared in PBS and the pH was adjusted to 7. After photosensitizer accumulation, the medium was replaced with ice cold PBS and cells were collected by incubation with trypsin as described above. The pellet was resuspended in 0.5 ml cold PBS and fluorescence of 50,000 cells was detected by flow cytometry using an excitation wavelength of 630 nm and detection in the FL3 photomultiplier tube (670 nm long pass filter) for PPIX and FL6 photomultiplier tube for Ce6. The median of cell fluorescence was used after subtraction of the median of the fluorescence of unlabeled cells as a measure of Ce6 or PpIX content in the tumor cells. In all experiments with sensitized cells, care was taken to minimize exposure of the cells to ambient light.

2.5. PDT Treatment

Cells were plated at a density of 1 × 10^4 per well in flat bottom 96-well plates (Nunc GmbH, Wiesbaden, Germany) in 6 replicates per data

point and grown for 6–8 h in medium with 10% FCS. Sensitization of the cells with 5 or 10 μM Ce6 with or without 1.5 μM KO143 was performed for 4 h in 100 μl of fresh medium with 2% FCS. The medium was replaced with 100 μl of medium without phenol red (Invitrogen/Gibco, Karlsruhe, Germany) containing supplements and 2% serum as listed above. At the end of the incubation period, cells were gently washed with pre-warmed PBS and supplied with serum free DMEM medium without phenol red. Irradiation took place using a 670 nm diode laser light (CeramOptec GmbH, Bonn, Germany) delivered by a 600 μm fiber with an attached microlens (Biolitec AG, Jena, Germany) adjusted to 50 mW/cm^2 in a light tight box with a 37 °C warm plate. After irradiation with a series of light doses (0.5–8 J/cm^2), cells were incubated in 10% FCS-containing DMEM medium for 4 h at 37 °C in the incubator. For each experiment, a dark control was included in which cells were incubated with Ce6, but not irradiated. Moreover, light only controls were included in which cells were irradiated with the highest tested light dose without prior Ce6 sensitization.

2.6. Cell Viability Assay

After PDT, cell viability was quantified using the MTT assay following the instructions of the manufacturer (Sigma-Aldrich Chemie, Munich, Germany). In brief, 20 μl of 3-(4,5-dimethylthiazol-2-yl)-2,5-diphenyltetrazolium bromide (MTT) solution (5 mg/ml PBS) was added to 100 μl medium and left in the incubator for 4 h. Crystals were dissolved in 20% SDS overnight at 37 °C in the incubator and absorbance was measured at 560 nm using a FLUOstar OPTIMA microplate reader (BMG LABTECH, Jena, Germany). The absorbance of cell-free medium was also measured and referred to as blank. Viability was calculated by subtracting the blank values from the obtained reading for treated cells and results were expressed as % of the control cells.

2.7. Statistics

The number of experimental replicates is indicated in the figure legends. Significance levels (P) were calculated using Two-way ANOVA in the GraphPad Prism3 software package. Comparisons of samples exhibiting P values < 0.05 were considered to be significantly different.

3. Results

3.1. ABCG2 Expression in Inducible U251-V Cells

Cells were stained with the fluorescently labeled specific ABCG2 antibody 5D3 [21] for ABCG2 expression quantification (Fig. 1). Flow cytometry findings revealed low, but detectable surface expression of ABCG2 in the absence of the inducer doxycycline (Dox) in both U251-EV and U251-V cells, as apparent by a comparison to fluorescence intensities measured for the isotype control stained negative control cell population. Induction with Dox at concentrations of 1 ng/ml or more induced ABCG2 expression in U251-V in a manner that produced a broad distribution of fluorescence intensities in the histogram. Particularly, ABCG2 induction using 10,000 ng/ml Dox indicated three distinct cell populations with low, medium and high expression of induced ABCG2, as designated 1, 2 and 3, respectively, in Fig. 1a. The maximum of the first peak in this histogram is shifted approximately 50 fluorescence units compared to non-induced cells (Fig. 1a). The position of the peaks is the same for 1 ng/ml and 10,000 ng/ml Dox with a shift of the relative contribution of populations with higher ABCG2 expression, which is responsible for the increase in geometric mean values with increasing Dox concentration. 1 ng/ml was used in further experiments to induce ABCG2 in U251-V cells. U251-EV cells with or without 1 ng/ml Dox showed only one peak (not shown) and the same mean ABCG2 surface expression as the non-induced U251-V cells (Fig. 1b), most probably representing basic surface expression originating from endogenous ABCG2.

3.2. ABCG2-Mediated Ce6 Efflux Capacity is Saturable, Sensitive to Serum Concentration and can be Inhibited by KO143

3.2.1. Dose-Response and Inhibition Analyses, Effects of Serum

To investigate whether and to which extent the intracellular accumulation of Ce6 depends on ABCG2 expression and activity, we investigated Ce6-mediated fluorescence in Dox-treated U251-V vs. isogenic U251-EV cells at different concentrations of the photosensitizer, as well as in presence vs. absence of KO143, a specific ABCG2 inhibitor [22] As expected, flow cytometric analyses revealed two major peaks of Ce6-mediated fluorescence in ABCG2 expressing U251-V cells, which most probably correspond to the previously identified cell populations with high and low expression of the transgene, respectively. The peak representing cells with less Ce6 will be referred to as “weakly fluorescent cells” and the other one as “strongly fluorescent cells”. The number of weakly fluorescent cells was sensitive to both increasing extracellular Ce6 concentration and the presence of KO143, indicating both efflux capacity saturation and KO143-mediated inhibition of ABCG2-mediated efflux (Fig. 2a). In contrast, U251-EV cells revealed one major peak at a high fluorescence intensity, irrespective of the Ce6 concentration.

It has been described that the presence of serum protein has an activating effect on ABCG2-mediated drug efflux via translocation of the protein to the cytoplasmic membrane [23]. We tested the impact of serum protein on Ce6 accumulation in Dox-induced U251-V cells via flow cytometry. As expected, we found a decrease in both mean fluorescence intensities (Fig. 2b), as well as in the relative number of strongly fluorescent cells (Fig. 2c) with increasing serum concentrations during Ce6 incubation. Interestingly, uninduced U251-V cells revealed a stronger decrease in Ce6 accumulation with increasing serum protein when compared to isogenic U251-EV control cells under identical treatment conditions (Fig. 2d). These findings indicate enhanced Ce6 efflux capacities of U251-V, which may be a result of leaky expression of the transgene in the absence of Dox.

3.2.2. Serum Protein Increases ABCG2-Mediated Ce6 Efflux

We wanted to verify that reduced Ce6-mediated intracellular fluorescence is not solely caused by molecular interaction of the photosensitizer with serum protein (which may reduce the effective concentration within the culture medium). In other words, we wanted to investigate whether a response to serum protein-mediated cell signaling does indeed play an important role. Thus, we temporally decoupled Ce6- from serum treatment. Dox-induced U251-V were incubated with 40 μM Ce6 for 5 h in serum free medium and subsequently kept in Ce6-free but 0%, 2% or 10% FCS-containing medium for up to 16 h (Fig. 3). The Ce6 levels in the cells were determined by flow cytometry. Two peaks were seen in the histograms directly at the end of the incubation period. The relative distribution of the cells in either peak containing weakly or strongly fluorescent cells was affected by both the FCS concentration and the length of the post-incubation period. The percentage of cells in the peak containing strongly fluorescent cells continuously decreased with the increase in FCS concentration and longer post-incubation periods, indicating FCS-supported, ABCG2-mediated efflux.

The influence of endogenous ABCG2 on intracellular Ce6 efflux was further studied in U251-EV cells. Cells were incubated for either 5 or 12 h with either 40 or 160 μM Ce6 in serum free medium and the efflux was investigated as described for U251-V cells. The cellular Ce6 fluorescence decreased over time by 25 to 75% (Fig. 4). The higher the FCS concentration in the medium, the faster was the Ce6 efflux. After the shorter (5 h) incubation period, the efflux started with a considerable delay, especially when there was no FCS in the medium. When KO143 was present during the efflux period, the efflux was most of the time reduced to the level obtained without FCS.

3.2.3. PpIX Efflux

In order to put these results in context with the kinetics of other photosensitizers, U251-EV cells were also incubated with 5-ALA

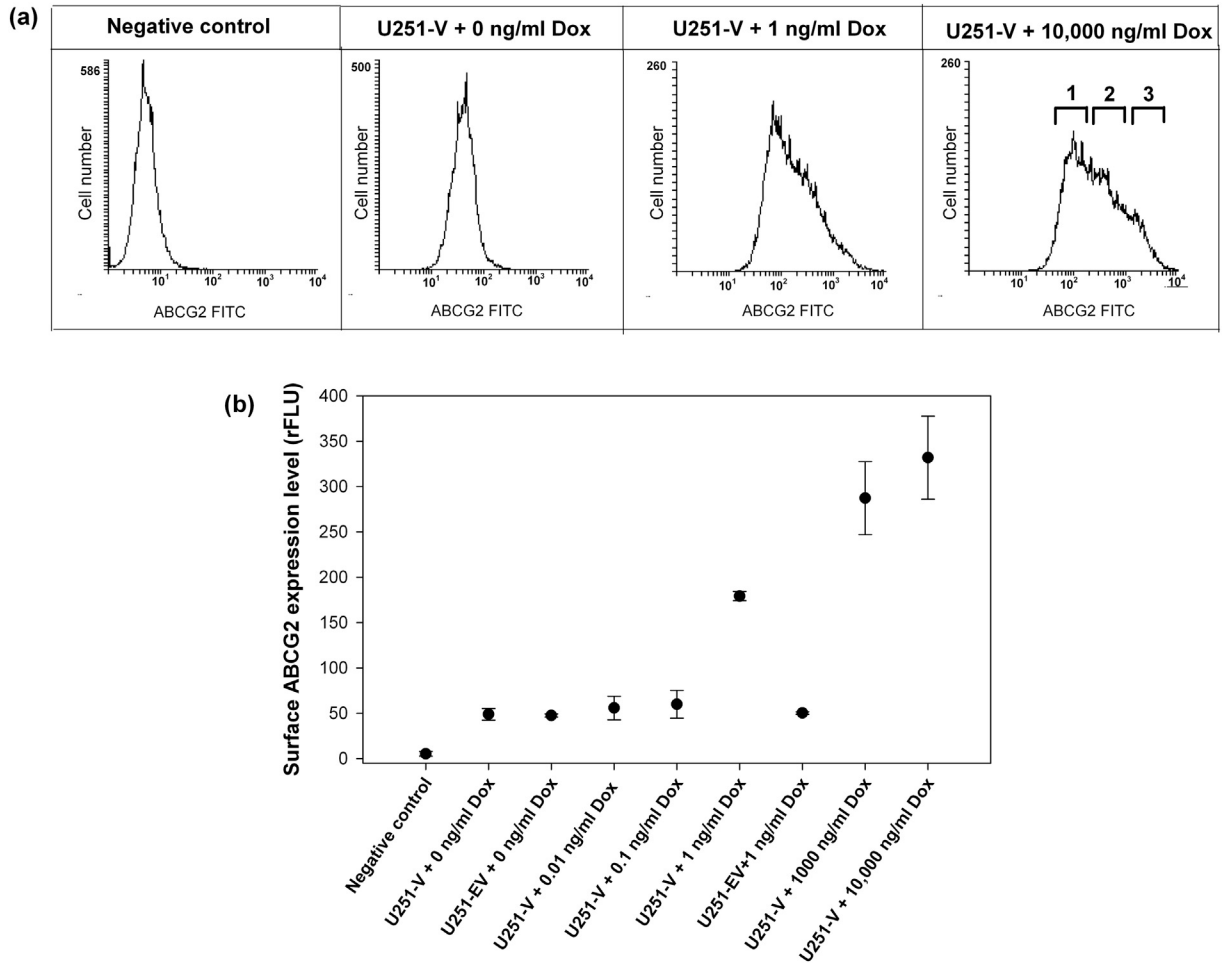

Fig. 1. ABCG2 induction by doxycycline: a) ABCG2 expression after incubating U251-V cells for 72 h with different doxycycline (Dox) concentrations as determined by flow cytometry. b) Dependence of cell surface ABCG2 protein expression on Dox concentration after incubation for 72 h for both U251-V and U251-EV cells. Shown is the average and standard deviation of errors for geometrical means of flow cytometry measurements (n = 3). U251-V, ABCG2 expression vector; U251-EV, empty vector.

(1.2 mM for 12 h without FCS). Fig. 5 shows the course of PpIX fluorescence, when the cells were then kept in medium without 5-ALA and 0%, 2% or 10% FCS respectively.

The dependence of efflux kinetics on FCS is more pronounced than with Ce6. A 50% decrease in PpIX concentration was observed after only 1 h in medium containing 10% FCS (Fig. 5). For cells incubated with Ce6 for 12 h, it required 4 h when Ce6 concentration was 40 μM and 8 h when the concentration was 160 μM to reach the same decrease in intracellular photosensitizer levels. A striking difference is also the further increase of sensitizer concentration in serum-free medium, obviously due to ongoing PpIX synthesis from 5-ALA at minimum PpIX efflux.

3.2.4. Inhibtion of Ce6 Efflux by Anti-ABCG2 Antibody and Sorafenib

Our results indicate an efficient inhibition of ABCG2-mediated efflux of Ce6 by KO143. To further assess the inhibiting activity of KO143, we compared it to inhibition mediated by i) the specific monoclonal ABCG2 antibody 5D3, and ii) the multikinase inhibitor sorafenib [24]. Similar to treatment with KO143, treatment with either 5D3 or sorafenib led to a single peak histogram in the flow cytometry analysis of Dox-treated U251-V cells (histograms not shown). But whereas KO143 and 5D restored Ce6 accumulation completely, sorafenib was not as efficient, leading to approx. 75% of Ce6-mediated fluorescence when compared to the inhibitor-free control. There was no significant difference between pre-incubating the cells with the inhibitor and co-incubating the inhibitor along with Ce6 (Fig. 6).

3.3. PDT Efficiency is Reduced by ABCG2 Expression

Irradiation of monolayer U251-V cells led to a light fluence- and Ce6 concentration-dependent phototoxicity. ABCG2 induction led to a significantly reduced phototoxicity as compared to non-induced cells or induced cells, which were co-incubated with KO143 (Fig. 7). The slightly higher response of KO143-treated induced cells as compared to the non-induced cells was not statistically significant. KO143 co-incubation showed a significant effect on phototoxicity only after ABCG2 induction.

3.4. Cancer Stem Cells are More Resistant to PDT due to High ABCG2 Levels

After 3 days of spheres cultivation, three dimensional cell structures could be seen (Fig. 8a). For U87 cells originating from spheres, ABCG2 expression as determined by flow cytometry was increased 2.1-fold (standard error: 0.14, $n = 2$) compared to adherent U87 cells grown as monolayers (Fig. 8b) and Ce6 accumulation in the monolayer cells grown after sphere dissociation was reduced to 16.9% (standard error: 0.015%, $n = 2$) (Fig. 8c).

Ce6-sensitized U87 cells in adherent monolayer cell culture exhibited a stronger phototoxicity than U87 cells grown in adherent monolayer after sphere dissociation. The light dose values to achieve 50% cell death were approximately 0.5 and 2 J/cm^2, respectively (Fig. 8d).

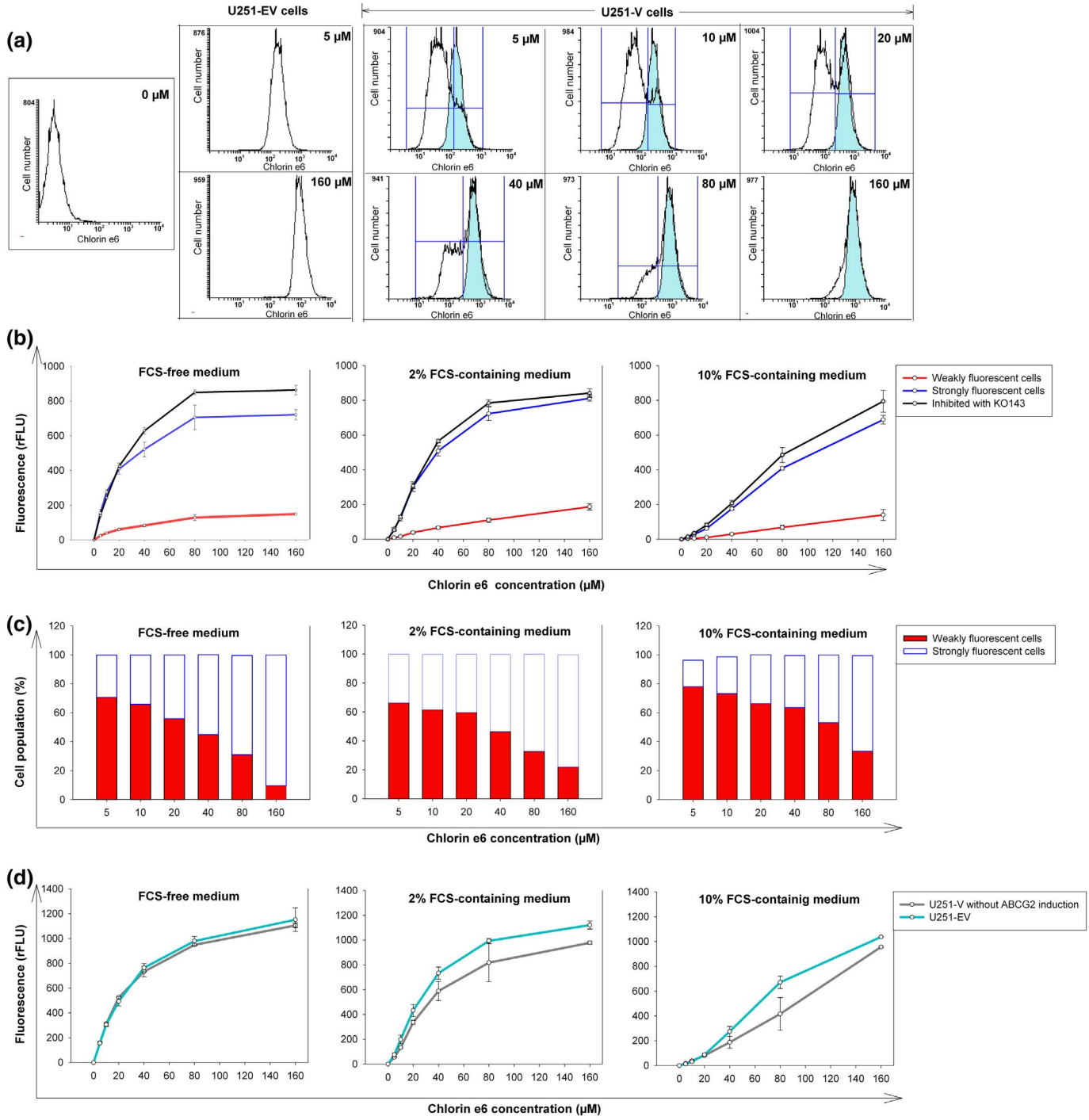

Fig. 2. Concentration and serum dependence of Ce6 uptake: a) Histograms of Ce6 uptake after incubation of U251-EV and ABCG2-induced U251-V cells for 4 h with the indicated concentrations of Ce6 in serum free medium without (white area) or with co-incubation of 1.5 µM KO143 (filled area overlay). b) Intracellular Ce6 levels as measured from FACS histograms without or with 2% or 10% FCS in the incubation medium (n = 3). Ce6 concentration-dependent geometrical mean intensities of weakly fluorescent and strongly fluorescent cells, as well as of the histograms of cells co-incubated with KO143 (n = 3; rFLU, relative Fluorescence Units). c) Relative contribution (area under curve) of the weakly fluorescent and of the strongly fluorescent cells. d) Comparison of U251-EV and U251-V cells without ABCG2 induction with respect to their uptake of Ce6 after 4 h incubation in serum free, 2% or 10% FCS-containing medium (n = 3). s for geometrical means of flow cytometry measurements (n = 3). U251-V, ABCG2 expression vector; U251-EV, empty vector.

4. Discussion

ABCG2 expression is associated with stem-like properties in GBM and is thought to be responsible for resistance to chemotherapy [25,26]. Photodynamic therapy of GBM may also be of limited effectiveness, if GBM stem-like cells accumulate less photosensitizer due to their high levels of ABCG2 and thus may survive light irradiation. On the other hand, ABCG2 activity can be blocked by a series of drugs, some of them being in clinical use, such as sorafenib [27]. For the purpose of improving the susceptibility of GBM stem-like cells to PDT, such ABCG2 inhibition needs to be performed only for a couple of hours thus limiting potential side effects. Overall side effects of such drugs will thus be considerably reduced compared to any combination with chemotherapy, which has to be applied for weeks or months.

We have used two different cell lines of glioblastoma origin with controllable ABCG2 expression and investigated the corresponding

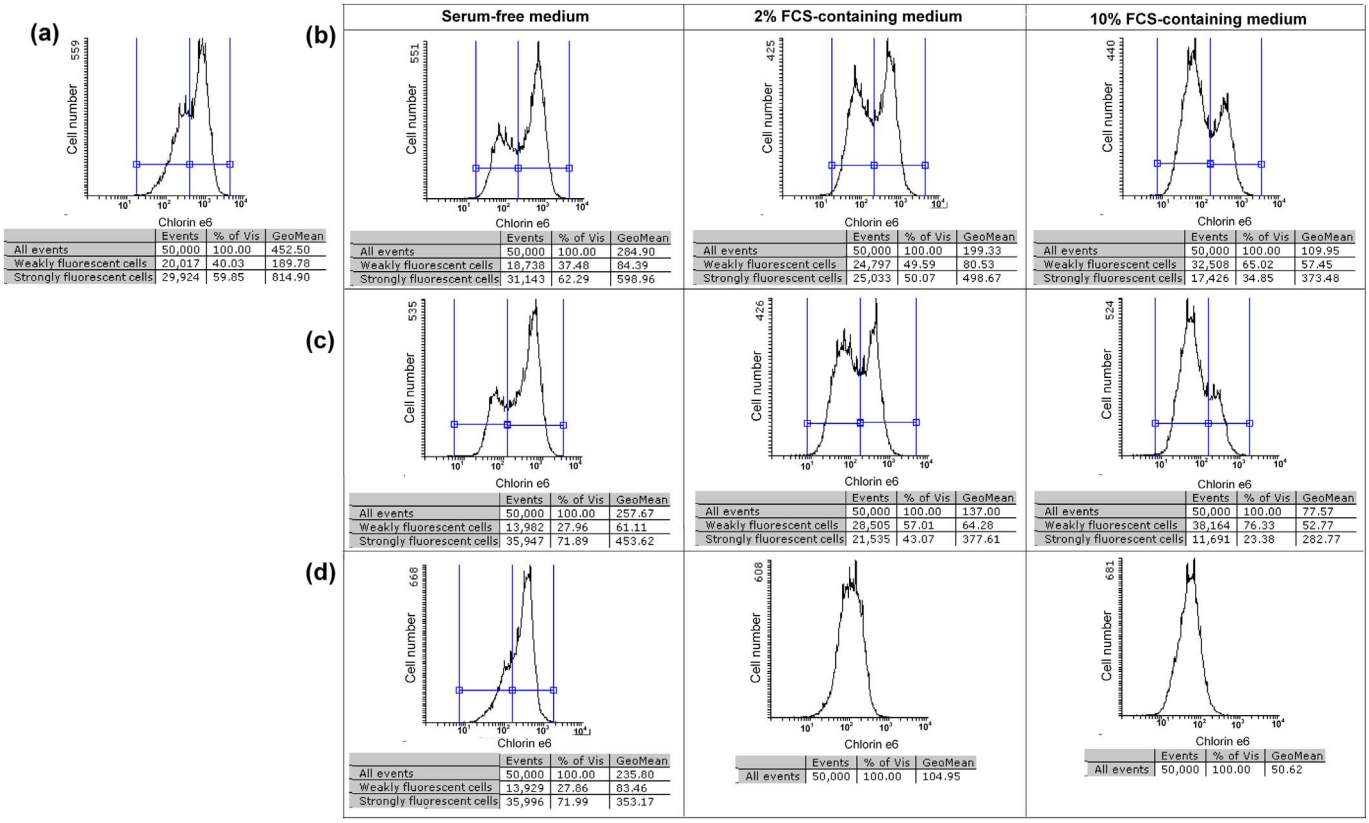

Fig. 3. Ce6 efflux dynamics depends on FCS concentration: Ce6 efflux of Dox-induced U251-V cells incubated for 5 h with 40 μM Ce6 in serum-free medium. Shown are histograms along with cell percentage of each peak and respective geometric means directly at the end of the 5 h incubation (a) and 2 h (b), 4 h (c) and 16 h (d) after Ce6 removal in presence of different FCS concentrations. One representative experiment is shown (n = 2).

consequences for Ce6 accumulation and phototoxicity. We have also studied the influence of the presence of serum proteins on the accumulation of the photosensitizer and the efficiency of ABCG2 sensitizer export.

U251 cells had been genetically engineered for doxycycline–inducible expression of ABCG2 (U251-V) and a corresponding isogenic empty vector control cell line (U251-EV), respectively. As expected, U251-EV cells did not express more ABCG2 when induced by Dox, while U251-V cells did. However, both cell lines do contain a certain level of endogenous, vector-independent ABCG2 shown in Fig. 1 and as suggested by the reduced efflux of Ce6 upon blocking of ABCG2 by KO143 shown in Fig. 4 for U251-EV cells. With regard to both Ce6 accumulation and surface staining using a fluorescently labeled ABCG2-specific antibody, U251-V cells revealed subpopulations which were sensitive to Dox concentration, indicating a heterogeneous ABCG2 expression in the genetically engineered cell line. The non-induced U251-V cells showed a slightly reduced Ce6 uptake in FCS containing medium compared to U251-EV cells, indicating that the ABCG2 plasmid did express some ABCG2 even in the absence of the inductor (Fig. 6), thus showing some “leakiness” of the expression system. In FCS-free medium, there was hardly any difference, an indication of a supportive effect of serum proteins on the efficiency of ABCG2.

The amount of serum proteins from the FCS in the incubation medium has a dual effect: 1. Ce6 binds to serum proteins and is less available for cellular uptake at high FCS concentrations [28], 2. ABCG2 efficiency is enhanced by FCS, leading to increased efflux of intracellular photosensitizer, as shown for 5-ALA induced PpIX [29]. The first effect is evident, when looking at the graphs in the top row of Fig. 2b; when ABCG2 is blocked with KO143 (top curves), the intracellular Ce6 fluorescence intensity decreases with increasing FCS concentration for any given Ce6 concentration. This effect is stronger for lower Ce6 concentrations, because at lower Ce6 concentrations, most of the Ce6 is bound to serum proteins, whereas at high Ce6 concentrations, most of the Ce6 is unbound and uptake into the cells is less dependent on FCS concentrations. The second effect is readily visible in Fig. 4, where efflux is fastest at the highest FCS concentration – unless ABCG2 is blocked by KO143.

Another interesting finding can be derived from the data presented in Fig. 2: the higher the intracellular Ce6 concentration, the larger the fraction of cells in the peak containing strongly fluorescent cells, which is at the same position (Ce6 fluorescence intensity) as when the cells are incubated with KO143. This suggests that Ce6 may inhibit ABCG2 activity at sufficiently high intracellular concentration. It has previously been shown that molecules can be substrates and inhibitors for ABCG2 at the same time, depending on their concentration, as e.g. reported for some tyrosine kinase inhibitors (gefitinib, imatinib) [30].

In our hands, ABCG2 activity could be blocked very effectively by either KO143 or an anti-ABCG2 antibody (5D3) (Fig. 6). 5D3 binding to ABCG2 is known to cause its endocytosis [31,32] which may explain the observed restoration of Ce6 cellular accumulation. It was not necessary to pre-incubate the induced U251-V cells with the inhibitor, co-incubation with Ce6 showed the same effect, meaning that the inhibitory effect is rather instantaneous. With sorafenib, a clinically validated multikinase inhibitor which was previously reported to also inhibit ABCG2 [27,33], we observed only incomplete inhibition, as the Ce6 levels did not reach levels obtained, when either KO143 or the anti-ABCG2 antibody 5D3 were used.

The most important question in the context of PDT is the consequence of an elevated ABCG2 expression for the phototoxicity. As expected, upon induction of ABCG2 expression, U251-V cells exhibited less phototoxicity (Fig. 7), which was, however, restored when ABCG2 was inhibited by co-incubation with KO143. The even higher phototoxicity observed for these cells compared to the non-induced cells, may be indicative of the activity of endogenous ABCG2 and “leakiness” of

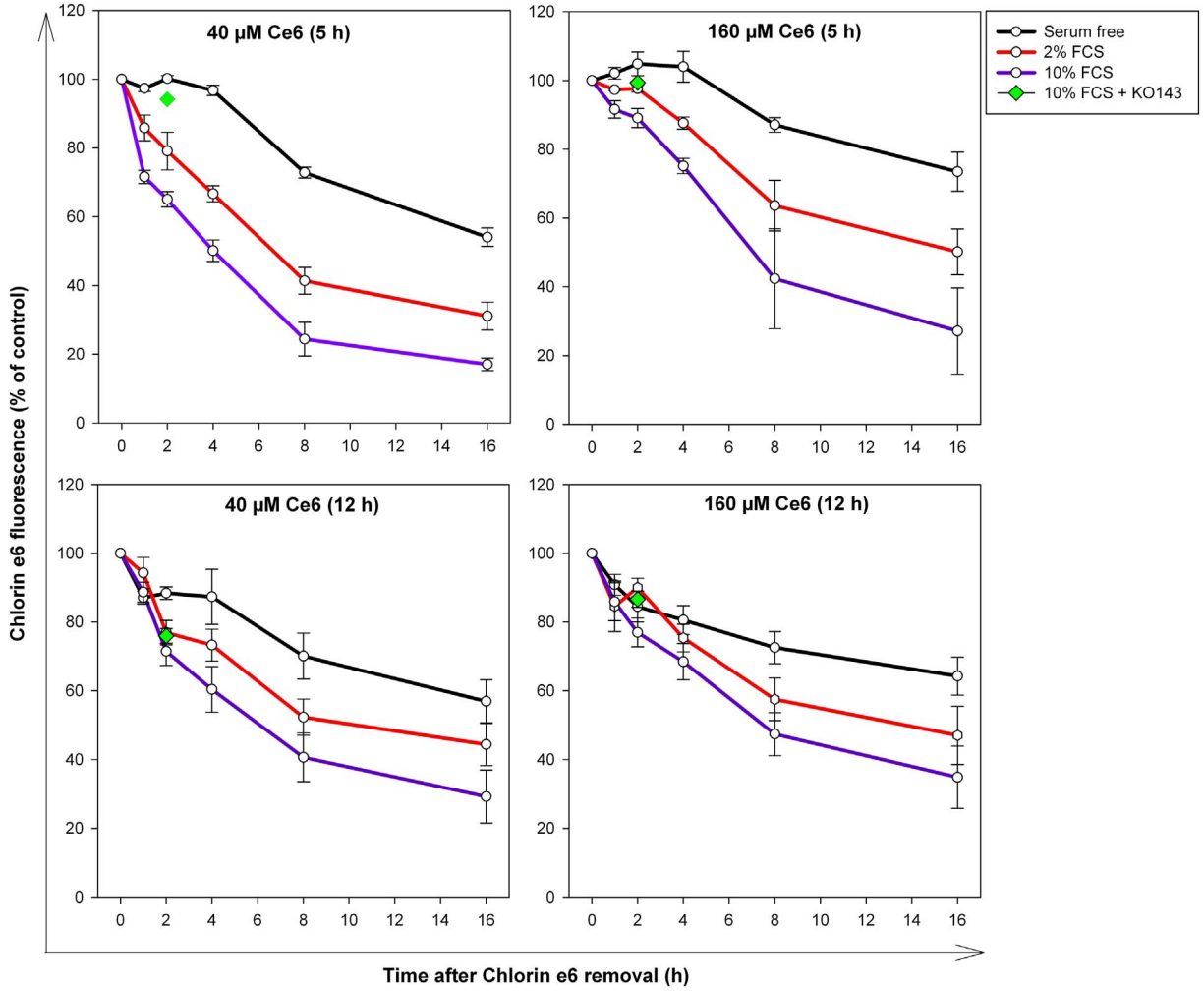

Fig. 4. Ce6 efflux dynamic depends on incubation time and Ce6 concentration. Loss of Ce6 from U251-EV cells after different Ce6 incubation conditions. Cells had been incubated in serum-free medium for 5 h (top row) or 12 h (bottom row) with 40 µM Ce6 (left column) or 160 µM Ce6 (right column). Fractions of retained Ce6 were determined by measurement of cellular fluorescence. Mean and standard error of three experiments each are shown. 100% correspond to the following mean fluorescence intensities (rFLU): 40 µM, 5 h: 697 ± 47; 160 µM, 5 h: 1019 ± 166; 40 µM, 12 h: 892 ± 126; 160 µM, 12 h: 1636 ± 248 (n = 3). rFLU, relative fluorescence units.

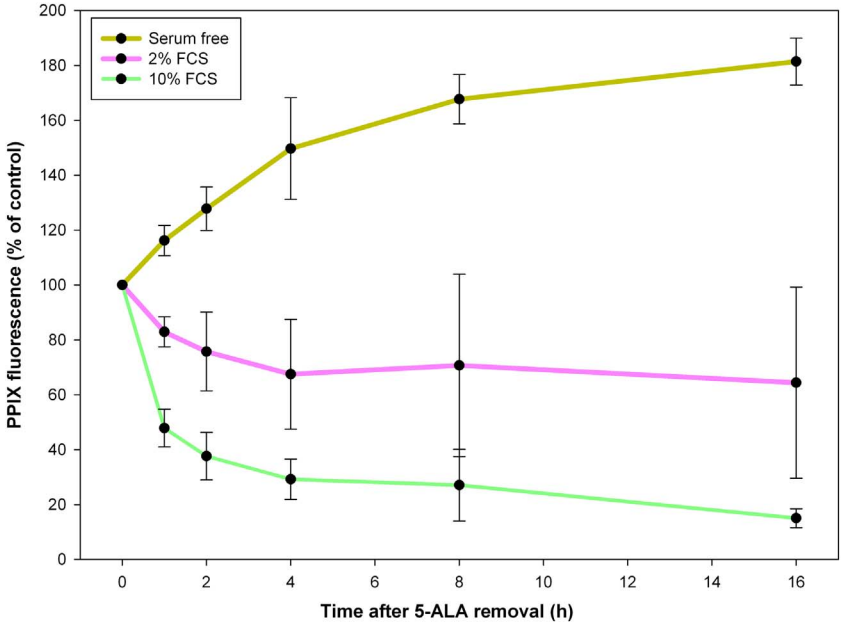

Fig. 5. Loss of 5-ALA-induced PpIX from U251-EV cells in dependence of FCS concentration. Cells had been incubated in serum free medium for 12 h at a concentration of 200 µg/ml 5-ALA (1.2 mM). The cells were transferred to 5-ALA-free medium and incubated in the absence or presence of 2 or 10% FCS for the indicated times. The retained PPIX fluorescence was determined by flow cytometry (n = 2).

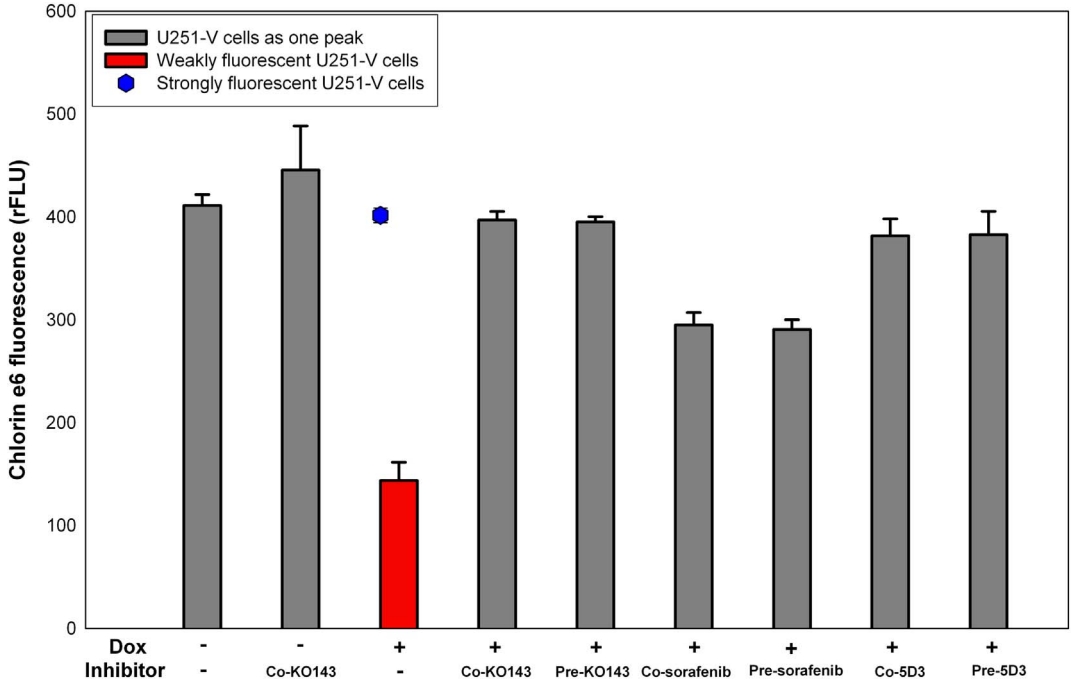

Fig. 6. Ce6 accumulation is reduced when ABCG2 is expressed and restored when it is inhibited by either co-incubation or pre-incubation with ABCG2 inhibitors such as 1.5 μM KO143, 3.2 μM sorafenib and 2 μg/ml of the antibody 5D3. U251-V cells were incubated for 5 h with 10 μM Ce6 in serum-free medium. Ce6 fluorescence was determined by flow cytometry. There was only one peak, when either of the inhibitors was applied and sorafenib showed the lowest ABCG2 inhibition efficiency. Shown are the mean values and standard errors of 2 independent experiments each (n = 2).Co: co-incubation with Ce6, pre: starting 1 h before Ce6 incubation.

the vector in the non-induced cells, as discussed above.

Finally, the association of ABCG2 expression with stemness properties of cancer cells was investigated. The growth of cells in spheres with appropriate culture medium is known to enrich the population of cells showing stem-like properties [34–36]. In a study of Schimanski et al. [37], cells isolated from human GBM tumors were grown in such spheres and exposed to ALA-based PDT. Although this investigation proved sufficient phototoxicity for a complete destruction of these presumably stem-like cells, it remained open, whether other growth conditions might have led to an even higher phototoxicity. In our investigation, we compared standard monolayer U87 cells with U87 cells grown in spheres. The experimental conditions were made as similar as possible by growing the cells from dissociated spheres also as monolayers until they adhered to the flasks before PDT was performed. Indeed, ABCG2 was increased and Ce6 concentration and PDT efficiency were decreased in the U87 cells originating from spheres. We expected a dual-peak in the ABCG2 flow cytometry results, corresponding to cell population fractions with normal unchanged ABCG2 expression and a more stem-like one with increased ABCG2. Instead, a single peak with elevated ABCG2 was observed, indicating a homogenous stimulation of ABCG2 expression (Fig. 8). The crucial clinical relevance of cancer stem cell niches for the growth and recurrence of glioblastoma and the association with ABCG2 has been pointed out earlier [8,9]. Unlike chemotherapy, PDT has the potential to effectively kill cancer stem cells if

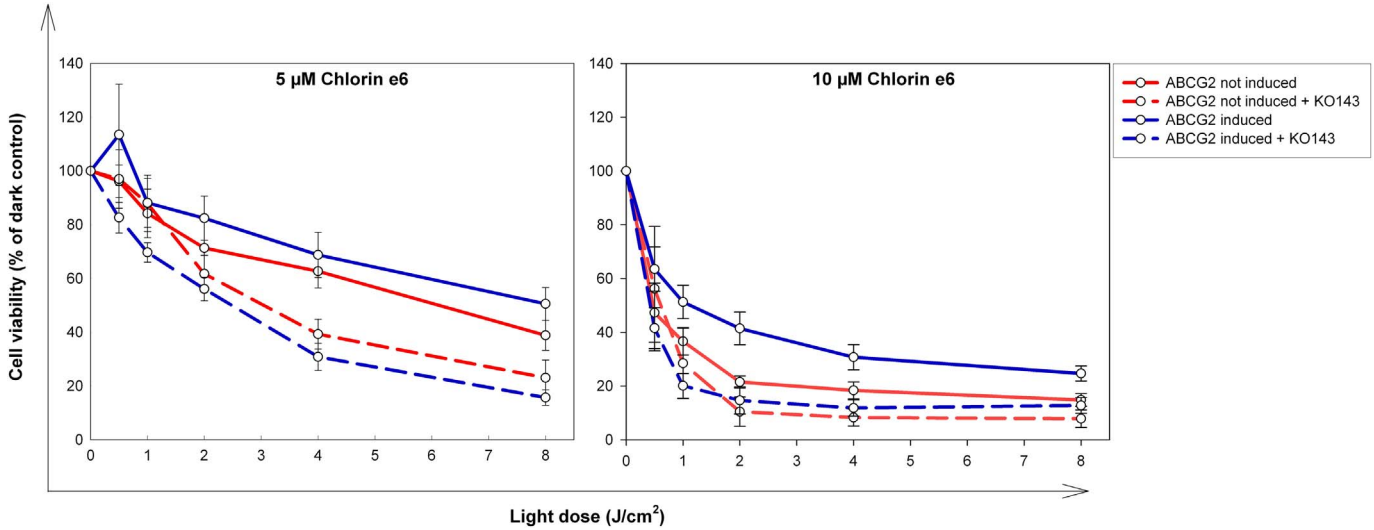

Fig. 7. PDT efficiency is reduced by ABCG2, but restored by the addition of KO143. Viability of U251-V cells incubated for 4 h with 5 μM (left) and 10 μM (right) Ce6 after PDT with 665 nm laser in dependence of the light dose. Viability was measured 4 h after irradiation. FCS concentration was 2% during the Ce6 incubation period, 0% during irradiation and 10% post irradiation. Mean values and standard errors are shown (n = 5). The differences in viability for "ABCG2 induced" versus "ABCG2 induced and inhibited" were statistically significant for all light doses above 0.5 J/cm^2 ($p < 0.01$).

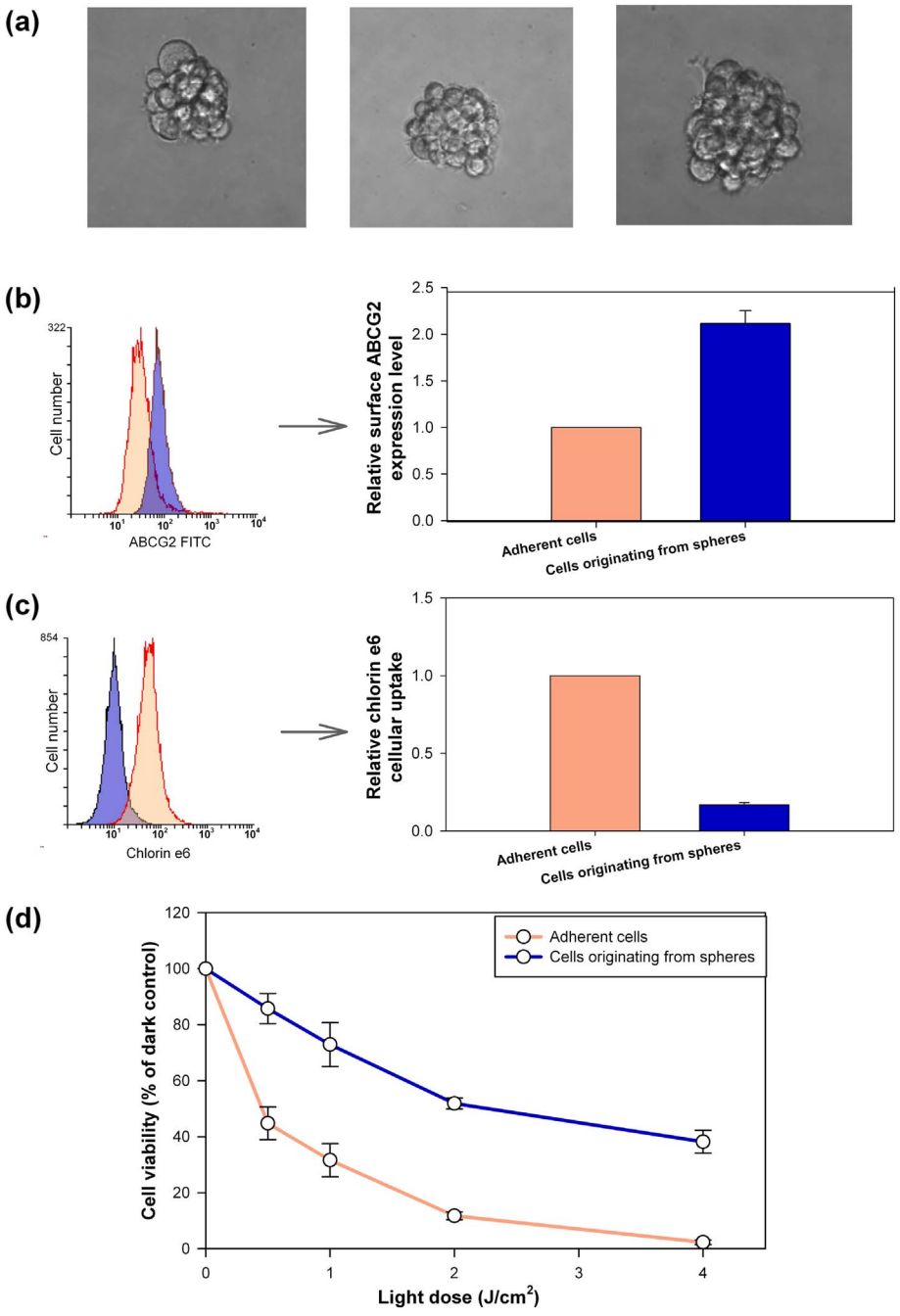

Fig. 8. U87 sphere cells express higher levels of ABCG2 than adherent cells and are more resistant to PDT: (a) Representative U87 spheres after culturing the cells for 3 days in ultra low attachment flasks and serum free medium. (b) Representative flow cytometry histograms and bar graph of ABCG2 expression and (c) Ce6 accumulation of U87 cells grown either as monolayer cell culture or spheres. (d) Ce6 PDT efficiency for U87 cells grown either as adherent monolayer or originating from spheres after being incubated for 5 h with 5 μM Ce6 in 2% FCS-containing medium. Mean values and standard error are shown (n = 2).

the uptake and accumulation of photosensitizer is enhanced by a short-term inhibition of ABCG2. Glioblastoma cells with stem-like properties are then photosensitized to the same degree as the rest of the tumor cells and the appropriate dose of light is expected to destroy these tumor-regenerating cells, which tend to resist chemo- or radiotherapy.

The limitations of the present study can be seen in the inhomogeneous ABCG2 expression of the induced U251-V cells, showing three cell populations with widely different ABCG2 expression (broad peaks instead of a distinct shift of a single peak (Fig. 1)) with respect to the non-induced controls. However, the results obtained do allow for clear conclusions. For future studies, the selection of a more uniformly ABCG2-expressing cell population will be tried. In addition it will be interesting to investigate the interaction between Ce6 and ABCG2 more comprehensively, as the results indicate that it may possess a substrate/inhibitor nature.

In conclusion, the experiments clearly show that stemness-associated ABCG2 expression leads to a reduced accumulation of the photosensitizer Ce6 and a correspondingly decreased photosensitivity of this crucial cell population. Short-term inhibition of ABCG2 by KO143 restores the photosensitivity. A combination of Ce6-based PDT with an inhibitor of ABCG2 may therefore be a promising modality to destroy stem-like cells in glioblastoma.

Acknowledgements

Dr. Sara A. Abdel Gaber was awarded a scholarship from Deutscher Akademischer Austauschdienst (DAAD). Apocare Pharma, Bielefeld, Germany provided chlorin e6 (Fotolon) and the laser device at no cost. The U251MG-L106 subclone and expression vectors were kindly provided by the Genome & Proteome Core Facility of the German Cancer Research Centre.

Conflicts of interest

None.

References

[1] R. Stupp, W.P. Mason, et al., Radiotherapy plus concomitant and adjuvant temozolomide for glioblastoma, N. Engl. J. Med. 352 (10) (2005) 987–996.
[2] S.S. Stylli, A.H. Kaye, Photodynamic therapy of cerebral glioma - a review. Part II - clinical studies, J. Clin. Neurosci. 13 (7) (2006) 709–717.
[3] S.S. Stylli, A.H. Kaye, et al., Photodynamic therapy of high grade glioma - long term survival, J. Clin. Neurosci. 12 (4) (2005) 389–398.
[4] S. Krishnamurthy, S.K. Powers, et al., Optimal light dose for interstitial photodynamic therapy in treatment for malignant brain tumors, Lasers Surg. Med. 27 (3) (2000) 224–234.
[5] A. Johansson, F. Faber, et al., Protoporphyrin IX fluorescence and photobleaching during interstitial photodynamic therapy of malignant gliomas for early treatment prognosis, Lasers Surg. Med. 45 (4) (2013) 225–234.
[6] J. Akimoto, Photodynamic therapy for malignant brain tumors, Neurol. Med. Chir. (Tokyo) 56 (4) (2016) 151–157.
[7] A.E. Stacy, P.J. Jansson, et al., Molecular pharmacology of ABCG2 and its role in chemoresistance, Mol. Pharmacol. 84 (5) (2013) 655–669.
[8] A.M. Bleau, J.T. Huse, et al., The ABCG2 resistance network of glioblastoma, Cell Cycle 8 (18) (2009) 2936–2944.
[9] T. Hide, K. Makino, et al., New treatment strategies to eradicate cancer stem cells and niches in glioblastoma, Neurol. Med. Chir. (Tokyo) 53 (11) (2013) 764–772.
[10] R.W. Robey, K. Steadman, et al., ABCG2-mediated transport of photosensitizers: potential impact on photodynamic therapy, Cancer Biol. Ther. 4 (2) (2005) 187–194.
[11] J.A. Hargus, F.R. Fronczek, et al., Mono-(L)-aspartylchlorin-e6, Photochem. Photobiol. 83 (5) (2007) 1006–1015.
[12] M. Pietruska, S. Sobaniec, et al., Clinical evaluation of photodynamic therapy efficacy in the treatment of oral leukoplakia, Photodiagn. Photodyn. Ther. 11 (1) (2014) 34–40.
[13] W. Ji, J.W. Yoo, et al., The effect of Radachlorin(R) PDT in advanced NSCLC: a pilot study, Photodiagn. Photodyn. Ther. 10 (2) (2013) 120–126.
[14] C. Simon, C. Mohrbacher, et al., In vitro studies of different irradiation conditions for Photodynamic inactivation of Helicobacter pylori, J. Photochem. Photobiol. B 141 (2014) 113–118.
[15] M.F. Wu, M. Deichelbohrer, et al., Chlorin e6 mediated photodynamic inactivation for multidrug resistant *Pseudomonas aeruginosa keratitis* in mice in vivo, Sci Rep 7 (2017) 44537.
[16] K. Winkler, C. Simon, et al., Photodynamic inactivation of multidrug-resistant *Staphylococcus aureus* by chlorin e6 and red light (lambda = 670 nm), J. Photochem. Photobiol. B 162 (2016) 340–347.
[17] J. Akimoto, J. Haraoka, et al., Preliminary clinical report on safety and efficacy of photodynamic therapy using talaporfin sodium for malignant gliomas, Photodiagn. Photodyn. Ther. 9 (2) (2012) 91–99.
[18] Y. Muragaki, J. Akimoto, et al., Phase II clinical study on intraoperative photodynamic therapy with talaporfin sodium and semiconductor laser in patients with malignant brain tumors, J. Neurosurg. 119 (4) (2013) 845–852.
[19] L. Gonzalez-Lobato, R. Real, et al., Differential inhibition of murine Bcrp1/Abcg2 and human BCRP/ABCG2 by the mycotoxin fumitremorgin C, Eur. J. Pharmacol. 644 (1–3) (2010) 41–48.
[20] S. Wittig-Blaich, R. Wittig, et al., Systematic screening of isogenic cancer cells identifies DUSP6 as context-specific synthetic lethal target in melanoma, Oncotarget 8 (14) (2017) 23760–23774.
[21] I. Kasza, G. Varady, et al., Expression levels of the ABCG2 multidrug transporter in human erythrocytes correspond to pharmacologically relevant genetic variations, PLoS One 7 (11) (2012) e48423.
[22] J.D. Allen, A. van Loevezijn, et al., Potent and specific inhibition of the breast cancer resistance protein multidrug transporter in vitro and in mouse intestine by a novel analogue of fumitremorgin C, Mol. Cancer Ther. 1 (6) (2002) 417–425.
[23] C. Hu, H. Li, et al., Analysis of ABCG2 expression and side population identifies intrinsic drug efflux in the HCC cell line MHCC-97L and its modulation by Akt signaling, Carcinogenesis 29 (12) (2008) 2289–2297.
[24] D. Strumberg, H. Richly, et al., Phase I clinical and pharmacokinetic study of the novel Raf kinase and vascular endothelial growth factor receptor inhibitor BAY 43-9006 in patients with advanced refractory solid tumors, J. Clin. Oncol. 23 (5) (2005) 965–972.
[25] M.D. Sorensen, S. Fosmark, et al., Chemoresistance and chemotherapy targeting stem-like cells in malignant glioma, Adv. Exp. Med. Biol. 853 (2015) 111–138.
[26] S. Warrier, P. Pavanram, et al., Study of chemoresistant CD133 + cancer stem cells from human glioblastoma cell line U138MG using multiple assays, Cell Biol. Int. 36 (12) (2012) 1137–1143.
[27] T. Mazard, A. Causse, et al., Sorafenib overcomes irinotecan resistance in colorectal cancer by inhibiting the ABCG2 drug-efflux pump, Mol. Cancer Ther. 12 (10) (2013) 2121–2134.
[28] H. Mojzisova, S. Bonneau, et al., The pH-dependent distribution of the photosensitizer chlorin e6 among plasma proteins and membranes: a physico-chemical approach, Biochim. Biophys. Acta 1768 (2) (2007) 366–374.
[29] T. Ogino, H. Kobuchi, et al., Serum-dependent export of protoporphyrin IX by ATP-binding cassette transporter G2 in T24 cells, Mol. Cell. Biochem. 358 (1–2) (2011) 297–307.
[30] R.W. Robey, C. Ierano, et al., The challenge of exploiting ABCG2 in the clinic, Curr. Pharm. Biotechnol. 12 (4) (2011) 595–608.
[31] C. Ozvegy-Laczka, R. Laczko, et al., Interaction with the 5D3 monoclonal antibody is regulated by intramolecular rearrangements but not by covalent dimer formation of the human ABCG2 multidrug transporter, J. Biol. Chem. 283 (38) (2008) 26059–26070.
[32] M. Studzian, G. Bartosz, et al., Endocytosis of ABCG2 drug transporter caused by binding of 5D3 antibody: trafficking mechanisms and intracellular fate, Biochim. Biophys. Acta 1853 (8) (2015) 1759–1771.
[33] Y. Wei, Y. Ma, et al., New use for an old drug: inhibiting ABCG2 with sorafenib, Mol. Cancer Ther. 11 (8) (2012) 1693–1702.
[34] K. Christensen, C. Aaberg-Jessen, et al., Immunohistochemical expression of stem cell, endothelial cell, and chemosensitivity markers in primary glioma spheroids cultured in serum-containing and serum-free medium, Neurosurgery 66 (5) (2010) 933–947.
[35] S.C. Yu, Y.F. Ping, et al., Isolation and characterization of cancer stem cells from a human glioblastoma cell line U87, Cancer Lett. 265 (1) (2008) 124–134.
[36] X. Yuan, J. Curtin, et al., Isolation of cancer stem cells from adult glioblastoma multiforme, Oncogene 23 (58) (2004) 9392–9400.
[37] A. Schimanski, L. Ebbert, et al., Human glioblastoma stem-like cells accumulate protoporphyrin IX when subjected to exogenous 5-aminolaevulinic acid, rendering them sensitive to photodynamic treatment, J. Photochem. Photobiol. B 163 (2016) 203–210.

Journal of Photochemistry & Photobiology, B: Biology 210 (2020) 111963

Contents lists available at ScienceDirect

Journal of Photochemistry & Photobiology, B: Biology

journal homepage: www.elsevier.com/locate/jphotobiol

ABCG2 influence on the efficiency of photodynamic therapy in glioblastoma cells

Patricia Müller[a,b,*], Sara A. Abdel Gaber[a,c,*], Wolfgang Zimmermann[b,d], Rainer Wittig[e], Herbert Stepp[a,d]

[a] Laser Forschungslabor, LIFE Center, University Hospital, LMU Munich, Fraunhoferstr. 20, 82152 Planegg, Germany
[b] Labor für Tumorimmunologie, LIFE Center, University Hospital, LMU Munich, Fraunhoferstr. 20, 82152, Planegg, Germany
[c] Nanomedicine Department, Institute of Nanoscience and Nanotechnology, Kafrelsheikh University, Kafrelsheikh, 33516, Egypt
[d] Department of Urology, University Hospital, LMU Munich, Fraunhoferstr. 20, 82152 Planegg, Germany
[e] Institut für Lasertechnologien in der Medizin und Messtechnik an der Universität Ulm, Helmholtzstr. 12, 89081 Ulm, Germany

ARTICLE INFO

Keywords:
Photodynamic therapy
5-aminolevulinic acid
Protoporphyrin IX (PpIX)
ABCG2
Glioblastoma
Cancer stem cells

ABSTRACT

Background: Photodynamic therapy with 5-aminolevulinic acid (5-ALA PDT) is a promising novel therapeutic approach in the therapy of malignant brain tumors. 5-ALA occurs as a natural precursor of protoporphyrin IX (PpIX), a tumor-selective photosensitizer. The ATP-binding cassette transporter ABCG2 plays a physiologically significant role in porphyrin efflux from living cells. ABCG2 is also associated with stemness properties. Here we investigate the role of ABCG2 on the susceptibility of glioblastoma cells to 5-ALA PDT.

Methods: Accumulation of PpIX in doxycycline-inducible U251MG glioblastoma cells with or without induction of ABCG2 expression or ABCG2 inhibition by KO143 was analyzed using flow cytometry. In U251MG cells, ABCG2 was inducible by doxycycline after stable transfection with a tet-on expression plasmid. U251MG cells with high expression of ABCG2 were enriched and used for further experiments (sU251MG-V). PDT was performed on monolayer cell cultures by irradiation with laser light at 635 nm.

Results: Elevated levels of ABCG2 in doxycycline induced sU251MG-V cells led to a diminished accumulation of PpIX and higher light doses were needed to reduce cell viability. By inhibiting the ABCG2 transporter with the efficient and non-toxic ABCG2 inhibitor KO143, PpIX accumulation and PDT efficiency could be strongly enhanced.

Conclusion: Glioblastoma cells with high ABCG2 expression accumulate less photosensitizer and require higher light doses to be eliminated. Inhibition of ABCG2 during photosensitizer accumulation and irradiation promises to restore full susceptibility of this crucial tumor cell population to photodynamic treatment.

1. Introduction

Glioblastoma multiforme (GBM) is the most common and most aggressive type of primary malignant brain tumor in adults [1]. It is a heterogeneous tumor with widespread invasion throughout the brain and no clear tumor margins, which makes complete resection difficult. Currently, there is no curative treatment available [2]. Standard therapy, consisting of maximal surgical resection, radiotherapy and adjuvant chemotherapy with temozolomide, can prolong the median survival time up to 14.6 months. After relapse the median survival time is only 6.2 months [3]. To improve the poor prognosis new modalities are urgently needed.

Fluorescence guided resection (FGR) and photodynamic therapy (PDT) are promising novel therapeutic approaches that involve administration of the tumor-selective photosensitizer precursor 5-aminolevulinic acid [(5-ALA), gliolan®)] leading to intracellular formation of fluorescent and phototoxic protoporphyrin IX (PpIX). When PpIX is excited by visible light (for maximal tissue penetration usually at a wavelength of 635 nm) it generates reactive oxygen species [4–8]. This photochemical reaction causes apoptosis and necrosis in tumor tissue due to the toxicity of singlet oxygen, occlusion of tumor vessels, and activation of the immune system which may result in tumor cell destruction [9].

5-ALA occurs as the natural precursor of PpIX in the heme biosynthesis pathway. Exogenously administered, it results in a highly selective PpIX accumulation in tumor tissue due to multifactorial

* Corresponding author at: Laser Forschungslabor, LIFE Center, University Hospital, LMU Munich, Fraunhoferstr. 20, 82152 Planegg, Germany.
E-mail addresses: patricia.mueller2101@gmail.com (P. Müller), sara.abdelgaber.guc@gmail.com (S.A. Abdel Gaber).

https://doi.org/10.1016/j.jphotobiol.2020.111963
Received 8 January 2020; Received in revised form 12 July 2020; Accepted 14 July 2020
Available online 18 July 2020
1011-1344/

phenomena like increased expression of PpIX biosynthesis enzymes, reduced ferrochelatase activity and blood brain barrier leakage in tumors [10–13]. Due to this high tumor selectivity the normal brain is very well protected from 5-ALA-mediated PDT [14]. A randomized phase III study on 27 newly diagnosed GBM patients evaluated 5-ALA- and photofrin-based FGR and repetitive PDT in GBM [15]. The authors described a beneficial effect for the patients in the study group with a mean survival of 52.8 ± 26 weeks compared to 24.6 ± 11.5 weeks in the control group. Therefore, 5-ALA PDT offers a promising new option for the management of malignant gliomas.

PpIX and other photosensitizers like chlorin e6 as well as a large number of anticancer agents like topoisomerase inhibitors and tyrosine kinase inhibitors serve as substrates for ABCG2, a member of ATP-binding cassette transporter transmembrane proteins [16]. It acts as a drug efflux pump, therefore, provoking drug resistance in cancer. In normal tissue, ABCG2 has a variety of functions. It is expressed in the placenta and blood brain barrier where it protects the fetus/brain from harmful endo- and exotoxins.

It is also overexpressed in many cancer cells, especially in cancer stem cells (CSC) [17]. In malignant glioma it represents an important marker for the stemness phenotype [18]. CSC are thought to be responsible for tumorigenesis, resistance to chemo- and radiotherapy and, therefore, the main cause for tumor recurrence [19]. Thus, targeting CSC could increase the efficiency of tumor therapies.

With PpIX being a substrate of ABCG2, overexpression of ABCG2 potentially leads to less efficiency in the treatment with PDT. Here, we demonstrate the decrease of PpIX accumulation by ABCG2 and PDT efficiency in glioma cells using isogenic transfectants of the U251MG cell line carrying either an inducible vector coding for human ABCG2 (sU251MG-V) or the respective empty control vector (U251MG-EV). We also investigated the recovery of PpIX accumulation and PDT efficiency by inhibiting ABCG2 with KO143.

2. Material and Methods

2.1. Cell Culture and Maintenance

The U251MG cells used in this study (kindly provided by the Genome & Proteome Core Facility of the German Cancer Research Centre [Heidelberg, Germany]) are genetically engineered subclones containing a single Flp recombinase target (FRT) site for site-specific integration of a vector for doxycycline (Dox)-inducible expression of ABCG2 (resulting in U251MG-V) and the corresponding empty control vector (resulting in the isogenic control clone U251MG-EV), respectively. Stable transfectants were generated as described previously [20,21]. In U251MG-V cells, the ABCG2 expression is controlled by a tetracycline-responsive cytomegalovirus (CMV) promoter that gets activated by addition of doxycycline (Dox, Sigma-Aldrich Chemie GmbH, Taufkirchen, Germany). Full expression of ABCG2 was achieved after exposure to Dox for 48 h. The cell lines were maintained in the presence of 150 µg/ml hygromycin B in DMEM supplemented with 10% fetal calf serum (FCS), 100 IE/ml penicillin, 100 µg/ml streptomycin sulfate, 1 mM sodium pyruvate and 100 µM nonessential amino acid (all Merck-Millipore, Darmstadt, Germany) in a humidified incubator with 5% CO_2/air at 37 °C.

2.2. ABCG2 Induction and Photosensitization

Glioblastoma cells (2.5×10^5 per well) were seeded in 6-well plates (Sigma-Aldrich Chemie GmbH, Darmstadt, Germany) in DMEM containing 10% FCS and incubated overnight. For ABCG2 expression, the medium was changed the next day to DMEM containing 10% FCS, 150 µg/ml hygromycin B with 1 µg/ml doxycycline. After 48 h various concentrations of 5-aminolevulinic acid (5-ALA, Medac GmbH, Hamburg, Germany) diluted in DMEM containing 2% FCS were added. A 1 mg/ml stock solution was freshly prepared in phosphate buffered saline (PBS, Merck-Millipore, Darmstadt, Germany) with its pH adjusted to 7.4. Cells were incubated with 5-ALA for 4 h in the presence or absence of the ABCG2 inhibitors KO143 (Santa Cruz Biotechnology, Heidelberg, Germany) or sorafenib (LC Laboratories, Woburn, USA). Dimmed light was used when 5-ALA-treated cells were handled.

2.3. Flow Cytometric Analysis of Intracellular PpIX and ABCG2

After incubation with 5-ALA, cells were washed with pre-warmed PBS and dissociated by incubation with 200 µl Biotase per 6-well plate (Merck-Millipore, Darmstadt, Germany) for 20 min. The reaction was stopped by adding PBS and after centrifugation at 251 x *g*/1500 rpm for 5 min, cells were resuspended in 0.5 ml PBS. Cellular protoporphyrin IX (PpIX) contents were measured using a flow cytometer (BD FACSCalibur, Heidelberg, Germany) with an excitation wavelength of 488 nm and fluorescence detection with filter 3 (670 nm long pass filter). A minimum of 3×10^4 viable cell events were recorded per sample. BD CellQuest™ software (version 4.0.2) was used for data acquisition and data were processed with FlowJo software (version 10.0.8r1; Tree Star, Ashland, Oregon, USA).

For ABCG2 quantification cells were handled as mentioned before, but after centrifugation, cells were incubated for 1 h on ice with 2 µg of mouse-monoclonal ABCG2 antibody 5D3 (Santa Cruz Biotechnology, Heidelberg, Germany) diluted in 100 µl ice cold PBS. Cells were washed with PBS three times to remove unbound antibody. An isotype matched control antibody (normal mouse $IgG2_b$, Santa Cruz Biotechnology, Heidelberg, Germany) was used as a negative control. Cells were then incubated on ice for 30 min with 1 µg goat anti-mouse polyclonal antibodies conjugated with DyLight 488 (ThermoFisher Scientific GmbH, Schwerte, Germany) diluted with PBS in the dark. Finally cells were washed twice with PBS and fluorescence was detected with filter 1 (530/30 nm band pass filter).

2.4. Enrichment of ABCG2-Positive Cells by Fluorescence Activated Cell Sorting

ABCG2 expression was induced for 48 h by incubation with doxycycline as described above. Cells were washed with PBS, detached with Biotase, resuspended in PBS and stained with 200 µg/ml FITC-conjugated anti-ABCG2 mouse monoclonal antibody (5D3; Santa Cruz Biotechnology, Heidelberg, Germany) for 20 min on ice in the dark. Cells were washed with PBS and then incubated for 10 min with PBS containing 5% FCS, 1 mM EDTA (Sigma-Aldrich Chemie GmbH, Darmstadt, Germany) and 0.5 mg/ml propidium iodide (BD BioSciences, Heidelberg, Germany). Cells were sorted using the FACSAria III (BD Biosciences, Heidelberg, Germany) into a tube with 20% FCS DMEM and 10 mM HEPES (ThermoFisher Scientific GmbH, Germany). The cells were recovered by centrifugation at 251 x *g*/1500 rpm for 5 min and cultured in DMEM with 20% FCS in a humidified incubator as above.

2.5. In Vitro Photodynamic Treatment

After 4 h incubation with 5-ALA the medium was replaced with DMEM without phenol red and FCS. Irradiation was performed with a red light laser at a wavelength of 635 nm (Ceralas PDT, Biolitec, Jena, Germany) with light doses ranging from 0 J/cm^2 to 13 J/cm^2. After irradiation, cells were cultured in DMEM medium containing 10% FCS and phenol red for 24 h at 37 °C.

2.6. Cell Viability Assay

Cell viability was determined 24 h after photodynamic therapy (PDT) by using the MTT assay as described elsewhere [22]. Briefly, Thiazolyl Blue Tetrazolium Bromide (MTT, Sigma-Aldrich Chemie GmbH, Taufkirchen, Germany) was dissolved in PBS at a concentration

of 5 mg/ml and sterilized using a 0.2 µm filter. 100 µl of MTT solution was added to 1000 µl of medium and cells were incubated for 1 h at 37 °C. The insoluble formazan was solubilized in 1000 µl of DMSO (Sigma-Aldrich Chemie GmbH, Taufkirchen, Germany) after removing the MTT medium and 100 µl were transferred to a 96-well plate. Absorbance was measured at 560 nm using a FLUOStar OPTIMA microplate reader (BMG LABTECH, Jena, Germany). The absorbance of DMSO was also measured and referred to as blank. Viability was calculated by subtracting the blank values from the obtained reading for treated cells and results were expressed as percent of control cells.

2.7. Statistical Analysis

Statistical analyses were performed using XLSTAT (Microsoft Excel Plugin). Pairwise significance was tested using student's *t*-test. Light dose dependent cell survival curves and time dependent PpIX efflux curves were analyzed pairwise using ANOVA, defining light dose or time as the one and the two curves to compare as the other independent variable. P values $< .05$ were considered to be statistically significant.

3. Results

3.1. Enrichment of Glioblastoma Cells Featuring Strong and Inducible Expression of ABCG2

To analyze the homogeneity and level of ABCG2 expression, the cell line U251MG-V was incubated for 48 h with or without 1 µg/ml Dox and stained with an anti-ABCG2 primary antibody (5D3) and DyLight 488 secondary antibody. As a control, U251MG-EV cells were used which were generated applying the same recombination vector but without ABCG2 cDNA (empty vector). In Dox-induced U251MG-V cells, three distinct cell populations with low, medium and high expression of ABCG2 could be deduced from the fluorescence histogram with the lowest fluorescence peak being the largest (Fig. 1a). As expected, no inducible expression of ABCG2 was observed for U251MG-EV cells. To enrich U251MG-V for high level ABCG2-expressing cells, U251MG-V cells were induced with Dox, stained with the 5D3 antibody and sorted by fluorescence activated cell sorting (FACS). The resulting sU251MG-V cells also showed distinct cell populations, but the relative contribution of populations was different, with the peak corresponding to the cell population with the highest ABCG2 expression now being the largest. This indicates that the cell sorting process largely eliminated the lowest expressing ABCG2 cells leaving just medium and highly ABCG2 expressing cells resulting in an increased mean fluorescence intensity. Note that the peak positions of the individual peaks are almost the same in both cell lines. Non-induced sU251MG-V cells sorted for high ABCG2 expression revealed a slightly stronger ABCG2 expression compared to the U251MG-EV cells indicating a low ABCG2 expression, probably as a result of some "leaky" expression of the transgene in the absence of Dox.

3.2. Optimization of ABCG2 Induction Conditions

In order to determine the optimal Dox concentration for maximal ABCG2 expression in sorted sU251MG-V cells, we incubated the cells with various amounts of Dox ranging from 0.1 ng/ml up to 10,000 ng/ml for 48 h and detected the ABCG2 expression by flow cytometry after staining with the anti-ABCG2 antibody 5D3 (Fig. 2a). Incubation with Dox at concentrations of 10 ng/ml or more induced a strong and broad distribution staining intensity in sU251MG-V cells. Two distinct cell populations with medium and high ABCG2 expression using a Dox concentration of 10 ng/ml or more could be detected, with the second population being the largest. The maximum of the high fluorescence peak in this histogram is separated by approximately 160 fluorescence units compared to the non-induced cells and does not shift further with increasing Dox concentrations up to 10,000 ng/ml. In order to achieve a stable and efficient ABCG2 gene expression response we continued our experiments with a Dox concentration of 1000 ng/ml (Fig. 2b). This Dox concentration appears to be nontoxic as no difference of cell viability measured by the MTT assay after incubation with various amounts of Dox up to 10,000 ng/ml for 48 h was seen (data not shown).

3.3. 5-ALA-Induced PpIX Accumulation Is Impaired by ABCG2 Expression

To investigate whether and to which extent the intracellular

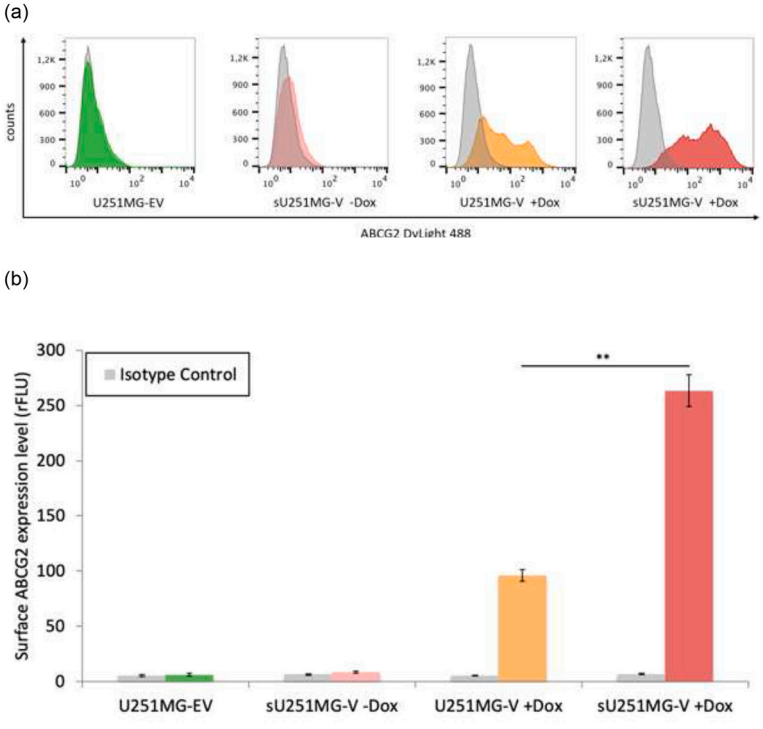

Fig. 1. ABCG2 induction after incubation with 1 µg/ml Dox for 48 h a) Representative histograms for U251MG-EV, sU251MG-V and U251MG-V cells as determined by flow cytometry. b) Cell surface ABCG2 protein expression of these cells after staining with a primary ABCG2 antibody (5D3) and DyLight488 secondary antibody. Shown is the average and standard deviation of geometrical means of flow cytometry measurements ($n = 3$).

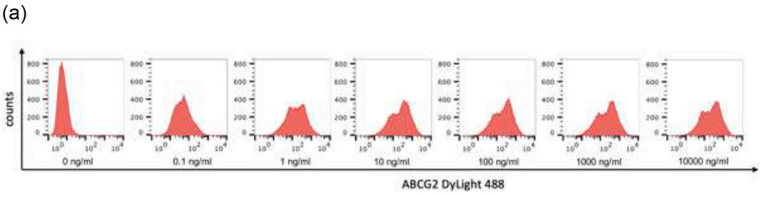

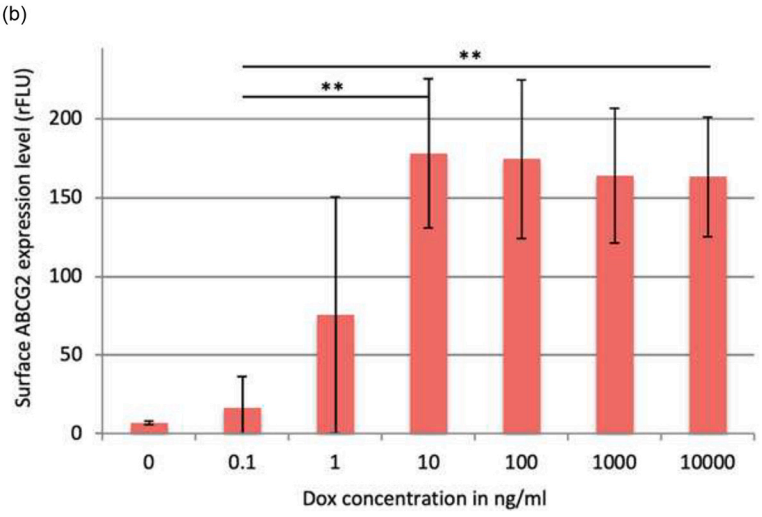

Fig. 2. Effect of Dox on the ABCG2 expression in sU251MG-V cells. a) ABCG2 expression after incubating cells for 48 h with various amounts of Dox as determined by flow cytometry. Shown are representative histograms from one of at least three independent experiments. b) Dependence of cell surface ABCG2 protein expression on Dox concentrations after incubation for 48 h. Shown is the average and standard deviation of geometric means of fluorescence measured by flow cytometry ($n = 4$).

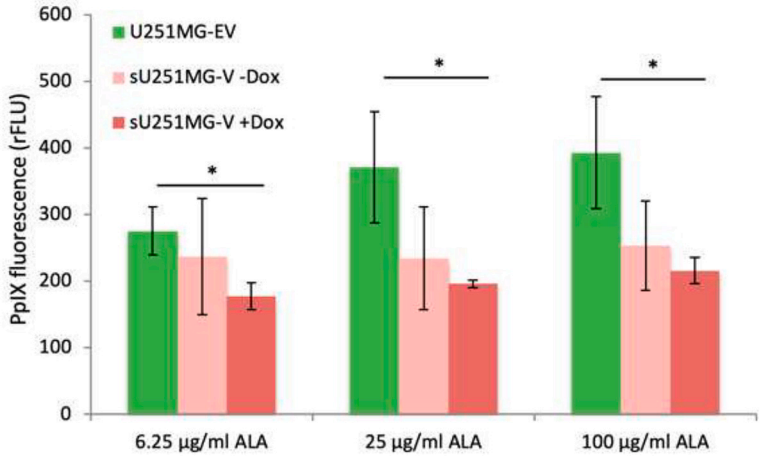

Fig. 3. PpIX accumulation is dependent on 5-ALA concentration and ABCG2 expression. Cells were incubated for 48 h in the presence or absence of 1 µg/ml Dox followed by a 4 h incubation period with various amounts of 5-ALA in 2% FCS containing medium. PpIX fluorescence was determined by flow cytometry. Shown are the mean values and standard deviations of three independent experiments ($n = 3$). *Statistically significant difference with $.05 < p < .005$, other relations were not significant.

accumulation of PpIX is influenced by ABCG2 expression, we investigated PpIX-mediated fluorescence in sU251MG-V cells with or without ABCG2 induction by Dox in comparison to isogenic U251MG-EV cells at different concentrations of 5-ALA. Cells were incubated for 4 h with 6.25, 25 or 100 µg/ml 5-ALA and PpIX fluorescence was determined by flow cytometry. Shown are the mean values and standard deviation of three independent experiments. PpIX accumulated with increasing 5-ALA concentrations and was reduced by induction of ABCG2 expression (Fig. 3). After Dox treatment the highly ABCG2-expressing sU251MG-V cells showed the lowest mean fluorescence intensity of PpIX whereas the U251MG-EV accumulated the highest concentration of PpIX. Interestingly, non-induced sU251MG-V cells revealed a lower mean fluorescence intensity of PpIX when compared to the U251MG-EV cells, which may be the result of a leaky expression of the transgene in the absence of Dox as already noted above (Fig. 3).

3.4. PpIX Accumulation Can Be Restored by ABCG2 Inhibition

As overexpression of ABCG2 reduced 5-ALA-mediated PpIX accumulation, we wanted to know, whether the presence of the pharmacological ABCG2 inhibitor KO143 could restore PpIX formation. Flow cytometric analysis revealed a higher mean PpIX fluorescence in all cell lines in the presence of KO143 (Fig. 4a). The KO143-induced increase in PpIX fluorescence was not statistically significant for U251MG-EV cells, whereas it was highly significant for the cell lines with higher levels of ABCG2 (Fig. 4b). This was the case for all 5-ALA concentrations used (see supplementary Fig. 1), indicating that the PpIX accumulation can be completely restored by the ABCG2 inhibitor KO143 independent of the amount of the PpIX precursor 5-ALA present in the media.

Interestingly, we could not detect an increase in PpIX accumulation when we co-incubated the cells with sorafenib or 5D3 antibody known to block the transporter function of ABGC2 for a number of drugs (Fig. 5), whereas accumulation of Ce6, a chemically synthesized porphyrin derivative, was increased when cells were co-incubated with these inhibitors [21].

Taken together our results indicate an efficient inhibition of ABCG2-mediated efflux of PpIX in induced sU251MG-V cells by the potent

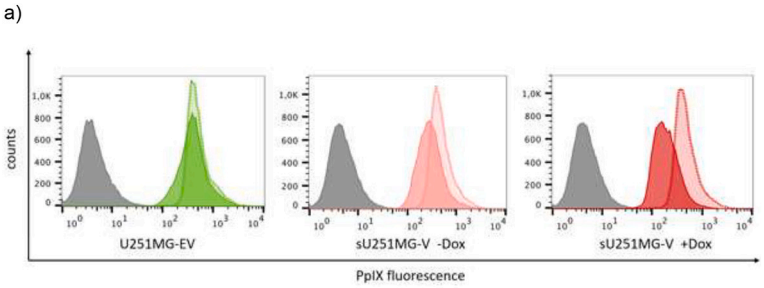

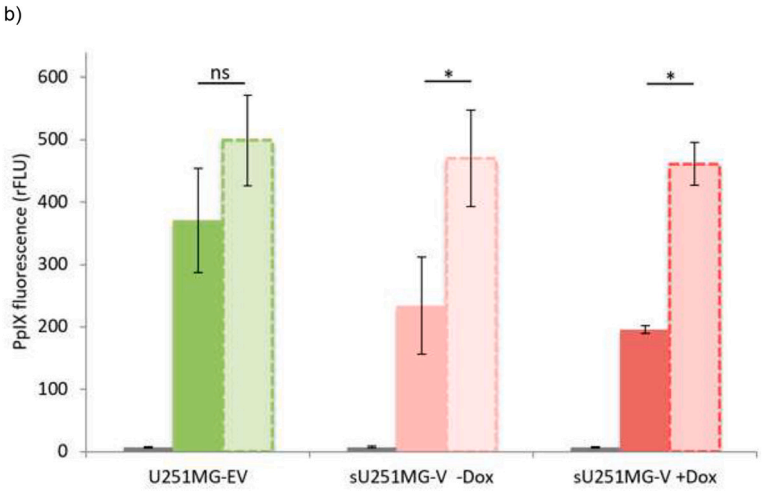

Fig. 4. Effect of KO143 on the accumulation of PpIX in U251MG-EV and sU251MG-V (non-induced) and sU251MG-V (induced) cells. Cells were incubated with 0 (grey fill color) or 25 μg/ml 5-ALA for 4 h at 37 °C in the dark in the absence (darker colors) or presence (lighter colors) of 1.5 μM KO143. The cells were then washed, collected and subsequently analyzed for PpIX accumulation by flow cytometry. a) representative flow cytometry histograms, b) mean values and standard deviation of three independent experiments ($n = 3$). *: p-value < .05, ns: p-value > .05.

ABCG2 inhibitor KO143.

3.5. ABCG2 Induction Reduces Phototoxicity, but PDT Efficiency Can Be Restored by ABCG2 Inhibition

PDT efficiency of monolayer U251MG-EV cells and sU251MG-V cells depends on light dose and 5-ALA concentration (Fig. 6 for 25 μg/ml 5-ALA, see supplementary Fig. 3 for 6.25 μg/ml and 100 μg/ml 5-ALA). As expected, the empty vector U251MG-EV cells did not respond to induction of ABCG2 by Dox. The survival was quite similar ($p = .93$, .75 and .62 for 5-ALA concentrations of 6.25, 25 and 100 μg/ml, respectively). A decrease in cell survival was however noted, when U251MG-EV cells were co-incubated with KO143, indicating the presence of some endogenous and functional ABCG2 ($p = .002$, .056 and .068, respectively, exceeding significance level, when the data point at 100% is excluded from statistical analysis).

Induction of ABCG2 in sU251MG-V cells led to an increase in cell survival. This difference was statistically significant only for the lowest 5-ALA concentration tested, however ($p = .017$, .1 and .063, respectively). While this increase in cell survival by a strong induction of ABCG2 expression was rather moderate, blocking of ABCG2 by KO143 led to a dramatic decrease in cell survival for all conditions tested ($p < .0001$ for all 5-ALA concentrations).

Compared to non-induced sU251MG-V cells, U251MG-EV cells were more sensitive to PDT (6.25 μg/ml $p < .0001$, 25 μg/ml $p = .001$, 100 μg/ml $p = .04$), indicating some "leakiness" of expression of the vector in the absence of Dox.

There was no statistically significant difference for 25 μg/ml 5-ALA

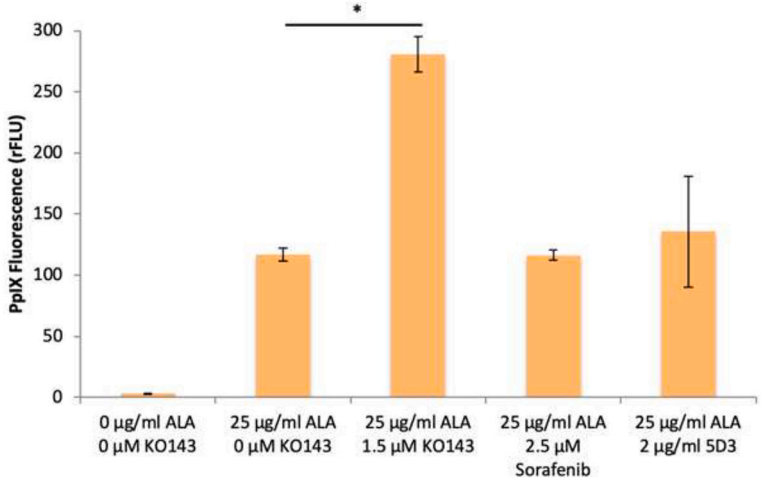

Fig. 5. PpIX accumulation is reduced when ABCG2 is expressed and restored when it is inhibited by co-incubation with the ABCG2 inhibitor KO143. Dox-induced U251MG-V cells were incubated for 4 h with 25 μg/ml 5-ALA. PpIX fluorescence was determined by flow cytometry. Shown are the mean values and standard deviations of 3 independent experiments (n = 3). *p-value < .05, ns: p-value > .05.

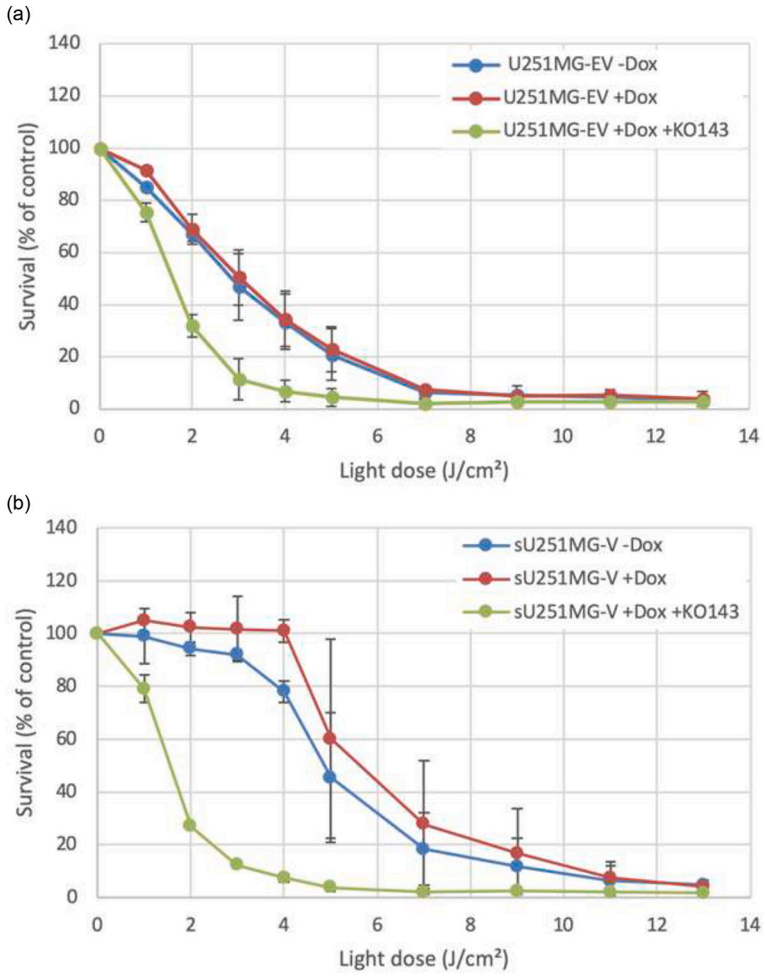

Fig. 6. Light dose dependent survival rates (MTT-assay 24 h after irradiation) of a) U251MG-EV and b) sU251MG-V cells, incubated for 4 h with 25 μg/ml 5-ALA in the presence or absence of the ABCG2 inhibitor KO143 (blue: without Dox, red and green: with Dox, green: KO143 in addition). FCS concentration was 2% during the 5-ALA incubation period, 0% during irradiation and 10% post irradiation. Mean values and standard errors of 3 biologically independent experiments are shown. (For interpretation of the references to color in this figure legend, the reader is referred to the web version of this article).

and 100 μg/ml 5-ALA phototoxicity between induced sU251MG-V cells and U251MG-EV cells when co-incubated with KO143 ($p > .9$), indicating that KO143 is a potent ABCG2 inhibitor inactivating efficiently low and high levels of ABCG2.

4. Discussion

4.1. Cellular Models for ABCG2 Expression

One of the less addressed questions with 5-ALA based PDT is, whether tumor stem cells might be resistant to PDT or at least require higher drug and light doses to be eliminated. While Schimanski et al. [23] could show that 5-ALA PDT is able to kill tumor stem cells, the authors did not show, whether non-stem cells from the same primary tumors would have been more susceptible to PDT. Fujishiro et al. [13] even found increased levels of PpIX in cells grown to enhance stem-like features and also showed increased susceptibility to PDT. However, the cells were cultivated in different media, especially containing different serum content, which might have influenced the PpIX accumulation capacity. It therefore remains to be clarified, whether more stem-like cells might accumulate less PpIX and/or are more resistant to PDT.

A crucial parameter associated with relative stem cell resistance to chemotherapy is the expression of the membrane transporter ABCG2. If the photosensitizer in use is a substrate of ABCG2 and ABCG2 is overexpressed in the stem cells of a tumor, PDT might fail to eradicate the tumor completely. It was therefore our aim to investigate, to which degree PpIX might be a substrate of ABCG2 and if so, whether this leads to a reduced cell death and finally, whether established inhibitors of ABCG2 are able to restore the susceptibility of these cells to PDT.

In earlier investigations, we have studied the correlation of ABCG2 expression and cell survival following PDT with the photosensitizer chlorin e6 (Ce6) [21]. Ce6 is a preformed photosensitizer, whereas 5-ALA itself is not photoactive and needs to be converted to the photosensitizer PpIX inside the cell's mitochondria. Interestingly, ABCG2 is – at least in some cell lines – also present in the outer mitochondrial membrane and found responsible for PpIX transport from mitochondria into the cytosol [24]. A small molecule inhibitor of ABCG2 has indeed altered the intracellular distribution pattern of PpIX in some cancer cells [25]. As a consequence of these findings, the interaction of ABCG2 with PpIX must be expected to be different and more complex than with other photosensitizers.

In order to study the influence of ABCG2 on PpIX accumulation and photosensitivity with minimal confounding factors, we chose a model, where the expression of ABCG2 could be switched on with minimal additional modification in the cell. Others have used models, where parental cells were induced to express ABCG2 by prolonged exposure to certain drugs such as mitoxantrone [26] or transfection with the ABCG2 encoding sequences [27]. The problem with such models is that it remains unclear, which additional changes in gene expression may have been induced. Another approach is to screen several cell lines

representing the same cancer type for their relative ABCG2 expression levels and select the highest and the lowest expressing ones to be the cellular models to study the role of ABCG2 in photosensitivity [25,28]. However, due to the heterogeneous genetic background these models are probably not exclusively studying the effect of ABCG2. We therefore adopted site-specific genetic engineering to create isogenic cell clones, which theoretically only differ in the presence of the ABCG2 coding sequence. In our previous study, this model has shown heterogeneous expression of ABCG2 following induction [21]. To enhance the performance, cell sorting was conducted using flow cytometry technique and as seen in Fig. 1, the fraction of highly ABCG2 expressing cells considerably increased.

4.2. PpIX is a Substrate for ABCG2

Our results are in agreement with other studies showing that cells expressing high levels of ABCG2 accumulate significantly less PpIX than cells with lower ABCG2 expression level (Fig. 3) [25,29,30]. To prove the role of ABCG2 as a transporter of PpIX, co-administration of the potent ABCG2 inhibitor KO143 was tested and it was indeed associated with a significant restoration of PpIX accumulation capacity similar to or even higher than levels observed with cells with minimal ABCG2 expression (Fig. 4). KO143 is an analogue of fumitremorgin C and one should keep in mind that apart from inhibiting ABCG2, it may also inhibit both ABCB1 and ABCC1, albeit at a higher concentration [31].

Yoshioka et al. showed that PpIX accumulation in cancer cells treated with 5-ALA can furthermore be promoted by inhibition of one of the Ras downstream elements, the Ras/mitogen-activated protein kinase (MEK). MEK inhibition reduced PpIX efflux from cancer cells by decreasing the expression level of ATP binding cassette subfamily B member 1 (ABCB1) transporter. In addition, the activity of ferrochelatase (FECH), the enzyme responsible for converting PpIX to heme, was reduced by MEK inhibition [32,33].

In contrast to our previous study with chlorin e6 [21], neither the ABCG2 antibody 5D3 nor the tyrosine kinase inhibitor sorafenib exerted a significant effect on photosensitizer retention. Sorafenib itself was proven to be a substrate for ABCG2 [34]. But another study suggested that sorafenib is also an ABCG2 inhibitor at higher concentrations, however its potency in restoring the cellular accumulation of mitoxantrone was significantly inferior to KO143 [35], which is confirmed by our study to be the case for PpIX too. A possible explanation for the superior inhibitory action of KO143 is its ability to inhibit both the mitochondrial and the cell surface ABCG2 as proven by Kobuchi et al. [24].

Overall, the PpIX levels did not correlate very well with the cell surface ABCG2 expression: while the induction of the ABCG2 vector by Dox increased ABCG2 on the cell membrane dramatically (Fig. 1), the reduction of intracellular PpIX versus the non-induced cells was rather moderate (Fig. 3). The leakiness of the vector itself, which caused only a minimal increase of surface ABCG2 expression already led to a considerable reduction of PpIX levels. Compared to the empty vector cells, the highly ABCG2-expressing cells still accumulated approximately half of the PpIX concentration under similar conditions, although one might have expected a much stronger reduction.

Interestingly, the application of KO143 was very effective in increasing the PpIX levels even in the empty vector cells, where the presence of some endogenous ABCG2 is to be expected. In summary, our results suggest that minimal ABCG2 expression, which is present in uninduced sU251MG-V and maybe even in U251MG-EV cells, could be sufficient for large parts of its biological function. In a similar case, leaky expression of the hepsin protease transgene in the prostate cancer cell line PC-3 resulted in considerable biological activity [36], which demonstrates the limitations of inducible gene expression systems and the relevance of the utilization of isogenic empty vector control cell lines for accurate data interpretation.

4.3. Serum Promotes ABCG2 Efflux Activity

The role of ABCG2 in PpIX transport can also be studied in PpIX efflux experiments. It has long been known that PpIX accumulation and efflux depend a lot on the presence or absence of serum in the cell culture medium [37]. The potential role of ABCG2 in this pharmacokinetic aspect of intra- and extracellular PpIX has been investigated by Ogino et al. [38] when studying ABCG2-expressing T24 urothelial carcinoma cells. With serum-containing medium, intracellular PpIX was much reduced and found in the extracellular medium, because serum albumin can bind extracellular PpIX and thus shift the partitioning equilibrium. This could very effectively be blocked by co-incubation with the ABCG2 inhibitor fumitremorgin C. We could confirm this qualitatively when comparing our empty vector U251MG-EV cells with the induced sU251MG-V cells (see supplementary Fig. 2). ABCG2 enhanced the efflux of PpIX in the presence of serum in the incubation medium, although the empty vector cells also lost PpIX in a serum dependent manner.

4.4. 5-ALA PDT is Hindered by ABCG2 Expression and Restored by KO143

Three different concentrations of 5-ALA and 9 different light doses were tested for their PDT efficiency in the different cell lines to cover all possible cell death mechanisms inducible by PDT. In the low concentration and light dose regime, cell death is mainly caused by apoptosis, whereas with high concentration and light doses, mainly immediate necrosis is observed as we have shown earlier [39]. It would be intriguing to investigate, whether delivery of KO143 favors apoptosis by confining PpIX stronger and longer inside the mitochondria. The steeper slopes of the survival curves at low light doses may indicate this, but employment of apoptosis assays is certainly required to clarify this question, which was outside the scope of the current study.

Switching on ABCG2 expression by Dox in sU251MG-V cells did result in a statistically significant, however not very drastic increase in cell survival (Fig. 6). This is consistent with the relatively moderate decrease in PpIX accumulation (Fig. 3), although the ABCG2 expression was very effectively upregulated (Fig. 1). Empty vector cells were much more vulnerable, which is again consistent with the considerably higher PpIX content. This indicates some unintended ABCG2 expression by the uninduced vector (leakiness). When KO143 was co-incubated, all cells, even the empty vector cells, showed increased susceptibility to PDT, as could have been expected by the increased PpIX fluorescence measured. This indicates the presence of some endogenous ABCG2. Overall, the observed PDT response is consistent with the PpIX content, but to a lesser degree with the observed (measurable) level of ABCG2 expression, where induction of the vector led to a very prominent ABCG2 signal, while the improvement of survival was quite moderate. On the other hand, KO143 co-delivery was quite effective in sensitizing the cells to PDT. In our previous study with chlorin e6 as a photosensitizer [21], the survival decrease, which could be induced by KO143 was by far less pronounced. This might be due to the hypothesized location of ABCG2 not only in the cell membrane but also in the mitochondrial membrane [24,25], where it influences PpIX, but not chlorin e6 accumulation.

Our results clearly demonstrate that ABCG2 modulates PpIX accumulation, FCS dependent efflux of PpIX and effectivity of PDT. The influence of factors other than ABCG2 expression is largely excluded by employing the model with a switchable ABCG2 expression vector. If cancer stem cells overexpress ABCG2 as part of their stem-like properties, a reduction of responsivity to PDT must be expected. This is, however, in contradiction to the work by Fujishiro et al. [13], who found an increased responsivity of stem-like cells to 5-ALA-PDT, despite significantly increased ABCG2 levels compared to the parental line. There were, however, many additional differences in the expression profile. On the other hand, Palasuberniam et al. [25] had shown that high ABCG2 transporter activity in triple negative breast cancer cells

leads to reduced PpIX accumulation and reduced effectivity of 5-ALA-PDT. It, therefore, remains to be shown, how the different expression profiles of stem-like cells in primary tumor tissue influence the PpIX content and the susceptibility to PDT. In conclusion, the negative impact of ABCG2 on 5-ALA-PDT can be avoided by the co-application of KO143 and even extremely high levels of ABCG2 do not completely inhibit PpIX accumulation and phototoxic cell death can still be achieved in vitro.

Supplementary data to this article can be found online at https://doi.org/10.1016/j.jphotobiol.2020.111963.

Declaration of Competing Interest

The authors declare that they have no known competing financial interests or personal relationships that could have appeared to influence the work reported in this paper.

Acknowledgements

This work was supported by the FöFoLe-Program of the Medical Faculty of the Ludwig-Maximilians-University Munich, Germany. The U251MG-L106 subclone and expression vectors were kindly provided by the Genome & Proteome Core Facility of the German Cancer Research Centre.

References

[1] Q.T. Ostrom, L. Bauchet, F.G. Davis, I. Deltour, J.L. Fisher, C.E. Langer, M. Pekmezci, J.A. Schwartzbaum, M.C. Turner, K.M. Walsh, M.R. Wrensch, J.S. Barnholtz-Sloan, The epidemiology of glioma in adults: a "state of the science" review, Neuro. Oncol. 16 (2014) 896–913.
[2] F. Hanif, K. Muzaffar, K. Perveen, S.M. Malhi, U. Simjee Sh, Glioblastoma multiforme: A review of its epidemiology and pathogenesis through clinical presentation and treatment, Asian Pac. J. Cancer Prev. 18 (2017) 3–9.
[3] R. Stupp, W.P. Mason, M.J. van den Bent, M. Weller, B. Fisher, M.J. Taphoorn, K. Belanger, A.A. Brandes, C. Marosi, U. Bogdahn, J. Curschmann, R.C. Janzer, S.K. Ludwin, T. Gorlia, A. Allgeier, D. Lacombe, J.G. Cairncross, E. Eisenhauer, R.O. Mirimanoff, R. European Organisation for, T. Treatment of Cancer Brain, G. Radiotherapy, G. National Cancer Institute of Canada Clinical Trials, Radiotherapy plus concomitant and adjuvant temozolomide for glioblastoma, N Engl. J. Med. 352 (2005) 987–996.
[4] W. Stummer, U. Pichlmeier, T. Meinel, O.D. Wiestler, F. Zanella, H.J. Reulen, Fluorescence-guided surgery with 5-aminolevulinic acid for resection of malignant glioma: a randomised controlled multicentre phase III trial, Lancet Oncol. 7 (2006) 392–401.
[5] T.S. Zavadskaya, Photodynamic therapy in the treatment of glioma, Exp. Oncol. 37 (2015) 234–241.
[6] P. Agostinis, K. Berg, K.A. Cengel, T.H. Foster, A.W. Girotti, S.O. Gollnick, S.M. Hahn, M.R. Hamblin, A. Juzeniene, D. Kessel, M. Korbelik, J. Moan, P. Mroz, D. Nowis, J. Piette, B.C. Wilson, J. Golab, Photodynamic therapy of cancer: an update, CA Cancer J. Clin. 61 (2011) 250–281.
[7] T.J. Beck, F.W. Kreth, W. Beyer, J.H. Mehrkens, A. Obermeier, H. Stepp, W. Stummer, R. Baumgartner, Interstitial photodynamic therapy of nonresectable malignant glioma recurrences using 5-aminolevulinic acid induced protoporphyrin IX, Lasers. Surg. Med. 39 (2007) 386–393.
[8] A. Johansson, F. Faber, G. Kniebuhler, H. Stepp, R. Sroka, R. Egensperger, W. Beyer, F.W. Kreth, Protoporphyrin IX fluorescence and photobleaching during interstitial photodynamic therapy of malignant gliomas for early treatment prognosis, Lasers. Surg. Med. 45 (2013) 225–234.
[9] J. Akimoto, Photodynamic therapy for malignant brain tumors, Neurol. Med. Chir. (Tokyo) 56 (2016) 151–157.
[10] L. Teng, M. Nakada, S.G. Zhao, Y. Endo, N. Furuyama, E. Nambu, I.V. Pyko, Y. Hayashi, J.I. Hamada, Silencing of ferrochelatase enhances 5-aminolevulinic acid-based fluorescence and photodynamic therapy efficacy, Br. J. Cancer 104 (2011) 798–807.
[11] X. Yang, W. Li, P. Palasuberniam, K.A. Myers, C. Wang, B. Chen, Effects of silencing heme biosynthesis enzymes on 5-aminolevulinic acid-mediated protoporphyrin IX fluorescence and photodynamic therapy, Photochem. Photobiol. 91 (2015) 923–930.
[12] S.R. Ennis, A. Novotny, J. Xiang, P. Shakui, T. Masada, W. Stummer, D.E. Smith, R.F. Keep, Transport of 5-aminolevulinic acid between blood and brain, Brain Res. 959 (2003) 226–234.
[13] T. Fujishiro, N. Nonoguchi, M. Pavliukov, N. Ohmura, S. Kawabata, Y. Park, Y. Kajimoto, T. Ishikawa, I. Nakano, T. Kuroiwa, 5-Aminolevulinic acid-mediated photodynamic therapy can target human glioma stem-like cells refractory to antineoplastic agents, Photodiag. Photodyn. Ther. 24 (2018) 58–68.
[14] H. Stepp, W. Stummer, 5-ALA in the management of malignant glioma, Lasers. Surg. Med. 50 (2018) 399–419.
[15] M.S. Eljamel, C. Goodman, H. Moseley, ALA and Photofrin fluorescence-guided resection and repetitive PDT in glioblastoma multiforme: a single centre Phase III randomised controlled trial, Lasers Med. Sci. 23 (2008) 361–367.
[16] M.I. Khot, C.L. Downey, G. Armstrong, H.S. Svavarsdottir, F. Jarral, H. Andrew, D.G. Jayne, The role of ABCG2 in modulating responses to anti-cancer photodynamic therapy, Photodiag. Photodyn. Ther. 29 (2019) 101579.
[17] W. Mo, J.T. Zhang, Human ABCG2: structure, function, and its role in multidrug resistance, Int. J. Biochem. Mol. Biol. 3 (2012) 1–27.
[18] A.M. Bleau, J.T. Huse, E.C. Holland, The ABCG2 resistance network of glioblastoma, Cell Cycle 8 (2009) 2936–2944.
[19] W. Wang, K. Tabu, Y. Hagiya, Y. Sugiyama, Y. Kokubu, Y. Murota, S.I. Ogura, T. Taga, Enhancement of 5-aminolevulinic acid-based fluorescence detection of side population-defined glioma stem cells by iron chelation, Sci. Rep. 7 (2017) 42070.
[20] S. Wittig-Blaich, R. Wittig, S. Schmidt, S. Lyer, M. Bewerunge-Hudler, S. Gronert-Sum, O. Strobel-Freidekind, C. Muller, M. List, A. Jaskot, H. Christiansen, M. Hafner, D. Schadendorf, I. Block, J. Mollenhauer, Systematic screening of isogenic cancer cells identifies DUSP6 as context-specific synthetic lethal target in melanoma, Oncotarget 8 (2017) 23760–23774.
[21] S.A. Abdel Gaber, P. Muller, W. Zimmermann, D. Huttenberger, R. Wittig, M.H. Abdel Kader, H. Stepp, ABCG2-mediated suppression of chlorin e6 accumulation and photodynamic therapy efficiency in glioblastoma cell lines can be reversed by KO143, J. Photochem. Photobiol. B. 178 (2018) 182–191.
[22] T.L. Riss, R.A. Moravec, A.L. Niles, S. Duellman, H.A. Benink, T.J. Worzella, L. Minor, Cell Viability Assays, in: G.S. Sittampalam, N.P. Coussens, H. Nelson, M. Arkin, D. Auld, C. Austin, ... J. Weidner (Eds.), Assay Guidance Manual, 2004 Bethesda, MD.
[23] A. Schimanski, L. Ebbert, M.C. Sabel, G. Finocchiaro, K. Lamszus, C. Ewelt, N. Etminan, J.C. Fischer, R.V. Sorg, Human glioblastoma stem-like cells accumulate protoporphyrin IX when subjected to exogenous 5-aminolaevulinic acid, rendering them sensitive to photodynamic treatment, J. Photochem. Photobiol. B. 163 (2016) 203–210.
[24] H. Kobuchi, K. Moriya, T. Ogino, H. Fujita, K. Inoue, T. Shuin, T. Yasuda, K. Utsumi, T. Utsumi, Mitochondrial localization of ABC transporter ABCG2 and its function in 5-aminolevulinic acid-mediated protoporphyrin IX accumulation, PLoS One 7 (2012) e50082.
[25] P. Palasuberniam, X. Yang, D. Kraus, P. Jones, K.A. Myers, B. Chen, ABCG2 transporter inhibitor restores the sensitivity of triple negative breast cancer cells to aminolevulinic acid-mediated photodynamic therapy, Sci. Rep. 5 (2015) 13298.
[26] R.W. Robey, O. Polgar, J. Deeken, K.W. To, S.E. Bates, ABCG2: determining its relevance in clinical drug resistance, Cancer Metastasis Rev. 26 (2007) 39–57.
[27] A.N. Robinson, B.G. Tebase, S.C. Francone, L.M. Huff, H. Kozlowski, D. Cossari, J.M. Lee, D. Esposito, R.W. Robey, M.M. Gottesman, Co-expression of ABCB1 and ABCG2 in a cell line model reveals both independent and additive transporter function, Drug Metab. Dispos. 47 (2019) 715–723.
[28] M. Galetti, P.G. Petronini, C. Fumarola, D. Cretella, S. La Monica, M. Bonelli, A. Cavazzoni, F. Saccani, C. Caffarra, R. Andreoli, A. Mutti, M. Tiseo, A. Ardizzoni, R.R. Alfieri, Effect of ABCG2/BCRP expression on efflux and uptake of Gefitinib in NSCLC cell lines, PLoS One 10 (2015) e0141795.
[29] N. Kawai, Y. Hirohashi, Y. Ebihara, T. Saito, A. Murai, T. Saito, T. Shirosaki, T. Kubo, M. Nakatsugawa, T. Kanaseki, T. Tsukahara, T. Shichinohe, L. Li, S. Hirano, T. Torigoe, ABCG2 expression is related to low 5-ALA photodynamic diagnosis (PDD) efficacy and cancer stem cell phenotype, and suppression of ABCG2 improves the efficacy of PDD, PLoS One 14 (2019) e0216503.
[30] T. Teshigawara, M. Mizuno, T. Ishii, Y. Kitajima, F. Utsumi, J. Sakata, H. Kajiyama, K. Shibata, M. Ishizuka, F. Kikkawa, Novel potential photodynamic therapy strategy using 5-Aminolevulinic acid for ovarian clear-cell carcinoma, Photodiag. Photodyn. Ther. 21 (2018) 121–127.
[31] L.D. Weidner, S.S. Zoghbi, S. Lu, S. Shukla, S.V. Ambudkar, V.W. Pike, J. Mulder, M.M. Gottesman, R.B. Innis, M.D. Hall, The Inhibitor Ko143 Is Not Specific for ABCG2, J. Pharmacol. Exp. Ther. 354 (2015) 384–393.
[32] E. Yoshioka, V.S. Chelakkot, M. Licursi, S.G. Rutihinda, J. Som, L. Derwish, J.J. King, T. Pongnopparat, K. Mearow, M. Larijani, A.M. Dorward, K. Hirasawa, Enhancement of cancer-specific protoporphyrin IX fluorescence by targeting oncogenic Ras/MEK pathway, Theranostics 8 (2018) 2134–2146.
[33] V.S. Chelakkot, J. Som, E. Yoshioka, C.P. Rice, S.G. Rutihinda, K. Hirasawa, Systemic MEK inhibition enhances the efficacy of 5-aminolevulinic acid-photodynamic therapy, Br. J. Cancer 121 (2019) 758–767.
[34] W.C. Huang, Y.L. Hsieh, C.M. Hung, P.H. Chien, Y.F. Chien, L.C. Chen, C.Y. Tu, C.H. Chen, S.C. Hsu, Y.M. Lin, Y.J. Chen, BCRP/ABCG2 inhibition sensitizes hepatocellular carcinoma cells to sorafenib, PLoS One 8 (2013) e83627.
[35] Y. Wei, Y. Ma, Q. Zhao, Z. Ren, Y. Li, T. Hou, H. Peng, New use for an old drug: inhibiting ABCG2 with sorafenib, Mol. Cancer Ther. 11 (2012) 1693–1702.
[36] R. Willbold, K. Wirth, T. Martini, H. Sultmann, C. Bolenz, R. Wittig, Excess hepsin proteolytic activity limits oncogenic signaling and induces ER stress and autophagy in prostate cancer cells, Cell Death Dis. 10 (2019) 601.
[37] P. Steinbach, H. Weingandt, R. Baumgartner, M. Kriegmair, F. Hofstadter, R. Knuchel, Cellular fluorescence of the endogenous photosensitizer protoporphyrin IX following exposure to 5-aminolevulinic acid, Photochem. Photobiol. 62 (1995) 887–895.
[38] T. Ogino, H. Kobuchi, K. Munetomo, H. Fujita, M. Yamamoto, T. Utsumi, K. Inoue, T. Shuin, J. Sasaki, M. Inoue, K. Utsumi, Serum-dependent export of protoporphyrin IX by ATP-binding cassette transporter G2 in T24 cells, Mol. Cell. Biochem. 358 (2011) 297–307.
[39] R. Kammerer, A. Buchner, P. Palluch, T. Pongratz, K. Oboukhovskij, W. Beyer, A. Johansson, H. Stepp, R. Baumgartner, W. Zimmermann, Induction of immune mediators in glioma and prostate cancer cells by non-lethal photodynamic therapy, PLoS One 6 (2011) e21834.

References

ABDEL GABER, S. A., MULLER, P., ZIMMERMANN, W., HUTTENBERGER, D., WITTIG, R., ABDEL KADER, M. H. & STEPP, H. 2018. ABCG2-mediated suppression of chlorin e6 accumulation and photodynamic therapy efficiency in glioblastoma cell lines can be reversed by KO143. *J Photochem Photobiol B,* 178**,** 182-191.

ABRAHAMSE, H. & HAMBLIN, M. R. 2016. New photosensitizers for photodynamic therapy. *Biochem J,* 473**,** 347-64.

AKIMOTO, J. 2016. Photodynamic Therapy for Malignant Brain Tumors. *Neurol Med Chir (Tokyo),* 56**,** 151-7.

ALEXANDER, B. M. & CLOUGHESY, T. F. 2017. Adult Glioblastoma. *J Clin Oncol,* 35**,** 2402-2409.

ALIFIERIS, C. & TRAFALIS, D. T. 2015. Glioblastoma multiforme: Pathogenesis and treatment. *Pharmacol Ther,* 152**,** 63-82.

ANAND, S., HONARI, G., HASAN, T., ELSON, P. & MAYTIN, E. V. 2009. Low-dose methotrexate enhances aminolevulinate-based photodynamic therapy in skin carcinoma cells in vitro and in vivo. *Clin Cancer Res,* 15**,** 3333-43.

ANAYO, L., MAGNUSSEN, A., PERRY, A., WOOD, M. & CURNOW, A. 2018. An experimental investigation of a novel iron chelating protoporphyrin IX prodrug for the enhancement of photodynamic therapy. *Lasers Surg Med,* 50**,** 552-565.

BEGICEVIC, R. R. & FALASCA, M. 2017. ABC Transporters in Cancer Stem Cells: Beyond Chemoresistance. *Int J Mol Sci,* 18.

BERTONCELLO, I. & WILLIAMS, B. 2004. Hematopoietic stem cell characterization by Hoechst 33342 and rhodamine 123 staining. *Methods Mol Biol,* 263**,** 181-200.

BROWN, D. V., FILIZ, G., DANIEL, P. M., HOLLANDE, F., DWORKIN, S., AMIRIDIS, S., KOUNTOURI, N., NG, W., MOROKOFF, A. P. & MANTAMADIOTIS, T. 2017. Expression of CD133 and CD44 in glioblastoma stem cells correlates with cell proliferation, phenotype stability and intra-tumor heterogeneity. *PLoS One,* 12**,** e0172791.

CASTANO, A. P., MROZ, P. & HAMBLIN, M. R. 2006. Photodynamic therapy and anti-tumour immunity. *Nat Rev Cancer,* 6**,** 535-45.

CHELAKKOT, V. S., SOM, J., YOSHIOKA, E., RICE, C. P., RUTIHINDA, S. G. & HIRASAWA, K. 2019. Systemic MEK inhibition enhances the efficacy of 5-aminolevulinic acid-photodynamic therapy. *Br J Cancer*.

CHEN, X., WANG, C., TENG, L., LIU, Y., YANG, G., WANG, L., LIU, H., LIU, Z., ZHANG, D., ZHANG, Y., GUAN, H., LI, X., FU, C., ZHAO, B., YIN, F. & ZHAO, S. 2014. Calcitriol enhances 5-aminolevulinic acid-induced fluorescence and the effect of photodynamic therapy in human glioma. *Acta Oncol,* 53**,** 405-13.

CHENG, L., HUANG, Z., ZHOU, W., WU, Q., DONNOLA, S., LIU, J. K., FANG, X., SLOAN, A. E., MAO, Y., LATHIA, J. D., MIN, W., MCLENDON, R. E., RICH, J. N. & BAO, S. 2013. Glioblastoma stem cells generate vascular pericytes to support vessel function and tumor growth. *Cell,* 153**,** 139-52.

CLAES, A., IDEMA, A. J. & WESSELING, P. 2007. Diffuse glioma growth: a guerilla war. *Acta Neuropathol,* 114**,** 443-58.

CLARKE, M. F., DICK, J. E., DIRKS, P. B., EAVES, C. J., JAMIESON, C. H., JONES, D. L., VISVADER, J., WEISSMAN, I. L. & WAHL, G. M. 2006. Cancer stem cells--perspectives on current status and future directions: AACR Workshop on cancer stem cells. *Cancer Res,* 66**,** 9339-44.

CLOUGHESY, T. F., CAVENEE, W. K. & MISCHEL, P. S. 2014. Glioblastoma: from molecular pathology to targeted treatment. *Annu Rev Pathol,* 9**,** 1-25.

COLLAUD, S., JUZENIENE, A., MOAN, J. & LANGE, N. 2004. On the selectivity of 5-aminolevulinic acid-induced protoporphyrin IX formation. *Curr Med Chem Anticancer Agents,* 4**,** 301-16.

CRAMER, S. W. & CHEN, C. C. 2019. Photodynamic Therapy for the Treatment of Glioblastoma. *Front Surg,* 6**,** 81.

CRESPO, I., VITAL, A. L., GONZALEZ-TABLAS, M., PATINO MDEL, C., OTERO, A., LOPES, M. C., DE OLIVEIRA, C., DOMINGUES, P., ORFAO, A. & TABERNERO, M. D. 2015. Molecular and Genomic Alterations in Glioblastoma Multiforme. *Am J Pathol,* 185**,** 1820-33.

DA ROCHA FILHO, H. N., DA SILVA, E. C., SILVA, F. R., COURROL, L. C., DE MESQUITA, C. H. & BELLINI, M. H. 2015. Expression of Genes Involved in Porphyrin Biosynthesis Pathway in the Human Renal Cell Carcinoma. *J Fluoresc,* 25**,** 1363-9.

DAVIS, M. E. 2016. Glioblastoma: Overview of Disease and Treatment. *Clin J Oncol Nurs,* 20**,** S2-8.

DEAN, M., FOJO, T. & BATES, S. 2005. Tumour stem cells and drug resistance. *Nat Rev Cancer,* 5**,** 275-84.

DING, X. W., WU, J. H. & JIANG, C. P. 2010. ABCG2: a potential marker of stem cells and novel target in stem cell and cancer therapy. *Life Sci,* 86**,** 631-7.

DOLMANS, D. E., FUKUMURA, D. & JAIN, R. K. 2003. Photodynamic therapy for cancer. *Nat Rev Cancer,* 3**,** 380-7.

ELEOUET, S., ROUSSET, N., CARRE, J., VONARX, V., VILATTE, C., LOUET, C., LAJAT, Y. & PATRICE, T. 2000. Heterogeneity of delta-aminolevulinic acid-induced protoporphyrin IX fluorescence in human glioma cells and leukemic lymphocytes. *Neurol Res,* 22**,** 361-8.

EMA. 2007. *Gliolan Approval Records* [Online]. Available: http://www.ema.europa.eu/ema/index.jsp?curl=pages/medicines/human/medicines/000744/human_med_000807.jsp&mid=WC0b01ac058001d124 [Accessed].

ENNIS, S. R., NOVOTNY, A., XIANG, J., SHAKUI, P., MASADA, T., STUMMER, W., SMITH, D. E. & KEEP, R. F. 2003. Transport of 5-aminolevulinic acid between blood and brain. *Brain Res,* 959**,** 226-34.

ESTELLER, M., GARCIA-FONCILLAS, J., ANDION, E., GOODMAN, S. N., HIDALGO, O. F., VANACLOCHA, V., BAYLIN, S. B. & HERMAN, J. G. 2000. Inactivation of the DNA-repair gene MGMT and the clinical response of gliomas to alkylating agents. *N Engl J Med,* 343**,** 1350-4.

FDA. 2011. *PHOTOFRIN (porfimer sodium) INJECTION* [Online]. Available: https://www.accessdata.fda.gov/drugsatfda_docs/label/2011/020451s020lbl.pdf [Accessed].

FDA. 2018. *Aminolevulinic acid hydrochloride, known as ALA HCl (Gleolan, NX Development Corp.) as an aoptical imaging agent indicated in patients with gliomas* [Online]. Available:

https://www.fda.gov/Drugs/InformationOnDrugs/ApprovedDrugs/ucm562645.htm [Accessed Jan 19, 2018].
FISHER, C. J., NIU, C., FOLTZ, W., CHEN, Y., SIDOROVA-DARMOS, E., EUBANKS, J. H. & LILGE, L. 2017. ALA-PpIX mediated photodynamic therapy of malignant gliomas augmented by hypothermia. *PLoS One,* 12**,** e0181654.
FISHER, C. J., NIU, C. J., LAI, B., CHEN, Y., KUTA, V. & LILGE, L. D. 2013. Modulation of PPIX synthesis and accumulation in various normal and glioma cell lines by modification of the cellular signaling and temperature. *Lasers Surg Med,* 45**,** 460-8.
FONKEM, E. & WONG, E. T. 2012. NovoTTF-100A: a new treatment modality for recurrent glioblastoma. *Expert Rev Neurother,* 12**,** 895-9.
GOLDING, J. P., WARDHAUGH, T., PATRICK, L., TURNER, M., PHILLIPS, J. B., BRUCE, J. I. & KIMANI, S. G. 2013. Targeting tumour energy metabolism potentiates the cytotoxicity of 5-aminolevulinic acid photodynamic therapy. *Br J Cancer,* 109**,** 976-82.
GUNAYDIN, G., GEDIK, M. E. & AYAN, S. 2021. Photodynamic Therapy for the Treatment and Diagnosis of Cancer-A Review of the Current Clinical Status. *Front Chem,* 9**,** 686303.
HAGIYA, Y., FUKUHARA, H., MATSUMOTO, K., ENDO, Y., NAKAJIMA, M., TANAKA, T., OKURA, I., KURABAYASHI, A., FURIHATA, M., INOUE, K., SHUIN, T. & OGURA, S. 2013. Expression levels of PEPT1 and ABCG2 play key roles in 5-aminolevulinic acid (ALA)-induced tumor-specific protoporphyrin IX (PpIX) accumulation in bladder cancer. *Photodiagnosis Photodyn Ther,* 10**,** 288-95.
HEGI, M. E., DISERENS, A. C., GORLIA, T., HAMOU, M. F., DE TRIBOLET, N., WELLER, M., KROS, J. M., HAINFELLNER, J. A., MASON, W., MARIANI, L., BROMBERG, J. E., HAU, P., MIRIMANOFF, R. O., CAIRNCROSS, J. G., JANZER, R. C. & STUPP, R. 2005. MGMT gene silencing and benefit from temozolomide in glioblastoma. *N Engl J Med,* 352**,** 997-1003.
HIROHASHI, Y., TORIGOE, T., TSUKAHARA, T., KANASEKI, T., KOCHIN, V. & SATO, N. 2016. Immune responses to human cancer stem-like cells/cancer-initiating cells. *Cancer Sci,* 107**,** 12-7.
HIRSCHBERG, H., UZAL, F. A., CHIGHVINADZE, D., ZHANG, M. J., PENG, Q. & MADSEN, S. J. 2008. Disruption of the blood-brain barrier following ALA-mediated photodynamic therapy. *Lasers Surg Med,* 40**,** 535-42.
HIRSCHMANN-JAX, C., FOSTER, A. E., WULF, G. G., NUCHTERN, J. G., JAX, T. W., GOBEL, U., GOODELL, M. A. & BRENNER, M. K. 2004. A distinct "side population" of cells with high drug efflux capacity in human tumor cells. *Proc Natl Acad Sci U S A,* 101**,** 14228-33.
INOUE, K., KARASHIMA, T., KAMADA, M., SHUIN, T., KURABAYASHI, A., FURIHATA, M., FUJITA, H., UTSUMI, K. & SASAKI, J. 2009. Regulation of 5-aminolevulinic acid-mediated protoporphyrin IX accumulation in human urothelial carcinomas. *Pathobiology,* 76**,** 303-14.
ITO, S., RACHINGER, W., STEPP, H., REULEN, H. J. & STUMMER, W. 2005. Oedema formation in experimental photo-irradiation therapy of brain tumours using 5-ALA. *Acta Neurochir (Wien),* 147**,** 57-65; discussion 65.
IYER, A. K., GREISH, K., SEKI, T., OKAZAKI, S., FANG, J., TAKESHITA, K. & MAEDA, H. 2007. Polymeric micelles of zinc protoporphyrin for tumor targeted delivery based on EPR effect and singlet oxygen generation. *J Drug Target,* 15**,** 496-506.

JOHANSSON, A., FABER, F., KNIEBUHLER, G., STEPP, H., SROKA, R., EGENSPERGER, R., BEYER, W. & KRETH, F. W. 2013. Protoporphyrin IX fluorescence and photobleaching during interstitial photodynamic therapy of malignant gliomas for early treatment prognosis. *Lasers Surg Med,* 45**,** 225-34.

JOHANSSON, A., PALTE, G., SCHNELL, O., TONN, J. C., HERMS, J. & STEPP, H. 2010. 5-Aminolevulinic acid-induced protoporphyrin IX levels in tissue of human malignant brain tumors. *Photochem Photobiol,* 86**,** 1373-8.

KAWAI, N., HIROHASHI, Y., EBIHARA, Y., SAITO, T., MURAI, A., SAITO, T., SHIROSAKI, T., KUBO, T., NAKATSUGAWA, M., KANASEKI, T., TSUKAHARA, T., SHICHINOHE, T., LI, L., HIRANO, S. & TORIGOE, T. 2019. ABCG2 expression is related to low 5-ALA photodynamic diagnosis (PDD) efficacy and cancer stem cell phenotype, and suppression of ABCG2 improves the efficacy of PDD. *PLoS One,* 14**,** e0216503.

KEMMNER, W., WAN, K., RUTTINGER, S., EBERT, B., MACDONALD, R., KLAMM, U. & MOESTA, K. T. 2008. Silencing of human ferrochelatase causes abundant protoporphyrin-IX accumulation in colon cancer. *FASEB J,* 22**,** 500-9.

KHOT, M. I., DOWNEY, C. L., ARMSTRONG, G., SVAVARSDOTTIR, H. S., JARRAL, F., ANDREW, H. & JAYNE, D. G. 2020. The role of ABCG2 in modulating responses to anti-cancer photodynamic therapy. *Photodiagnosis Photodyn Ther,* 29**,** 101579.

KIM, J. E., CHO, H. R., XU, W. J., KIM, J. Y., KIM, S. K., KIM, S. K., PARK, S. H., KIM, H., LEE, S. H., CHOI, S. H., PARK, S. & PARK, C. K. 2015. Mechanism for enhanced 5-aminolevulinic acid fluorescence in isocitrate dehydrogenase 1 mutant malignant gliomas. *Oncotarget,* 6**,** 20266-77.

KIRSON, E. D., DBALY, V., TOVARYS, F., VYMAZAL, J., SOUSTIEL, J. F., ITZHAKI, A., MORDECHOVICH, D., STEINBERG-SHAPIRA, S., GURVICH, Z., SCHNEIDERMAN, R., WASSERMAN, Y., SALZBERG, M., RYFFEL, B., GOLDSHER, D., DEKEL, E. & PALTI, Y. 2007. Alternating electric fields arrest cell proliferation in animal tumor models and human brain tumors. *Proc Natl Acad Sci U S A,* 104**,** 10152-7.

KLEIHUES, P. & OHGAKI, H. 1999. Primary and secondary glioblastomas: from concept to clinical diagnosis. *Neuro Oncol,* 1**,** 44-51.

KOBUCHI, H., MORIYA, K., OGINO, T., FUJITA, H., INOUE, K., SHUIN, T., YASUDA, T., UTSUMI, K. & UTSUMI, T. 2012. Mitochondrial localization of ABC transporter ABCG2 and its function in 5-aminolevulinic acid-mediated protoporphyrin IX accumulation. *PLoS One,* 7**,** e50082.

KONDO, T., SETOGUCHI, T. & TAGA, T. 2004. Persistence of a small subpopulation of cancer stem-like cells in the C6 glioma cell line. *Proc Natl Acad Sci U S A,* 101**,** 781-6.

KRISHNAMURTHY, P. C., DU, G., FUKUDA, Y., SUN, D., SAMPATH, J., MERCER, K. E., WANG, J., SOSA-PINEDA, B., MURTI, K. G. & SCHUETZ, J. D. 2006. Identification of a mammalian mitochondrial porphyrin transporter. *Nature,* 443**,** 586-9.

KUROKAWA, H., ITO, H., TERASAKI, M. & MATSUI, H. 2019. Hyperthermia enhances photodynamic therapy by regulation of HCP1 and ABCG2 expressions via high level ROS generation. *Sci Rep,* 9**,** 1638.

LAKIN, N., RULACH, R., NOWICKI, S. & KURIAN, K. M. 2017. Current Advances in Checkpoint Inhibitors: Lessons from Non-Central Nervous System Cancers and Potential for Glioblastoma. *Front Oncol,* 7**,** 141.

LAYER, G., REICHELT, J., JAHN, D. & HEINZ, D. W. 2010. Structure and function of enzymes in heme biosynthesis. *Protein Sci,* 19**,** 1137-61.

LE RHUN, E., PREUSSER, M., ROTH, P., REARDON, D. A., VAN DEN BENT, M., WEN, P., REIFENBERGER, G. & WELLER, M. 2019. Molecular targeted therapy of glioblastoma. *Cancer Treat Rev,* 80**,** 101896.

LEE, P. J., JIANG, B. H., CHIN, B. Y., IYER, N. V., ALAM, J., SEMENZA, G. L. & CHOI, A. M. 1997. Hypoxia-inducible factor-1 mediates transcriptional activation of the heme oxygenase-1 gene in response to hypoxia. *J Biol Chem,* 272**,** 5375-81.

LIETKE, S., SCHMUTZER, M., SCHWARTZ, C., WELLER, J., SILLER, S., AUMILLER, M., HECKL, C., FORBRIG, R., NIYAZI, M., EGENSPERGER, R., STEPP, H., SROKA, R., TONN, J. C., RUHM, A. & THON, N. 2021. Interstitial Photodynamic Therapy Using 5-ALA for Malignant Glioma Recurrences. *Cancers (Basel),* 13.

LIU, Y. L., ANG, S. O., WEIGENT, D. A., PRCHAL, J. T. & BLOOMER, J. R. 2004. Regulation of ferrochelatase gene expression by hypoxia. *Life Sci,* 75**,** 2035-43.

MAHMOUDI, K., GARVEY, K. L., BOURAS, A., CRAMER, G., STEPP, H., JESU RAJ, J. G., BOZEC, D., BUSCH, T. M. & HADJIPANAYIS, C. G. 2019. 5-aminolevulinic acid photodynamic therapy for the treatment of high-grade gliomas. *J Neurooncol,* 141**,** 595-607.

MAO, Q. 2008. BCRP/ABCG2 in the placenta: expression, function and regulation. *Pharm Res,* 25**,** 1244-55.

MATHEWS, M. S., CHIGHVINADZE, D., GACH, H. M., UZAL, F. A., MADSEN, S. J. & HIRSCHBERG, H. 2011. Cerebral edema following photodynamic therapy using endogenous and exogenous photosensitizers in normal brain. *Lasers Surg Med,* 43**,** 892-900.

MAXWELL, R., JACKSON, C. M. & LIM, M. 2017. Clinical Trials Investigating Immune Checkpoint Blockade in Glioblastoma. *Curr Treat Options Oncol,* 18**,** 51.

MAYTIN, E. V., ANAND, S., RIHA, M., LOHSER, S., TELLEZ, A., ISHAK, R., KARPINSKI, L., SOT, J., HU, B., DENISYUK, A., DAVIS, S. C., KYEI, A. & VIDIMOS, A. 2018. 5-Fluorouracil Enhances Protoporphyrin IX Accumulation and Lesion Clearance during Photodynamic Therapy of Actinic Keratoses: A Mechanism-Based Clinical Trial. *Clin Cancer Res,* 24**,** 3026-3035.

MCNICHOLAS, K., MACGREGOR, M. N. & GLEADLE, J. M. 2019. In order for the light to shine so brightly, the darkness must be present-why do cancers fluoresce with 5-aminolaevulinic acid? *Br J Cancer,* 121**,** 631-639.

MROZ, P., YAROSLAVSKY, A., KHARKWAL, G. B. & HAMBLIN, M. R. 2011. Cell death pathways in photodynamic therapy of cancer. *Cancers (Basel),* 3**,** 2516-39.

MULLER, P., ABDEL GABER, S. A., ZIMMERMANN, W., WITTIG, R. & STEPP, H. 2020. ABCG2 influence on the efficiency of photodynamic therapy in glioblastoma cells. *J Photochem Photobiol B,* 210**,** 111963.

NAKANO, A., TSUJI, D., MIKI, H., CUI, Q., EL SAYED, S. M., IKEGAME, A., ODA, A., AMOU, H., NAKAMURA, S., HARADA, T., FUJII, S., KAGAWA, K., TAKEUCHI, K., SAKAI, A., OZAKI, S., OKANO, K., NAKAMURA, T., ITOH, K., MATSUMOTO, T. & ABE, M. 2011. Glycolysis inhibition inactivates ABC transporters to restore drug sensitivity in malignant cells. *PLoS One,* 6**,** e27222.

NAMATAME, H., AKIMOTO, J., MATSUMURA, H., HARAOKA, J. & AIZAWA, K. 2008. Photodynamic therapy of C6-implanted glioma cells in the rat brain employing second-

generation photosensitizer talaporfin sodium. *Photodiagnosis Photodyn Ther,* 5**,** 198-209.

NATARAJAN, K., XIE, Y., BAER, M. R. & ROSS, D. D. 2012. Role of breast cancer resistance protein (BCRP/ABCG2) in cancer drug resistance. *Biochem Pharmacol,* 83**,** 1084-103.

NAVONE, N. M., POLO, C. F., FRISARDI, A. L., ANDRADE, N. E. & BATTLE, A. M. 1990. Heme biosynthesis in human breast cancer--mimetic "in vitro" studies and some heme enzymic activity levels. *Int J Biochem,* 22**,** 1407-11.

NICOLAZZO, J. A. & KATNENI, K. 2009. Drug transport across the blood-brain barrier and the impact of breast cancer resistance protein (ABCG2). *Curr Top Med Chem,* 9**,** 130-47.

NIE, S., HUANG, Y., SHI, M., QIAN, X., LI, H., PENG, C., KONG, B., ZOU, X. & SHEN, S. 2018. Protective role of ABCG2 against oxidative stress in colorectal cancer and its potential underlying mechanism. *Oncol Rep,* 40**,** 2137-2146.

NOBUSAWA, S., WATANABE, T., KLEIHUES, P. & OHGAKI, H. 2009. IDH1 mutations as molecular signature and predictive factor of secondary glioblastomas. *Clin Cancer Res,* 15**,** 6002-7.

OGINO, T., KOBUCHI, H., MUNETOMO, K., FUJITA, H., YAMAMOTO, M., UTSUMI, T., INOUE, K., SHUIN, T., SASAKI, J., INOUE, M. & UTSUMI, K. 2011. Serum-dependent export of protoporphyrin IX by ATP-binding cassette transporter G2 in T24 cells. *Mol Cell Biochem,* 358**,** 297-307.

OHGAKI, H., DESSEN, P., JOURDE, B., HORSTMANN, S., NISHIKAWA, T., DI PATRE, P. L., BURKHARD, C., SCHULER, D., PROBST-HENSCH, N. M., MAIORKA, P. C., BAEZA, N., PISANI, P., YONEKAWA, Y., YASARGIL, M. G., LUTOLF, U. M. & KLEIHUES, P. 2004. Genetic pathways to glioblastoma: a population-based study. *Cancer Res,* 64**,** 6892-9.

OHGARI, Y., NAKAYASU, Y., KITAJIMA, S., SAWAMOTO, M., MORI, H., SHIMOKAWA, O., MATSUI, H. & TAKETANI, S. 2005. Mechanisms involved in delta-aminolevulinic acid (ALA)-induced photosensitivity of tumor cells: relation of ferrochelatase and uptake of ALA to the accumulation of protoporphyrin. *Biochem Pharmacol,* 71**,** 42-9.

OMOTO, K., MATSUDA, R., NAKAI, Y., TATSUMI, Y., NAKAZAWA, T., TANAKA, Y., SHIDA, Y., MURAKAMI, T., NISHIMURA, F., NAKAGAWA, I., MOTOYAMA, Y., NAKAMURA, M., FUJIMOTO, K. & HIROYUKI, N. 2019. Expression of peptide transporter 1 has a positive correlation in protoporphyrin IX accumulation induced by 5-aminolevulinic acid with photodynamic detection of non-small cell lung cancer and metastatic brain tumor specimens originating from non-small cell lung cancer. *Photodiagnosis Photodyn Ther,* 25**,** 309-316.

ONIZUKA, H., MASUI, K. & KOMORI, T. 2020. Diffuse gliomas to date and beyond 2016 WHO Classification of Tumours of the Central Nervous System. *Int J Clin Oncol,* 25**,** 997-1003.

OSTROM, Q. T., PATIL, N., CIOFFI, G., WAITE, K., KRUCHKO, C. & BARNHOLTZ-SLOAN, J. S. 2020. CBTRUS Statistical Report: Primary Brain and Other Central Nervous System Tumors Diagnosed in the United States in 2013-2017. *Neuro Oncol,* 22**,** iv1-iv96.

OTSUKA, S., MATSUMOTO, K., NAKAJIMA, M., TANAKA, T. & OGURA, S. 2015. Oxygen Availability for Porphyrin Biosynthesis Enzymes Determines the Production of Protoporphyrin IX (PpIX) during Hypoxia. *PLoS One,* 10**,** e0146026.

PALASUBERNIAM, P., YANG, X., KRAUS, D., JONES, P., MYERS, K. A. & CHEN, B. 2015. ABCG2 transporter inhibitor restores the sensitivity of triple negative breast cancer cells to aminolevulinic acid-mediated photodynamic therapy. *Sci Rep,* 5**,** 13298.

PETRECCA, K., GUIOT, M. C., PANET-RAYMOND, V. & SOUHAMI, L. 2013. Failure pattern following complete resection plus radiotherapy and temozolomide is at the resection margin in patients with glioblastoma. *J Neurooncol,* 111**,** 19-23.

QUIRK, B. J., BRANDAL, G., DONLON, S., VERA, J. C., MANG, T. S., FOY, A. B., LEW, S. M., GIROTTI, A. W., JOGAL, S., LAVIOLETTE, P. S., CONNELLY, J. M. & WHELAN, H. T. 2015. Photodynamic therapy (PDT) for malignant brain tumors--where do we stand? *Photodiagnosis Photodyn Ther,* 12**,** 530-44.

ROBEY, R. W., IERANO, C., ZHAN, Z. & BATES, S. E. 2011. The challenge of exploiting ABCG2 in the clinic. *Curr Pharm Biotechnol,* 12**,** 595-608.

SAI, D. L., LEE, J., NGUYEN, D. L. & KIM, Y. P. 2021. Tailoring photosensitive ROS for advanced photodynamic therapy. *Exp Mol Med,* 53**,** 495-504.

SATHORNSUMETEE, S., REARDON, D. A., DESJARDINS, A., QUINN, J. A., VREDENBURGH, J. J. & RICH, J. N. 2007. Molecularly targeted therapy for malignant glioma. *Cancer,* 110**,** 13-24.

SAWAMOTO, M., IMAI, T., UMEDA, M., FUKUDA, K., KATAOKA, T. & TAKETANI, S. 2013. The p53-dependent expression of frataxin controls 5-aminolevulinic acid-induced accumulation of protoporphyrin IX and photo-damage in cancerous cells. *Photochem Photobiol,* 89**,** 163-72.

SHELEG, S. V., ZHAVRID, E. A., KHODINA, T. V., KOCHUBEEV, G. A., ISTOMIN, Y. P., CHALOV, V. N. & ZHURAVKIN, I. N. 2004. Photodynamic therapy with chlorin e(6) for skin metastases of melanoma. *Photodermatol Photoimmunol Photomed,* 20**,** 21-6.

SHENG, T., ONG, Y., BUSCH, T. M. & ZHU, T. C. 2020. Reactive oxygen species explicit dosimetry to predict local tumor growth for Photofrin-mediated photodynamic therapy. *Biomed Opt Express,* 11**,** 4586-4601.

SINHA, A. K., ANAND, S., ORTEL, B. J., CHANG, Y., MAI, Z., HASAN, T. & MAYTIN, E. V. 2006. Methotrexate used in combination with aminolaevulinic acid for photodynamic killing of prostate cancer cells. *Br J Cancer,* 95**,** 485-95.

STEPP, H. & STUMMER, W. 2018. 5-ALA in the management of malignant glioma. *Lasers Surg Med,* 50**,** 399-419.

STUMMER, W., PICHLMEIER, U., MEINEL, T., WIESTLER, O. D., ZANELLA, F., REULEN, H. J. & GROUP, A. L.-G. S. 2006. Fluorescence-guided surgery with 5-aminolevulinic acid for resection of malignant glioma: a randomised controlled multicentre phase III trial. *Lancet Oncol,* 7**,** 392-401.

STUPP, R., MASON, W. P., VAN DEN BENT, M. J., WELLER, M., FISHER, B., TAPHOORN, M. J., BELANGER, K., BRANDES, A. A., MAROSI, C., BOGDAHN, U., CURSCHMANN, J., JANZER, R. C., LUDWIN, S. K., GORLIA, T., ALLGEIER, A., LACOMBE, D., CAIRNCROSS, J. G., EISENHAUER, E., MIRIMANOFF, R. O., EUROPEAN ORGANISATION FOR, R., TREATMENT OF CANCER BRAIN, T., RADIOTHERAPY, G. & NATIONAL CANCER INSTITUTE OF CANADA CLINICAL TRIALS, G. 2005. Radiotherapy plus concomitant and adjuvant temozolomide for glioblastoma. *N Engl J Med,* 352**,** 987-96.

STUPP, R., TAILLIBERT, S., KANNER, A. A., KESARI, S., STEINBERG, D. M., TOMS, S. A., TAYLOR, L. P., LIEBERMAN, F., SILVANI, A., FINK, K. L., BARNETT, G. H., ZHU, J. J., HENSON, J. W., ENGELHARD, H. H., CHEN, T. C., TRAN, D. D., SROUBEK, J., TRAN, N. D., HOTTINGER, A. F., LANDOLFI, J., DESAI, R., CAROLI, M., KEW, Y., HONNORAT, J., IDBAIH, A., KIRSON, E. D., WEINBERG, U., PALTI, Y., HEGI, M. E. & RAM, Z. 2015. Maintenance Therapy With Tumor-Treating Fields Plus Temozolomide vs Temozolomide Alone for Glioblastoma: A Randomized Clinical Trial. *JAMA,* 314**,** 2535-43.

SUN, W., KAJIMOTO, Y., INOUE, H., MIYATAKE, S., ISHIKAWA, T. & KUROIWA, T. 2013. Gefitinib enhances the efficacy of photodynamic therapy using 5-aminolevulinic acid in malignant brain tumor cells. *Photodiagnosis Photodyn Ther,* 10**,** 42-50.

TENG, L., NAKADA, M., ZHAO, S. G., ENDO, Y., FURUYAMA, N., NAMBU, E., PYKO, I. V., HAYASHI, Y. & HAMADA, J. I. 2011. Silencing of ferrochelatase enhances 5-aminolevulinic acid-based fluorescence and photodynamic therapy efficacy. *Br J Cancer,* 104**,** 798-807.

THON, N., TONN, J. C. & KRETH, F. W. 2019. The surgical perspective in precision treatment of diffuse gliomas. *Onco Targets Ther,* 12**,** 1497-1508.

VERMANDEL, M., DUPONT, C., LECOMTE, F., LEROY, H. A., TULEASCA, C., MORDON, S., HADJIPANAYIS, C. G. & REYNS, N. 2021. Standardized intraoperative 5-ALA photodynamic therapy for newly diagnosed glioblastoma patients: a preliminary analysis of the INDYGO clinical trial. *J Neurooncol,* 152**,** 501-514.

VLAMING, M. L., LAGAS, J. S. & SCHINKEL, A. H. 2009. Physiological and pharmacological roles of ABCG2 (BCRP): recent findings in Abcg2 knockout mice. *Adv Drug Deliv Rev,* 61**,** 14-25.

WANG, W., TABU, K., HAGIYA, Y., SUGIYAMA, Y., KOKUBU, Y., MUROTA, Y., OGURA, S. I. & TAGA, T. 2017. Enhancement of 5-aminolevulinic acid-based fluorescence detection of side population-defined glioma stem cells by iron chelation. *Sci Rep,* 7**,** 42070.

WELLER, M., STUPP, R., HEGI, M. & WICK, W. 2012. Individualized targeted therapy for glioblastoma: fact or fiction? *Cancer J,* 18**,** 40-4.

WYLD, L., TOMLINSON, M., REED, M. W. & BROWN, N. J. 2002. Aminolaevulinic acid-induced photodynamic therapy: cellular responses to glucose starvation. *Br J Cancer,* 86**,** 1343-7.

YANG, S. B., GAO, K. D., JIANG, T., CHENG, S. J. & LI, W. B. 2017. Bevacizumab combined with chemotherapy for glioblastoma: a meta-analysis of randomized controlled trials. *Oncotarget,* 8**,** 57337-57344.

YANG, X., LI, W., PALASUBERNIAM, P., MYERS, K. A., WANG, C. & CHEN, B. 2015. Effects of Silencing Heme Biosynthesis Enzymes on 5-Aminolevulinic Acid-mediated Protoporphyrin IX Fluorescence and Photodynamic Therapy. *Photochem Photobiol,* 91**,** 923-30.

YENARI, M. A. & HAN, H. S. 2012. Neuroprotective mechanisms of hypothermia in brain ischaemia. *Nat Rev Neurosci,* 13**,** 267-78.

YOSHIOKA, E., CHELAKKOT, V. S., LICURSI, M., RUTIHINDA, S. G., SOM, J., DERWISH, L., KING, J. J., PONGNOPPARAT, T., MEAROW, K., LARIJANI, M., DORWARD, A. M. & HIRASAWA, K. 2018. Enhancement of Cancer-Specific Protoporphyrin IX Fluorescence by Targeting Oncogenic Ras/MEK Pathway. *Theranostics,* 8**,** 2134-2146.

ZHANG, J., JIANG, C., FIGUEIRO LONGO, J. P., AZEVEDO, R. B., ZHANG, H. & MUEHLMANN, L. A. 2018. An updated overview on the development of new photosensitizers for anticancer photodynamic therapy. *Acta Pharm Sin B,* 8**,** 137-146.

ZHAO, S. G., CHEN, X. F., WANG, L. G., YANG, G., HAN, D. Y., TENG, L., YANG, M. C., WANG, D. Y., SHI, C., LIU, Y. H., ZHENG, B. J., SHI, C. B., GAO, X. & RAINOV, N. G. 2013. Increased expression of ABCB6 enhances protoporphyrin IX accumulation and photodynamic effect in human glioma. *Ann Surg Oncol,* 20**,** 4379-88.

ZHOU, H. M., ZHANG, J. G., ZHANG, X. & LI, Q. 2021. Targeting cancer stem cells for reversing therapy resistance: mechanism, signaling, and prospective agents. *Signal Transduct Target Ther,* 6**,** 62.

ZIMMERMANN, M. & STAN, A. C. 2010. PepT2 transporter protein expression in human neoplastic glial cells and mediation of fluorescently tagged dipeptide derivative beta-Ala-Lys-Nepsilon-7-amino-4-methyl-coumarin-3-acetic acid accumulation. *J Neurosurg,* 112**,** 1005-14.

Acknowledgements

At this point I would like to thank everyone who actively supported me in my doctoral thesis and without their help this dissertation would not have been realized in this form.

First and foremost, I am very grateful to my supervisor, Prof. Wolfgang Zimmermann, for his invaluable advice, his multiple suggestions in the design of the experimental setup and the detailed clarification of biological questions that would otherwise have remained unanswered.

The completion of my dissertation would not have been possible without the tremendous support of my advisor, Dr. Herbert Stepp, who always found enough time to discuss my progress, guided me through the whole project, read my numerous revisions within days, continuously supported me especially with statistics and, above all, always stayed patient and motivated me during rough times.

Moreover, I highly appreciate the support I received from Dr. Sara Abdel Gaber for convincing me to initially do this project, always offering me a helping hand as well as encouraging words and most importantly helping me to finalize our second paper together.

Special thanks go to Dr. Rainer Wittig for providing the cell line we used for this project. Furthermore, I would also like to acknowledge Birgit Stadlbauer and Dr. Gabriele Strauß for helping me with the cell culture and giving me technical support with the flow cytometer. I would like to extend my gratitude to all the other members from the LIFE Center for an incredible time spent at the lab together and especially the social lunch meetings during summer time.

My appreciation extends to the Medical Faculty of the LMU for the research fellowship (FöFoLe) and their financial support.

Finally, I would like to express my gratitude to my family and friends, who always offered me tremendous encouragement during this long process.